MICROGEL BASED ADHESIVES FOR WET PAPER STRENGTH

MICROGEL BASED ADHESIVES FOR WET PAPER STRENGTH

By

QUAN WEN, B. Eng., M. Eng.

A Thesis

Submitted to the School of Graduate Studies

in Partial Fulfillment of the Requirements

for the Degree

Doctor of Philosophy

McMaster University

DOCTOR OF PHILOSOPHY (2012) McMaster University

(Chemical Engineering) Hamilton, Ontario

TITLE: Microgel Based Adhesive for Wet Paper Strength

AUTHOR: Quan Wen

B.Eng. (Beihang University)

M.Eng. (Queen Mary, University of London)

SUPERVISOR: Professor Robert H. Pelton

NUMBER OF PAGES: vii, 127

Abstract

The interactions of microgel based adhesives with cellulose were studied by peel test of cellulose laminates and tensile test of handsheets. The objective of this project was to create design rules for microgel based adhesives so as to improve the wet paper strength.

Colloidal microgel based adhesives were formed by coating carboxylated poly(N-isopropylacrylamide) (PNIPAM) microgels with polyvinylamine (PVAm). The characterization of the microgel base adhesives were performed by electrophoretic mobilities, dynamic light scattering, and potentiometric titration. The microgel based adhesives were pH sensitive and their swelling behaviour was related to the composition of PVAm in the microgels. The maximum amount of PVAm binding to microgels depends on the location of charges in the microgels and the molecular weight of PVAm. The binding process of PVAm to microgels was monitored by quartz crystal microbalance measurements. It is proposed that the binding of PVAm to microgels is controlled by the rate of initial attachment of PVAm and the rate of reconfiguration of PVAm on the microgels.

The microgel based adhesives were laminated between oxidized cellulose films and the wet adhesion of microgel based adhesives with cellulose was studied by a 90° peel test. The wet delamination force was measured as a function of PVAm content, PVAm molecular weight, coverage of adhesives on cellulose films, size of adhesives, stiffness of adhesives and the roughness of cellulose films. The wet adhesion of microgel based adhesives with cellulose increased with PVAm content in the microgels, and decreased with microgel stiffness. The molecular weight of PVAm did not influence the performance of adhesives. The effect of microgel size on wet adhesion with cellulose was related to the roughness of cellulose films. Larger microgels did fill the voids between rough cellulose films to create more contact area with these films resulting in higher wet adhesion. By contrast, for smooth cellulose films, the size of microgels didn't affect the wet adhesion.

Finally, this basic research was extended to a practical situation. The microgel based adhesives were added to unbeaten, bleached softwood pulp to prepare handsheets and their ability to enhance wet paper strength was evaluated by tensile test. The wet paper strength increased with PVAm content of the microgels. For linear PVAm, high molecular weight PVAm was more effective as a wet strength adhesive while for PVAm coated microgels, the molecular weight was not significant for wet paper strength. With the aid of PVAm coating, solid carboxylated polystyrene particles improved the wet paper strength. However the wet strength of paper treated with PVAm coated microgels was larger than that treated with PVAm coated polystyrene by a factor of 2.

Acknowledgements

First, I wish to express my sincere gratitude to my supervisor, Dr. Robert Pelton for his constant guidance and encouragement throughout my graduate studies. I am also grateful for the opportunities Dr. Pelton provided to network with industry and meet other experts in conferences. I would like to thank the members of my Ph.D committee, Dr. Kari Dalnoki-Veress and Dr. Todd Hoare for their valuable advice and generous help on this research work.

I would like to thank the Natural Sciences and Engineering Research Council of Canada and BASF Canada for funding this work. Special acknowledgments go to Drs. Esser, Kroener, Mijolovic, and Stährfeldt, all from BASF in Europe, and with Prof. Boxin Zhao, University of Waterloo for their stimulating advice.

I would also like to acknowledge all the people that have collaborated kindly, without which this work would not have been possible. I would like to thank Ms. Marnie Timleck for her help with confocal microscopy, Dr. Steve Kornic for his training of nuclear magnetic resonance, Mr. Steve Koprich for his assistant with scanning electron microscopy, Dr. Shiping Zhu and Dr. Carlos Filipe for the access of their instruments, Mr. Zhilin Peng for his help of silicon wafer modification, Dr. Yuguo Cui for help with mathematical modeling, Dr. Wei Chen for training of wet adhesion measurements, Dr. Dan Zhang for sharing his knowledge of synthetic chemistry. Three brilliant summer students worked with me and contributed greatly to this work. I would like to thank Andrew Vincelli, Steven Zecchin and Antonyos Fahmy for their hard work and beautiful data analysis.

Special thanks are given to my colleagues in McMaster Interfacial Technologies Group and Department of Chemical Engineering for their support and friendship. I am indebted to Ms. Kathy Goodram, Ms. Lynn Falkiner, Ms. Nanci Cole, Ms. Andrea Vickers, Ms. Melissa Vasi, Ms. Francis Lima, and Ms. Sally Watson for their administrative assistance, Mr.Doug Keller, Mr.Paul Gatt, Ms. Justyna Derkach and Mr. Dan Wright for their technical assistance.

Finally, I would like to thank my parents for their love and support.

TABLE OF CONTENTS

Abbreviations

AFM	atomic force microscopy
APS	ammonium persulfate
BBA	1,4-bis(aminomethyl)benzene
CLSM	Confocal Laser Scanning Microscope
CMC	carboxymethylcellulose `
DLS	dynamic light scattering
DMAc/LiCl	dimethylacetamide/lithium chloride
EDC	N-(3-dimethylaminopropyl)-N'-ethylcarbodiimide hydrochloride
EMIMAC	1-ethyl-3-methylimidazolium acetate
IL	ionic liquid
LB	Langmuir-Blodgett
LCST	lower critical solution temperature
MAA	methylacrylic acid
MBA	N,N-Methylenebisacrylamide
MG	microgel
MW	molecular weight
MWCO	molecular weight cut-off
NIPAM	N-Isopropylacrylamide
NMMO	N-methylmorpholine N-oxide
NMR	nuclear magnetic resonance
PAE	polyamide-epichlorohydrin
PAE	poly(amideamine) epichlorohydrin
PAH	polyallylamine hydrochloride
PALS	phase analysis light scattering
PDADMAC	polydiallyldimethyl ammonium chloride
PNIPAM	carboxylated? poly(Nisopropylacrylamide)iii
PS	polystyrene
PVAm	polyvinylamine

QCM	Quartz crystal microbalance
RBA	relative bonded area
SDS	sodium dodecyl sulfate
SEM	scanning electron microscope?
Sulfo-NHS	*N*-hydroxysulfosuccinimide
TAPPI	Technical Association of the Pulp and Paper Industry
TEMPO	2,2,6,6-tetramethylpiperidine-1-oxyl
TMSC	trimethylssilyl cellulose
UF	Urea-Formaldehyde
VAA	vinylacetic acid

Chapter 1 Introduction

Generally speaking, paper loses 90% of its strength when it comes in contact with water.[1] This is because water molecules are able to enter the paper and weaken the fiber-fiber joints. However, for certain applications such as liquid packaging base paper, paper towels and tissue paper, the paper product is required to maintain some level of strength in a humid environment.[3] Therefore, water soluble polymers have been widely employed as wet-strength additives to maintain the strength of paper exposed to high humidity.

The traditional wet strength additives are linear cationic polymers which can adsorb onto wood fibers to reinforce the fiber-fiber joints[3]. The ability of linear polymers to enhance the wet strength of paper is limited by adsorption since linear polymers can only form a monolayer on the surface of fibers and the thickness of the adsorbed layer is on the scale of a few nanometers. To overcome this obstacle, polyelectrolyte complexes are introduced into paper as wet strength additive.[4-5] Polyelectrolyte complexes are formed from oppositely charged polyelectrolytes driven by electrostatic interactions. Compared with linear polymers, the complexes have the advantage of large bulk volume, resulting in an adsorbed layer on a surface with a thickness up to a few micrometers.[6] But it is difficult to prepare polyelectrolyte complexes without excess free polymer, which is a drawback considering the economic impact. Microgel based wet strength additives, introduced into paper by Miao, showed a dramatically improvement of wet paper strength.[6] However, there was a large size distribution of microgels synthesized by Miao, ranging from 0.1μm to 10μm, which made the size effect of strength additives on wet paper strength difficult to determine.

This thesis focuses on the improvement of wet paper strength by microgel-based adhesives. By introducing carboxylated microgels as templates, monodispersed cationic microgels were prepared and used as wet strength adhesives. Both wet adhesion to cellulose membranes and wet paper strength were studied in terms of microgel surface chemical and bulk physical properties.This study could be useful to the papermaking industry for wet-strength resins and high strength paper.

1.1 Literature review

1.1.1 Structure of fibers

Paper is formed by anionic cellulose fibers joined together by removing water from a pulp suspension[7]. Other materials such as polymeric additives and filler particles are added to pulp suspensions, depending on the final application. Figure 1 illustrates the structures of a paper surface and a wood fiber. The wood fibers distribute in paper stochastically, and the aspect ratio of wood fibers ranges from 50 to 100 according to the precise species[8].

The cross section of wood fiber consists of many layers. As shown in Figure 1, the center of the wood fiber is hollow tube called the lumen, surrounded by three layers of secondary wall. The micro fibrils are spirally distributed around the axis of fiber length at different angles depending on the layers in the secondary wall of wood fibers. The fibrils in secondary wall consist mostly of cellulose molecules, and the fibrils in the matrix are primarily hemicelluloses and lignin.

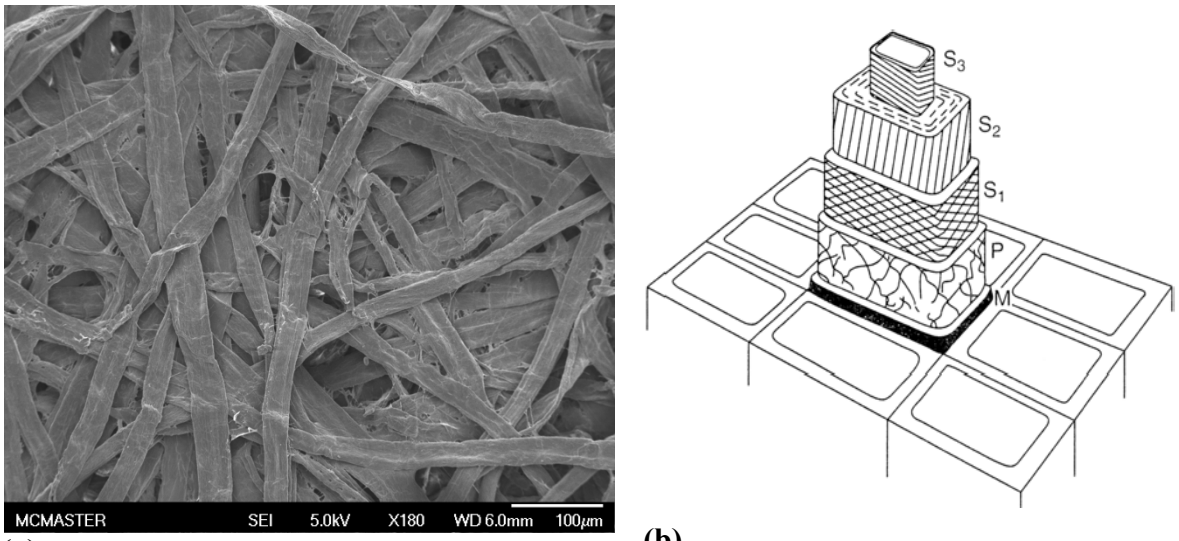

(a) **(b)**

Figure 1 (a) microscopic image of a paper surface; (b) cell wall structure of a wood fiber (adapted from Booker et.al.[9]) . M, middle lamella; P, primary wall; S1,S2,S3, layers of secondary wall.

At the molecular level, the wood fibers composed of cellulose, hemicellulose and lignin. Cellulose is a linear polysaccharide consisting of a number of repeat units of glucose linked by ß-1,4 glycosidic bonds. Cellulose contains hydroxyl groups located at the C2, C3, and C6 positions. These hydroxyl groups can form a hydrogen bonding network contributing to the crystallinity of wood fibers[10]. Hemicellulose is branched polysaccharides containing different sugar monomers. Other than cellulose, hemicellulose has an amorphous structure and its resistance of hydrolysis is very low. Therefore, hemicelluloses are easily removed from wood fibers. The chemical structure of lignin is quite distinct from cellulose and hemicellulose. Lignins are carbohydrate complexes crosslinked by benzyl ester, benzyl either, and glycosidic linkages. The aromatic components of lignin prevent the adsorption of water to wood. Thus the major function of lignin is to transport water in wood. Due to the benzyl ester linkage, lignin can be hydrolyzed during the pulping process[11].

1.1.2 Properties of pulp fibers

As paper is made of crossed cellulose fibers with each other, the properties of pulp fibers strongly affect the paper strength in the following ways:

The geometry of pulp fibers. The distribution of pulp fibers in paper is determined by their geometric property. Generally speaking, paper made of short pulp fibers is more uniform. However, long pulp fibers contribute to the strength of paper since there are more interactions between the fibers.

The strength of pulp fibers. The strength of a fiber is recognized as the maximum strength of paper. But the strength of paper is determined by the weakest point. Thus, paper strength is usually weaker than the fiber strength.

The surface topography of pulp fibers. The real fiber surface is quite rough and contains many pores[12-14]. These pores are produced during the pulping process, and the porosity of cellulose fibers changes with their water content in cellulose fibers[15-16]. The roughness due to porosity increases the surface area of the pulp fibers. However this it is not necessary for strength enhancement, which is mostly determined by the contact area between fibers.

The fiber-fiber bonds. The bonds between cellulose fibers are essential for paper strength. The bonds existing in paper are mainly chemical bonds, intermolecular Van der Waals bonds, and the entanglement of polymer chains[17]. The strength of these bonds is determined by the surface chemistry and physical structure of the cellulose fibers. The hydrogen bonds between cellulose fibers assemble the fibers to form paper, while hydrogen bonds between fibrils in the fiber wall contribute to the rigidity of fibers. Covalent bonds also exist between fibers introduced by polymeric additives. Cellulose fibers are usually negatively charged, forming reactive sites for covalent bonds. These charges originate from carboxyl groups and sulfonic acid groups produced in the papermaking process[18]. Further, Back has claimed that heat treatment can improve the wet strength of paper, due to thermal crosslinking in cellulose[19]. The physical entanglements of polymer chains are located at the interfaces of fibers, since the fiber surface is covered by amorphous cellulose chains[20]. Among all the bonds formed between cellulose fibers, hydrogen bonds are believed to form the primary interaction.

1.1.3 Paper strength test

Paper strength can be categorized into *in-plane strength* and *out-of-plane strength*. In-plane strength represents the ability of paper to hold together under stretching, while out-of–plane strength shows the resistance of paper to certain loads in the thickness direction.

In-plane strength of paper is usually measured by tensile tests. These are carried out by measuring the maximum load applied to paper samples under constant a elongation rate. The tensile strength is defined as the maximum load divided by the width of the paper

samples. Sometimes, a tensile index is used for paper samples, defined as the tensile strength divided by the basis weight of the paper samples:

$$TI = \frac{T}{W} \qquad \text{Equation 1}$$

where TI is the tensile index expressed as Nm/g, T is the tensile strength expressed as N/m, and W is the basis weight, which is the weight per unit area of paper expressed as g/m^2.

Both the failure of fibers, and the failure of bonds between fibers can cause the tensile failure of paper. Many models have been developed to predict the tensile strength of paper. Shallhorn and Karnis established a model, according to which tensile strength is proportional to geometrical properties of fibers[21]. The model derived by Page entails that the strength of weakly bonded paper is determined by the bond strength between fibers, whereas the strength of strongly bonded paper is determined by the strength of fibers[22].

Out-of-plane strength is measured by the strength of paper in the thickness directions. Commonly, testing of out-of-plane strength is performed by a tensile tester or a Scott Bond Tester, illustrated below in Figures 2(a) and 2(b) respectively. The measurements are performed by applying force onto two surfaces of the paper specimen fixed to suitable metal blocks with double sided tapes, assuming that the adhesive does not affect paper strength. The tensile tester showed in Figure 2(a) gives the out-of-plane failure stress. The Scott Bond Tester showed in Figure 2(b) measures the delamination energy of paper caused by the striking of a pendulum on an aluminum block.

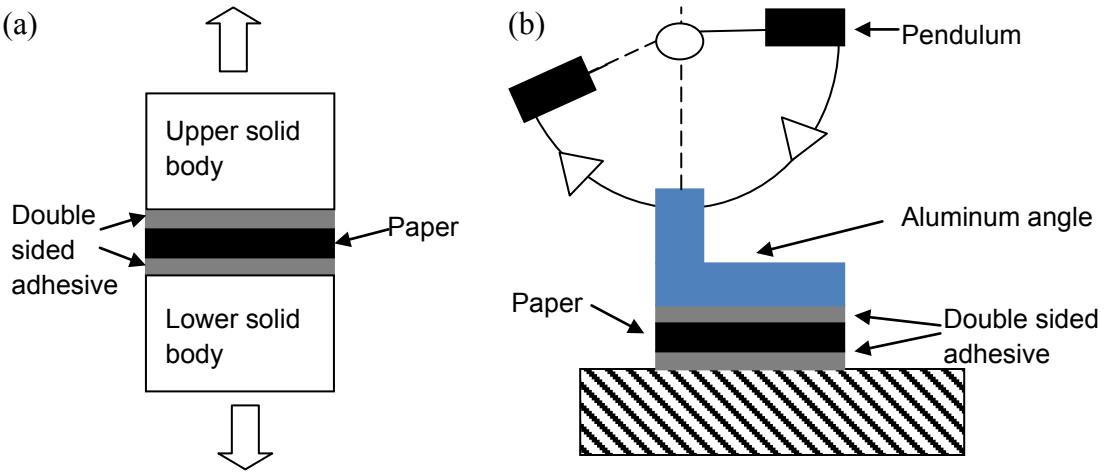

Figure 2 Measurements of out-of-plane strength(adapted from Retulainen [17])

1.1.4 Wet strength resins

Paper strength is strongly affected by the moisture in the environment. When paper comes in contact with water, the cellulose fibers swell and the hydrogen bonds between the fibers are diminished. Thus wet strength resins are added into paper pulp to reinforce the fiber-fiber bonds. The common characteristics of wet strength resins are:

Water-soluble. The paper is made from pulp suspension. The wet strength resins must be adsorbed onto cellulose fibers before being pressed to form paper sheets. Water soluble polymer can disperse easily well in pulp suspension, and deposit effectively onto cellulose fibers.

Cationic. Since the cellulose fibers are anionic, opposite charges can bring the polymer to the fiber surface by electrostatic interactions[23-24].

Reactive. Since the hydrogen bonds network in paper is destruct by water molecules, wet strength resins are needed to provide the secondary bonding network to hold the cellulose fibers together[3].

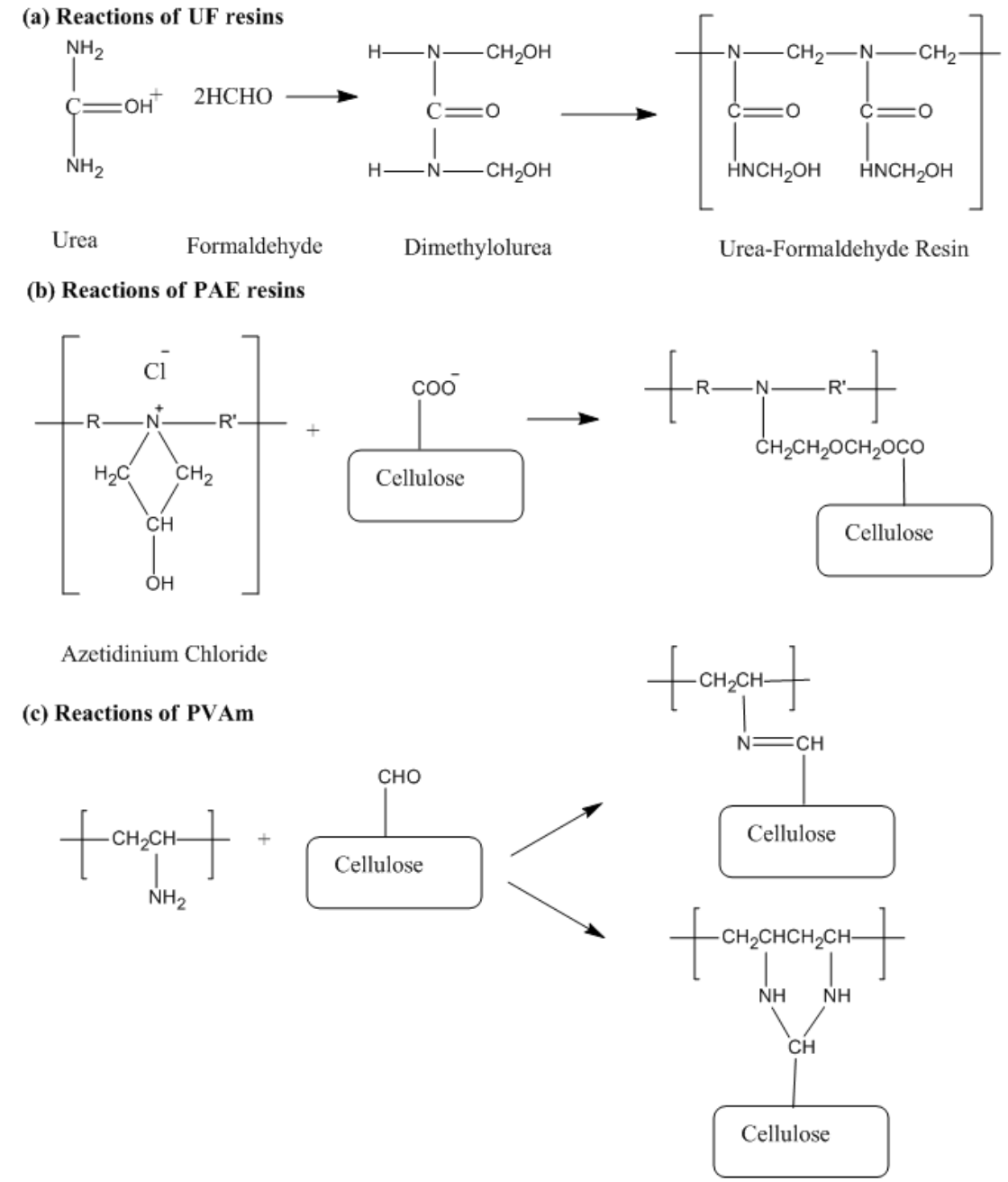

Figure 3 The reactions of wet strength resins

The earliest known traditional wet strength resin is Urea-Formaldehyde (UF), which can establish a network by self-crosslinking[25]. This reaction principle is illustrated in Figure 3(a). Actually, it is the reaction product of urea and formaldehyde that can form crosslink networks. However, the insolubility of dimethylolurea limits the application of UF as a wet strength resin. Although the solubility of UF resin can be modified, the usage of UF

is still reduced, since the performance of UF resin is affected by hemicelluloses, and the crosslink reaction requires heat and low pH[26].

Another commonly used wet strength resin is polyamide-epichlorohydrin (PAE). An early study concluded that PAE enhances the wet strength by homo-crosslinking, and PAE does not react with hydroxyl groups of fibers[27]. However, this study did not consider the carboxylic acid groups contained in fibers. Later, another mechanism was proposed, according to which the wet strength improvement is caused by the reaction between azetidinium groups of PAE and carboxylic acid groups on cellulose fibers[28]. It was also found that PAE could effectively improve the wet strength of carboxylated pulp[29]. Thus, it is now believed that the mechanism whereby PAE reinforces the wet strength is the formation of covalent bonds of PAE to cellulose fibers. However, because of the impact of organic chloride contained in PAE products on the environment, the use of PAE in paper mills is now limited[25, 30].

Recently, polyvinylamine (PVAm) has been considered as a wet strength resin.[31-33] PVAm is protonated so as to be positive charged when its pH is lower than 10. Thus PVAm can be quickly adsorbed onto anionic charged cellulose fibers driven by electrostatic interactions. The wet strength improvement caused by PVAm is achieved by covalent linkage between primary amine groups of PVAm and aldehyde groups of cellulose fibers introduced by TEMPO/NaBr/NaClO oxidation[34]. The reactions are shown above in Figure 3(c).

The effect of polymer as a wet-strength additive is influenced not only by chemical composition but also by physical morphology. Since wet strength additives have to be able to adsorb onto cellulose fibers to improve wet strength, the effect of wet strength additives is limited by adsorption. A polymer can only form monolayer on the surfaces, and the thickness of the polymer layer is determined by the physical morphology of the polymer.[35-36] As illustrated in Figure 4(a)(c), the thickness of the linear polymer layer on a fiber surface is of the order of 10nm, while the thickness of the colloidal polymer layer can reach several microns, depending on the size of the colloidal polymer. In addition, the fiber surface is covered with pores and the radius of pores in the fiber wall is in the range of 6.5 to 10 nm[37-38]. Thus, as shown in Figure 4(b), wet strength resins with small sizes can easily enter the fiber wall[39-41], and the improvement in wet strength of the paper is reduced. To overcome this obstacle, a colloidal polyelectrolyte complex is introduced as a wet strength resin. Polyelectrolyte complexes are formed by binding of oppositely charge polymers. Gardlund et al. prepared an anionic polyelectrolyte complex composed of PAE and carboxymethylcellulose (CMC) and found that this complex gave significant improvement on wet paper strength[4]. Feng et al. studied the wet adhesion between wet cellulose membranes and a polyelectrolyte complex formed by PVAm and CMC, and concluded that the wet adhesion enhancement was increased by the surface amine content originating from PVAm[5]. However, it is difficult to control the physical parameters of the complex. In addition, the preparation of a polyelectrolyte complex is always accompanied by excess free polymer in solution, which is waste material for commercial applications. Instead of changing the morphology of wet strength resins, Wagberg and Eriksson

modified the surface of cellulose fibers with multiple layers of polyelectrolytes by adsorbing oppositely charged polymer alternately[42-43]. Although building multiple layers of polyelectrolyte can improve the paper strength, it is difficult to apply this technique in the papermaking industry. To simplify the preparation process and utilize materials effectively, Miao synthesized PVAm microgels and studied the interactions between them and wet cellulose[6, 44]. Microgels are three-dimensional crosslink networks with average diameters ranging from 50nm to 5μm[45]. PVAm microgels increased the wet paper strength tremendously compared with linear PVAm, due to their large bulk volume[6]. But the variation in size of PVAm microgels is large, making the effect of microgel size to wet paper strength unclear.

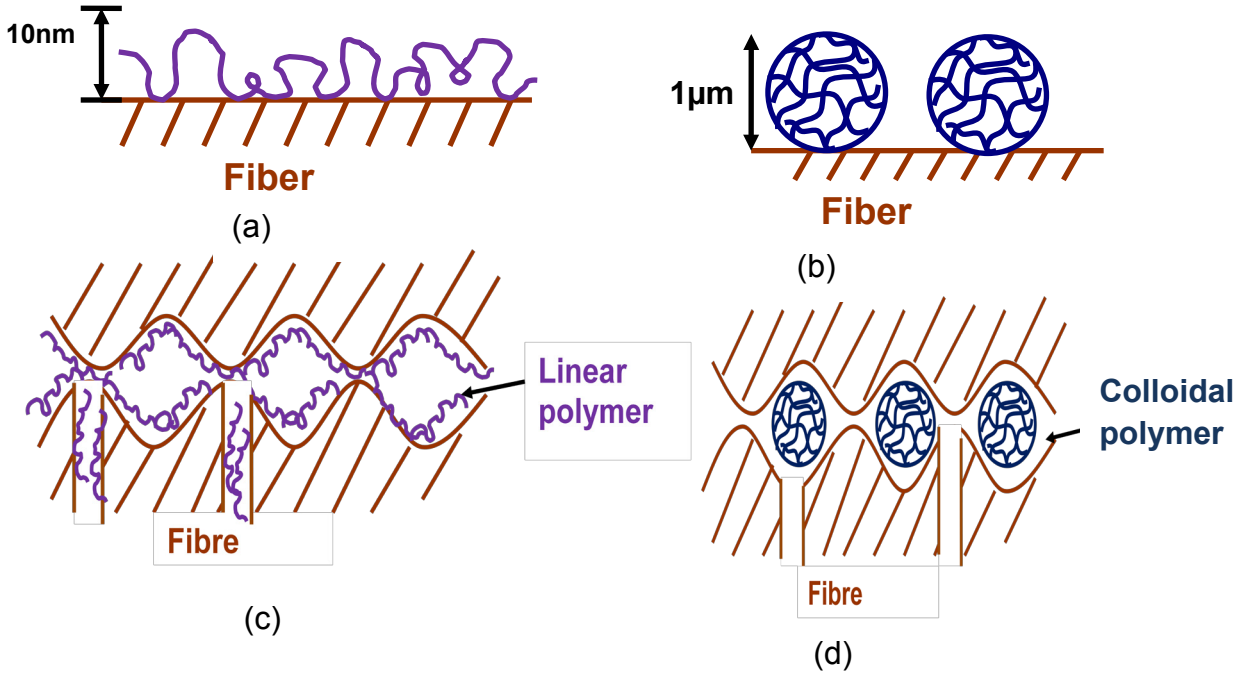

Figure 4 The impact of physical morphology of wet strength resins onto wet strength

1.1.5 Adhesion theory

An essential improvement of polymer adhesion to cellulose fibers is made by adding wet strength resins to paper pulp, to reinforce the fiber-fiber bonds. Generally, adhesion depends on the work required to separate materials. Thus, the work of adhesion is defined as the energy change due to the separation of joined surfaces:

$$W = \gamma_1 + \gamma_2 - \gamma_{12} \quad \text{.....Equation 2}$$

where γ_1 and γ_2 are the surface energies of the two bare surfaces and γ_{12} is the interfacial energy.

According to the forces acting on the surfaces, adhesion is classified as electrostatic adhesion, gravitational adhesion, liquid bridge adhesion and molecular adhesion. Electrostatic adhesion, gravitational adhesion and liquid bridge adhesion are easy to measure due to the long range adhesion forces, while molecular adhesion is hard to test since the adhesive force acts only at short range and is difficult to reproduce. Kevin Kendall has defined molecular adhesion as the force experienced when bodies make contact at the molecular level, with gaps near molecular dimensions[46]. When two polymer surfaces are close to each other within a distance of a few nanometers, adhesion is created by intermolecular interactions such as van der Waals interactions, hydrogen bonding, and covalent bonds[47-48].

1.1.6 Adhesion test

Usually, AFM (atomic force microscopy) is employed to measure molecular adhesion. As shown in Figure 5, there are three main components of AFM: a cantilever deflection sensor, a cantilever and a feedback loop. Small particles are attached to the tip of the cantilever to test interaction between surfaces. When there is an attraction between the cantilever tip and the sample, the cantilever is bent, which is detected by a laser. Since the cantilever is attached to piezoelectric material linked to a feedback loop, the bending of the cantilever results in a voltage change in the feedback loop. By controlling the voltage of the feedback loop, the distance between the cantilever tip and sample is kept constant, preventing sample from scratching the cantilever tip.

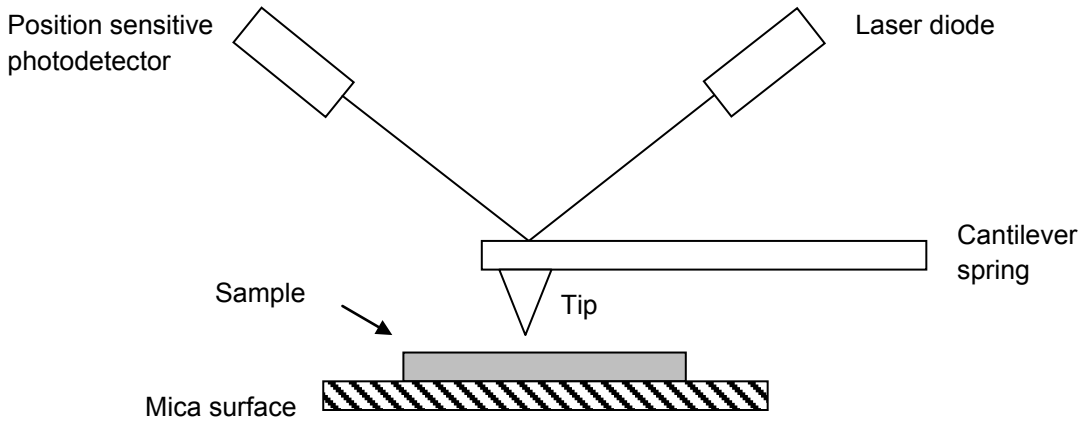

Figure 5 Major components of AFM(adapted from Takano et.al.[49])

Interactions between surfaces in polymer solutions have been extensively studied by AFM aided by a colloidal probe[50-57]. Due to the importance of polymer adhesion to cellulose fibers in the papermaking industry, AFM has also been used to study the interactions between polymer and cellulose. Amelina has measured the interactions between cellulose fibers in the present of polyethyleneimine[58]. Salmi et.al. studied the interactions between a polyelectrolyte complex and cellulose by gluing the colloidal

cellulose spheres to a cantilever and mica surfaces in polymer solutions[59]. Zauscher et al. studied the interactions between cellulose films and colloidal cellulose beads [60].

Although AFM gives precise measurements, it uses sensitive equipment and requires smooth surfaces. Hence, the system tested in AFM is quite different from system actually used in papermaking. To establish a simplified paper system and still keep the structural characteristics of paper, a 90° peeling test has been developed for measurements of polymer adhesion to cellulose[31, 61]. The experimental setup is illustrated in Figure 6. The cellulose laminates used in measurements consist of two cellulose membranes with different dimensions. The desired amount of polymer solution is added between the cellulose membranes. Teflon tape is placed on one end of the laminates for future separation. Before the test, the cellulose laminates are fixed on an aluminum wheel by double sided tape, and the top membrane is clipped by the screw grips. The desired force is obtained by applying a certain peel rate to the system and recorded along the length of the cellulose membranes. Usually, the delamination force is normalized by dividing by the width of the cellulose membranes. This cellulose adhesion measurement is accepted as a macroscopic model of fiber-fiber bonding.

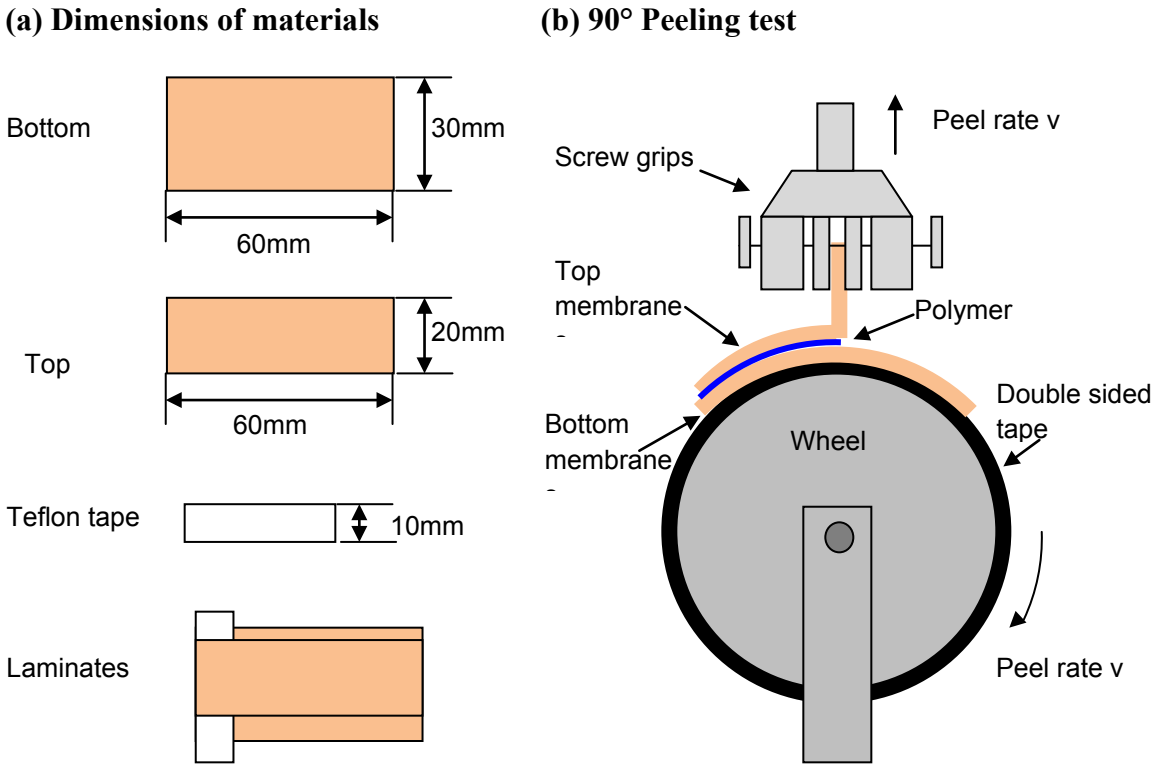

Figure 6 Scheme of cellulose peel test

Fig. 7 shows the typical curve obtained from peel test of cellulose laminates. In order to summarize the data, the force along the length of the wheel is averaged between 20mm and 60mm. The error reported on the figures in this thesis will represent not the error

along each trace but that of repeat tests at identical conditions (i.e. represents the variability between samples not within them). This cellulose adhesion measurement is accepted as a macroscopic model of fiber-fiber bonding.

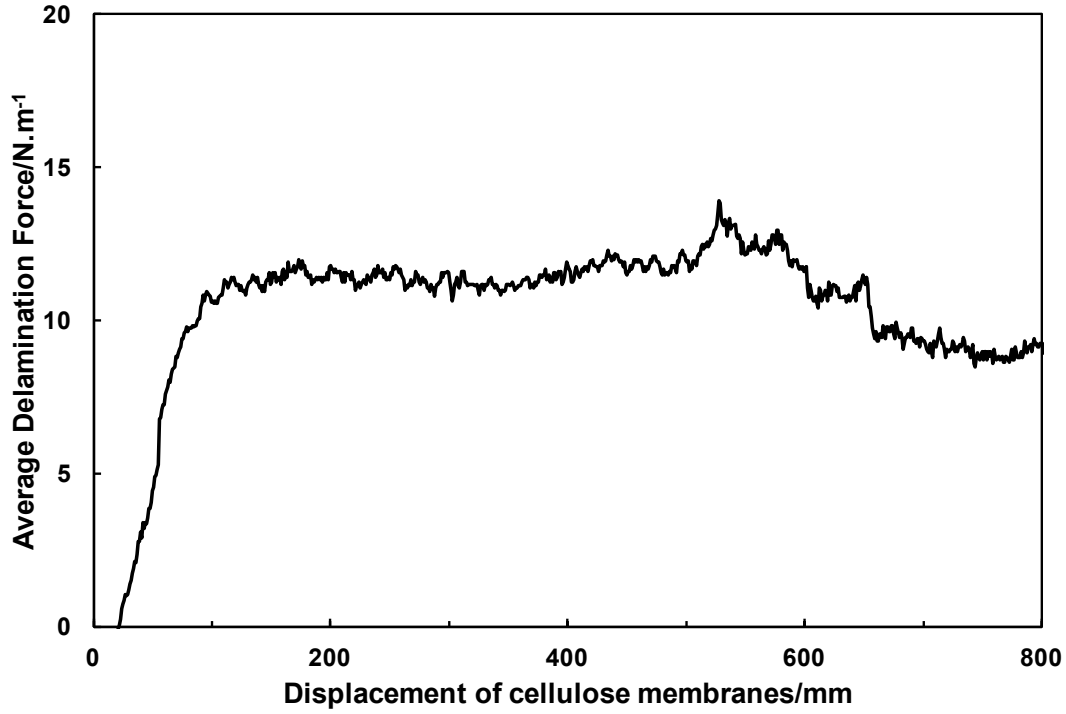

Figure 7 Typical curve generated from peel test

1.1.7 Peel mechanics

Peel tests are commonly used to evaluate the failure of adhesively bonded laminates, and require the laminates to be flexible. The laminates are peeled apart at a fixed angle at a constant rate, as illustrated in Figure 8. For a general peel test, the peel energy is defined by the peel geometry[62]:

$$G = \frac{F}{b}(1 - \cos\theta) \qquad \text{Equation 3}$$

where G is the total peel work, F is the force required to separate the laminates, b is the width of the lamianates and ϴ is the peel angle. Therefore, F is normalized by the width of the samples, and *G* is used as the delamination force in peel tests. The peel angle was chosen to be 90° in this project. Under these conditions, the delamination force was derived as

$G = F / b$ .....Equation 4

Since G represents the total energy dissipated during the peeling process, and fractures occurs accompanied by the creation of new surfaces, the work of adhesion (a thermodynamic therm) is included in G. In terms of materials properties and experimental parameters, G may also includes energy losses caused by plastic deformation of adhesives near the fracture surfaces, viscoelastic deformation of adhesives as the peel zone moves forward , and bending of the freed strip.[63]Usually, the contribution of the thermodynamic work is orders of magnitude smaller than other terms, and so, the peel energy is mostly determined by the dissipation of adhesive bonds.[64]

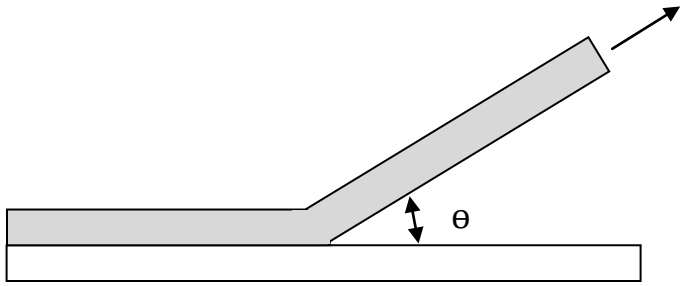

Figure 8 General peel test (adapted from Packham[2])

1.2 Objectives

The aim of this project was to develop design criteria for microgel based adhesives that can reinforce the wet strength of paper. The objectives are listed below:

To characterise the colloidal stable complexes formed by cationic PVAm and anionic microgels. Considerable attention is focused on the shape of the binding isotherm of PVAm to the microgels. From the viewpoint of industry, it is important to reduce the linear polymer residues in the solution after the formation of the complex. The mixing conditions in terms of adding sequences, and the effect of the ratio between PVAm and microgels, are studied.

To determine the role of PVAm in microgel based adhesives in terms of wet adhesion to smooth cellulose surfaces. It is hypothesized that only the surface chemistry of PVAm influences the adhesion. This study uses peel tests to measure the wet adhesion between microgels, with different distributions of PVAm, with cellulose surfaces.

To correlate the adhesive properties of microgel based adhesives to wet cellulose with physical properties of microgels. It is known that microgels work better on rough cellulose fibers as adhesives.[65] It is hypothesized that for suitable microgel sizes, the adsorption limitation of linear polymer adhesives can be overcome, so that more glue is

brought to fiber-fiber joints. Wet adhesion to cellulose is measured as a function of the crosslink density of microgels, the size of microgel particles, and roughness of the cellulose surfaces.

To develop design criteria of PVAm coated microgels in papermaking. Both linear and microgel based adhesives were introduced to pulp suspension. Tensile strength of the handsheet was correlated with the binding of polymer to fibers and the structure of the polymer adhesives. It is hypothesized that PVAm coated microgels provide wet paper strength comparable to PVAm microgels.

1.3 Thesis outline

Chapter 1: Introduction. This chapter presents the background of this project including the relevant literature, and research objectives. The thesis outline is also given.

Chapter 2: Cationic Polyvinylamine Binding to Anionic Microgels Yields Kinetically Controlled Structures. This chapter investigates the interaction between PVAm and carboxylate microgels in terms of surface charges, particle sizes and binding isotherm. The possibility of PVAm penetration into microgels is predicted by a model developed in this work. Further, the isoelectric point of microgels is estimated from a model based on the dissociation behaviour of PVAm and carboxylate microgels. This chapter has been published by Journal of Colloid and Interface Science.

Chapter3: Influence of microgel surface chemistry on wet adhesion. This chapter studies the factors affecting the adhesion of microgels to wet cellulose including binding between microgels and PVAm, the location of functional groups in microgels, the amine content of microgels, the molecular weight of PVAm, and the thickness of adhesive layers. A model predicting the influence of polymer dosage on wet adhesion to cellulose is developed and agrees well with the experimental results for both linear polymer and microgels. This chapter has been submitted to Langmuir.

Chapter 4: Influence of microgels physics on wet adhesion. This chapter presents physical factors affecting the wet adhesion between microgels and cellulose. These factors include the softness of microgels, the size of microgels and the roughness of cellulose films. We propose an explanation of the importance of microgels in wet strength improvement. This chapter is in preparation for publication.

Chapter 5: Influence of microgel based adhesives on wet paper strength. This chapter describes the influence of the morphology of polymer on wet paper strength. Linear polymers with different molecular weights, and microgels, are introduced to the handsheets by adsorption to pulp fibers. Binding isotherms of polymers to cellulose fibers are studied by titrating the solution removed from the pulp solution. The wet tensile strength of the handsheets is measured as a function of dosage of polymer, molecular weight of linear polymer, amine content of the microgels and the softness of the microgels. This chapter is in preparation for publication.

Chapter 6: Concluding remarks. This chapter summarise the major contributions of this study.

1.4 References

1. Smook, G. A., *Handbook for pulp & paper technologists* 2nd ed. ed.; Angus Wilde Publications: Vancouver, 1992.

2. Packham, D. E., *Handbook of adhesion*. 2nd ed. ed.; Hoboken, N.J.: John Wiley, 2005.

3. Espy, H. H., The mechanism of wet-strength development in paper: a review. *Tappi* **1995,** *78* (4), 90.

4. Gärdlund, L.; Wågberg, L.; Gernandt, R., Polyelectrolyte complexes for surface modification of wood fibres: II. Influence of complexes on wet and dry strength of paper. *Colloids and Surfaces A: Physicochemical and Engineering Aspects* **2003,** *218* (1-3), 137-149.

5. Feng, X.; Pouw, K.; Leung, V.; Pelton, R., Adhesion of Colloidal Polyelectrolyte Complexes to Wet Cellulose. *Biomacromolecules* **2007,** *8* (7), 2161.

6. Miao, C. W.; Pelton, R.; Chen, X. N.; Leduc, M., Microgels versus linear polymers for paper wet strength - size does matter. *Appita Journal* **2007,** *60* (6), 465-468.

7. Gernandt, R.; Wågberg, L.; Gärdlund, L.; Dautzenberg, H., Polyelectrolyte complexes for surface modification of wood fibres: I. Preparation and characterisation of complexes for dry and wet strength improvement of paper. *Colloids and Surfaces A: Physicochemical and Engineering Aspects* **2003,** *213* (1), 15-25.

8. Ilvessalo-Pfäffli, M.-S., *Fiber atlas: identification of papermaking fibers*. Springer Berlin 1995

9. Booker, R.; Sell, J., The nanostructure of the cell wall of softwoods and its functions in a living tree. *European Journal of Wood and Wood Products* **1998,** *56* (1), 1-8.

10. Klemm, D.; Philipp, B.; Heinze, T.; Heinze, U.; Wagenknecht, W., General Considerations on Structure and Reactivity of Cellulose: Section 2.1–2.1.4. In *Comprehensive Cellulose Chemistry*, Wiley-VCH Verlag GmbH & Co. KGaA: 2004; pp 9-29.

11. Scott, W. E. E.; Trosset, S. E., *Properties of paper: an introduction*. Technical Association of the Pulp and Paper Industry: 1989.

12. Pelton, R., A model of the external surface of wood pulp fibers. *Nordic Pulp & Paper Reserach Journal* **1993,** *8* (1).

13. Dunchesne, I.; Daniel, G., The ultrastructure of wood fibre surfaces as shown by a variety of microscopical methods. *Nordic Pulp & Paper Reserach Journal* **1999,** *14* (2), 129-139.

14. Snell, R.; Groom, L. H.; Rials, T. G., Characterizing the Surface Roughness of Thermomechanical Pulp Fibers with Atomic Force Microscopy. *Holzforschung* **2001,** *55* (5), 511-520.

15. Topgaard, D.; Söderman, O., Changes of cellulose fiber wall structure during drying investigated using NMR self-diffusion and relaxation experiments. *Cellulose* **2002,** *9* (2), 139-147.

16. Stone, J. E.; Scallan, A. M.; Aberson, G. M. A., The wall density of native cellulose fibers. *Pulp Pap-Canada* **1966,** *67*, 263-268.

17. Retulainen, E.; Niskanen, K.; Nilsen, N., *Paper Physics*. Fapet Oy: Hilsinkin, 1998; p 324.

18. Horvath, A. E.; Lindström, T., Indirect polyelectrolyte titration of cellulosic fibers– Surface and bulk charges of cellulosic fibers. *Nordic Pulp and Paper Research Journal* **2007,** *22* (1).

19. Back, E. L., Thermal auto-crosslinking in cellulose materials *Pulp Pap-Canada* **1967,** *68* (4).

20. Mckenzie, W. A., The structure and properties of paper. XXI: The diffusion theory of adhesion applied to interfibre bonding. *Appita* **1984**, 37(4) 301-303.

21. Shallhorn, P.; Karnis, A., Tear and tensile strength of mechanical pulps. *Pulp Pap-Canada* **1979,** *5* (4), 92-99.

22. Page, D. H., A theory for the tensile strength of paper. *Tappi* **1969,** *52* (4), 674-680.

23. Bates, N. A., Polyamide-Epichlorohydrin Wet-Strength Resin; I. Retention by Pulp. *Tappi* **1969,** *52* (6), 1157.

24. Ampulski, R.; Neal, C., The effect of inorganic ions on the adsorption and ion exchange of kymene 557H by bleached northern softwood kraft pulp. *Nordic Pulp & Paper Reserach Journal* **1989,** *4* (2), 155-163.

25. Roberts, J. C., *Paper chemistry*. Blackie ;Chapman and Hall: GlasgowNew York, 1991; p xiii, 234 p.

26. Fineman, M. N., The Role of Hemicelluloses in the Mechanism of Wet Strength. *Tappi* **1952,** *35* (7), 320.

27. Devore, I. D.; Fischer, A. S., *Wet-strength mechanism of polyaminoamide-epichlorohydrin resins*. TAPPI **1993**, 76 (8).

28. Espy, H. H.; Rave, W. T., *The mechanism of wet-strength development by alkaline-curing amino polymer-epichlorohydrin resins*. TAPPI **1988**, 71.

29. Wagberg, L.; Bjoeklund, M., On the mechanism behind wet strength development in papers containing wet strength resins. *Nordic Pulp & Paper Reserach Journal* **1993,** *8* (1), 53-58.

30. Obokata, T.; Yanagisawa, M.; Isogai, A., Characterization of polyamideamine-epichlorohydrin (PAE) resin: Roles of azetidinium groups and molecular mass of PAE in wet strength development of paper prepared with PAE. *J Appl Polym Sci* **2005,** *97* (6), 2249-2255.

31. Kurosu, K.; Pelton, R., Simple lysine-containing polypeptide and polyvinylamine adhesives for wet cellulose. *J Pulp Pap Sci* **2004,** *30* (8), 228-232.

32. Pelton, R.; Hong, J., Some properties of newsprint impregnated with polyvinylamine. *Tappi J.* **2002,** *1* (10), 21.

33. Saito, T.; Isogai, A., Wet Strength Improvement of TEMPO-Oxidized Cellulose Sheets Prepared with Cationic Polymers. *Ind. Eng. Chem. Res.* **2006,** *46* (3), 773-780.

34. John-Louis, D.; Robert, B.; Robert, P.; Marc, L., The mechanism of polyvinylamine wet-strengthening. *13th Fundamental Research Symposium* **2005**.

35. Peterson, C.; Kwei, T. K., The kinetics of polymer adosprtion onto solid surfaces. *The Journal of Physical Chemistry* **1961,** *65* (8), 1330-1333.

36. Kawaguchi, M.; Takahashi, A., Polymer adsorption at solid-liquid interfaces. *Advances in Colloid and Interface Science* **1992,** *37* (3-4), 219-317.

37. Andreasson, B.; Forsström, J.; Wågberg, L., The porous structure of pulp fibres with different yields and its influence on paper strength. *Cellulose* **2003,** *10* (2), 111-123.

38. Maloney, C. T.; Li, T.-Q.; Weise, U.; Paulapuro, H., Intra- and inter-fibre pore closure in wet pressing. *Appita* **1997**, 50(4) 301-303.

39. Andreasson, B.; Forsström, J.; Wågberg, L., Determination of Fibre Pore Structure: Influence of Salt, pH and Conventional Wet Strength Resins. *Cellulose* **2005,** *12* (3), 253-265.

40. Fatehi, P.; Xiao, H., Adsorption characteristics of cationic-modified poly (vinyl alcohol) on cellulose fibers–A qualitative analysis. *Colloids and Surfaces A: Physicochemical and Engineering Aspects* **2008,** *327* (1-3), 127-133.

41. Gimåker, M.; Wågberg, L., Adsorption of polyallylamine to lignocellulosic fibres: effect of adsorption conditions on localisation of adsorbed polyelectrolyte and mechanical properties of resulting paper sheets. *Cellulose* **2009,** *16* (1), 87-101.

42. Wagberg, L.; Decher, G.; Norgren, M.; Lindstrom, T.; Ankerfors, M.; Axnas, K., The Build-Up of Polyelectrolyte Multilayers of Microfibrillated Cellulose and Cationic Polyelectrolytes. *Langmuir* **2008,** *24* (3), 784-795.

43. Eriksson, M.; Torgnysdotter, A.; Wågberg, L., Surface Modification of Wood Fibers Using the Polyelectrolyte Multilayer Technique: Effects on Fiber Joint and Paper Strength Properties. *Ind. Eng. Chem. Res.* **2006,** *45* (15), 5279-5286.

44. Miao, C.; Chen, X.; Pelton, R., Adhesion of Poly(vinylamine) Microgels to Wet Cellulose. *Ind Eng Chem Res* **2007,** *46* (20), 6486.

45. Pelton, R., Temperature-sensitive aqueous microgels. *Advances in Colloid and Interface Science* **2000,** *85* (1), 1.

46. Kendall, K., *Molecular adhesion and its applications : the sticky universe*. Kluwer Academic/Plenum Publishers: New York, 2001; p 429.

47. Pocius, A. V., *Adhesion and adhesives technology: an introduction*. Hanser Publishers: Munich; Cincinati, 2002.

48. Kinloch, A. J., *Adhesion and adhesives: science and technology*. Chapman and Hall: London and New York, 1987.

49. Takano, H.; Kenseth, J. R.; Wong, S. S.; O'Brien, J. C.; Porter, M. D., Chemical and biochemical analysis using scanning force microscopy. *Chem. Rev.* **1999,** *99* (10), 2845.

50. Braithwaite, G. J. C.; Howe, A.; Luckham, P. F., Interactions between poly(ethylene oxide) layers adsorbed to glass surfaces probed by using a modified atomic force microscope. *Langmuir* **1996,** *12* (17), 4224-4237.

51. Hartley, P. G.; Larson, I.; Scales, P. J., Electrokinetic and Direct Force Measurements between Silica and Mica Surfaces in Dilute Electrolyte Solutions. *Langmuir* **1997,** *13* (8), 2207-2214.

52. Biggs, S., Steric and Bridging Forces between Surfaces Bearing Adsorbed Polymer: An Atomic Force Microscopy Study. *Langmuir* **1995,** *11* (1), 156-162.

53. Bosio, V.; Dubreuil, F.; Bogdanovic, G.; Fery, A., Interactions between silica surfaces coated by polyelectrolyte multilayers in aqueous environment: comparison between precursor and multilayer regime. *Colloids and Surfaces A: Physicochemical and Engineering Aspects* **2004,** *243* (1-3), 147-155.

54. Liu, J.-F.; Min, G.; Ducker, W. A., AFM Study of Adsorption of Cationic Surfactants and Cationic Polyelectrolytes at the Silica−Water Interface. *Langmuir* **2001,** *17* (16), 4895-4903.

55. Pedersen, H. G.; Bergström, L., Forces Measured between Zirconia Surfaces in Poly(acrylic acid) Solutions. *Journal of the American Ceramic Society* **1999,** *82* (5), 1137-1145.

56. J. Milling, A.; Vincent, B., Depletion forces between silica surfaces in solutions of poly(acrylic acid). *Journal of the Chemical Society, Faraday Transactions* **1997,** *93* (17), 3179-3183.

57. Bremmell, K. E.; Jameson, G. J.; Biggs, S., Forces between surfaces in the presence of a cationic polyelectrolyte and an anionic surfactant. *Colloids and Surfaces A: Physicochemical and Engineering Aspects* **1999,** *155* (1), 1-10.

58. Amelina, A. E.; Shchukin, D., E.; Parfenova, M., A.; Bessonov, I., A.; Videnskii, V., I., Adhesion of the cellulose fibers in liquid media : 1. Measurement of the contact friction force. *Colloid journal of the Russian Academy of Sciences* **1998**, 60 (5) , 537-540.

59. Salmi, J.; Österberg, M.; Laine, J., The effect of cationic polyelectrolyte complexes on interactions between cellulose surfaces. *Colloids and Surfaces A: Physicochemical and Engineering Aspects* **2007,** *297* (1-3), 122-130.

60. Zauscher, S.; Klingenberg, D. J., Normal Forces between Cellulose Surfaces Measured with Colloidal Probe Microscopy. *Journal of Colloid and Interface Science* **2000,** *229* (2), 497-510.

61. McLaren, A. D., Adhesion of high polymers to cellulose. Influence of structure, polarity, and tack temperature. *Journal of Polymer Science* **1948,** *3* (5), 652-662.

62. Zhao, B.; Kwon, H. J., Adhesion of Polymers in Paper Products from the Macroscopic to Molecular Level An Overview. *J.Adhes.Sci.Technol.* **2011,** *25* (6-7), 557-579.

63. Kinloch, A. J.; Lau, C. C.; Williams, J. G., The peeling of flexible laminates. *International Journal of Fracture* **1994,** *66* (1), 45-70.

64. Satas, D., *Handbook of pressure sensitive adhesive technology*. 2nd ed. -- ed.; New York: Van Nostrand Reinhold, 1989.

65. Miao, C.; Pelton, R.; Chen, X.; Leduc, M., Microgels versus Linear Polymers for Paper Wet Strength - Size Does Matter. *Appita Journal: Journal of the Technical Association of the Australian and New Zealand Pulp and Paper Industry* **2007,** *60* (6), 465.

Chapter 2 Cationic polyvinylamine binding to anionic microgels yields kinetically controlled structures

In chapter2, the preparation and characterization of microgels were conducted by myself with the help of Andrew M. Vincelli who worked as a summer student. I plotted the experimental data and Dr. Pelton helped to analyze the data. Dr. Pelton proposed that binding of PVAm to oppositely charged microgels was kinetically controlled. I wrote the first drafts and Dr. Pelton rewrote sections for the final version.

Journal of Colloid and Interface Science xxx (2012) xxx–xxx

Contents lists available at SciVerse ScienceDirect

Journal of Colloid and Interface Science

www.elsevier.com/locate/jcis

Cationic polyvinylamine binding to anionic microgels yields kinetically controlled structures

Quan Wen, Andrew M. Vincelli, Robert Pelton *

McMaster University, Department of Chemical Engineering, Hamilton, Canada

ARTICLE INFO

Article history:
Received 18 November 2011
Accepted 11 December 2011
Available online xxxx

Keywords:
Microgels
Polyvinylamine
Polyelectrolyte complexes
QCM
Electrokinetics
Microgel adsorption
Microgel swelling
Microgel charge distribution
Microgel binding isotherms
Microgel colloidal stability

ABSTRACT

Polyvinylamine (PVAm) binding (absorption and adsorption) to carboxylated microgels gave colloidally stable, cationic microgels that can be centrifuged, washed, freeze dried, and redispersed in water with no loss in colloidal stability. Because both PVAm and the carboxylated microgels are pH sensitive, changes in microgel swelling and electrophoretic mobility in response to pH change can be positive or negative depending upon pH and the PVAm content of the microgels. For a given PVAm molecular weight, the steady-state saturated mass fraction of bound PVAm in the microgels varied by a factor of four in our experiments. We proposed that the PVAm content at saturation was controlled by the relative rates of the initial attachment of PVAm chains versus the rate of attached chain spreading on and into the microgel structure. This explanation was further supported by a series of quartz crystal microbalance measurements.

Finally, PVAm binding to two types of PNIPAM microgels shows general features recently reported for other polyelectrolyte types. Specifically: (1) for surface localized anionic charges on the microgels, the mass fraction of bound PVAm increased with PVAm molecular weight and *vice versa*; (2) in virtually all conditions, the quantity of adsorbed cationic ammonium groups was much greater than the carboxylate content of the microgel; and (3) sodium chloride additions lowered the mass fraction of bound PVAm.

1. Introduction

For many applications of polyelectrolytes, including as flocculants, dispersants, and adhesives, the charged polymers must adsorb at solid/water interfaces. Polyelectrolyte adsorption on solid surfaces has been intensively studied. One universal observation is that adsorption leads to only a monolayer of polymer attached to a surface in water [1]. Multilayer adsorption from a simple polyelectrolyte solution only occurs when ionic strength is very high or the polymer is relatively hydrophobic, in other words, when the polyelectrolyte is very near phase separation. Monolayer or sub-monolayer adsorption is ideal for applications such as flocculation [2]. On the other hand, there are applications, where it would be desirable to increase the accumulation of polymer on surfaces. For example, we are interested in developing strength-enhancing polymers for paper. In papermaking, strength-enhancing polyelectrolytes are adsorbed onto fiber surfaces in dilute aqueous solution. The fibers are then filtered and pressed together to form a paper sheet. The quantity of polyelectrolyte glue between the fiber–fiber contact surfaces is limited by monolayer adsorption. Adding more polyelectrolyte will not give stronger paper. Thus, there is a need to overcome the "adsorbed monolayer limit" for some applications.

The literature describes a number of approaches to circumventing the adsorbed monolayer limitation to give larger assemblies of polymers on surfaces. Perhaps the oldest approach is to form colloidal sized polyelectrolyte complexes by mixing oppositely charged polymers [3,4]. If the polyelectrolyte complex particles are positively charged and the surface is negative, a monolayer of typically 200–500 nm particles can form on the surface [5]. Polyelectrolyte complexes are routinely used in papermaking technology, both for flocculation and as adhesives. They tend to be formed *in situ*, under poorly controlled conditions. Even in the research laboratory, it is difficult to prepare pure, monodisperse polyelectrolyte complexes without a significant presence of excess linear polymer.

Wagberg and coworkers [6] have shown that Decher's [7] layer-by-layer adsorption methodology is a controllable and reproducible way of introducing thick, mixed polyelectrolyte layers on cellulose fiber surfaces, leading to enhanced adhesion. Although effective, layer-by-layer approaches are not practical for large scale, commodity processes because of the many adsorption and washing steps.

* Corresponding author.
E-mail address: peltonrh@mcmaster.ca (R. Pelton).

0021-9797/$ - see front matter © 2011 Elsevier Inc. All rights reserved.
doi:10.1016/j.jcis.2011.12.035

Please cite this article in press as: Q. Wen et al., J. Colloid Interface Sci. (2012), doi:10.1016/j.jcis.2011.12.035

We recently showed an alternative approach to increasing the amount of polyelectrolyte adhesive adsorbed from solution using colloidal sized microgels instead of linear polymer [8–10]. In our preliminary work, polyvinylamine (PVAm) was the adhesive of interest, and we showed that microgels can indeed lead to stronger paper simply because one can incorporate much more of the polyvinylamine into the paper compared to linear polymer. For example, an adsorbed monolayer of PVAm on cellulose gives polymer coverages in the range 0.08–1.1 mg/m^2, whereas the hexagonal close packed array of 500 nm microgels, 50% swollen with water, corresponds to a coverage of 150 mg/m^2.

Our PVAm microgels were not ideal; they are difficult to make as monodisperse spheres. In addition, PVAm is an expensive material and it is wasteful to bury most of the amine functional groups inside microgel particles, where the amine groups will have little function. In this work, we describe the preparation and characterization of a more facile form of PVAm microgel obtained by adsorbing PVAm onto and into anionic PNIPAM hydrogels. We chose PNIPAM microgels because they are extremely uniform and because their composition can be controlled. For papermaking and other commodity applications, we propose that less exotic support microgels, such as crosslinked starch, may be more appropriate.

There have been a number of reports of polyelectrolyte and protein binding to microgels. A recent paper from Johansson et al. includes a good review of the previous literature [11]. In addition, there have been many reports of surfactant and drug uptake and release from microgels; this work is not reviewed herein. The binding of polyelectrolytes to oppositely charged microgels is mainly driven by the entropic gain from the release of counterions. Much like the behavior of polyelectrolyte complexes or layer-by-layer assemblies, the binding of an oppositely charged polyelectrolyte causes microgels to shrink and to show reversal of electrokinetic charge, measured by electrophoresis. Furthermore, initial shrinkage of the microgel periphery inhibits polyelectrolyte transport into the microgel [12].

The location of charged groups in the gels is important. Charges near the microgel surface are accessible to all sizes of polyelectrolyte, whereas interior charges can only be accessed by polyelectrolytes small enough to penetrate the microgel polymer network [12].

PNIPAM microgels are colloidally stable because: (1) surface chains impart steric stabilization below the volume phase transition temperature; (2) swollen microgels have a low combined Hamaker constant; and (3) the presence of charged groups gives an electrostatic contribution to stabilization. Polyelectrolyte binding often induces microgel aggregation at pH conditions approaching the isoelectric point [11,13], suggesting that in those cases, electrostatic stabilization is the predominant stabilization mechanism after polyelectrolyte binding. However, there are exceptions, where gels are reported to be stable at the isoelectric point [14].

The importance of the detailed polyelectrolyte structure is illustrated in a series of papers by Bysell et al. employing low molecular weight polypeptides and very large microgel particles [12,15–17]. They emphasized that the overall uptake of cationic polypeptides by anionic microgels is dominated by the charge content of the microgel, whereas the peptide charge distribution influenced uptake and release dynamics.

In this work, we examined the binding of PVAm in and on two types of anionic PNIPAM microgels. Those formed by copolymerization with vinylacetic acid (PNIPAM-co-VAA) display most of the carboxyl groups on the end of surface hairs [18]. At the other extreme, microgels formed with methacrylic acid (PNIPAM-co-MAA) have a majority of carboxylate groups in the gel interior. Both the carboxylated microgels and the polyelectrolyte are pH sensitive. The degree of ionization of PVAm is approximately a linear decreasing function of pH over the whole pH range – i.e. extreme polyelectrolyte behavior [19]. Similarly, the PNIPAM-co-MAA gels ionized over a broad pH range, whereas the ionization/pH behavior of PNIPAM-co-VAA was more akin to acetic acid because the carboxyl groups are relatively isolated [18].

The goals of our work were to determine the influence of PVAm molecular weight, microgel structure, pH and order of mixing on the properties of PVAm loaded gels. In particular, we were interested in approaches to maximize the amount of bound PVAm while minimizing the concentration of unbound PVAm. The excess, unbound PVAm is easily removed in the research laboratory, however, such a cleaning step is to be avoided in many commercial applications. Finally, the following sections will reveal that the composition of microgels with bound polyelectrolyte is kinetically controlled. We believe this is a general property of microgels that has not been recognized in the current literature.

2. Experimental

2.1. Materials

N-Isopropylacrylamide (NIPAM, 97%, Sigma–Aldrich) was purified by recrystallization from a 60:40 toluene:hexane mixture. N,N-methylenebisacrylamide (MBA, 99%, Aldrich), vinylacetic acid (VAA, 97%, Aldrich), methacrylic acid (MAA, 99%, Aldrich), sodium dodecyl sulfate (SDS, 98%, Aldrich), ammonium persulfate (APS, 99%, BDH) were all used as received from their respective suppliers. Three polyvinylamine (PVAm) solutions, LUPAMIN® 1595 (10 kDa), LUPAMIN® 5095 (45 kDa), LUPAMIN® 9095 (340 kDa) were provided by BASF (Ludwigshafen, Germany). These polymers were purified via dialysis and freeze dried. The degree of hydrolysis (MW/DH) was determined by 1H NMR – see examples provided as Supplementary data. The equivalent weights, a measure of the free amine content, of stock solutions prepared from freeze dried PVAm (MW/EW) were measured by conductometric titration.

2.2. Methods

2.2.1. Microgel preparation

Microgel was prepared following Hoare's method [18]. The polymerization was conducted in a 500 mL three-necked flask with a condenser, a glass stirring rod, and a Teflon paddle. NIPAM (1.4 g), MBA (0.1 g), SDS (0.05 g), and VAA (0.1 g) or MAA (0.07 g) were dissolved in 150 mL deionized water and heated to 70 °C. After the solution was preheated for 30 min, APS (0.1 g) was dissolved in 10 mL of water and injected into the flask. Polymerization proceeded for at least 6 h with a mixing rate of 200 rpm. After cooling to room temperature, microgels were purified and cleaned by at least five cycles of centrifugation (50 min at 50,000 rpm, Beckman model Optima L-80 XP) until the supernatant conductivity was less than 5 μs/cm. The purified microgel solution was freeze dried (Millrock Tech.) and stored at 4 °C.

2.2.2. PVAm binding studies

For most of our work, the concentrated microgel dispersion was added to more dilute PVAm solutions (Method 1), whereas in a few experiments concentrated PVAm solutions were added to diluted microgel suspensions (Method 2). For Method 1, 40 mg of freeze dried microgel was dispersed in 10 ml water and PVAm was dissolved in 70 mL water. The pH values of the solutions were adjusted to 7 ± 0.1 with HCl (0.1 N) or NaOH (0.1 N). After 4 h, the microgel dispersion was added to the stirred (magnetic stirrer) PVAm solution using a micropipette at the rate of 0.5 mL/min. For Method 2, PVAm was dissolved in 10 mL water, and 40 mg of dried microgel was dispersed in 70 mL water followed by pH adjustment. After 4 h, the PVAm solution was added to the stirred

Please cite this article in press as: Q. Wen et al., J. Colloid Interface Sci. (2012), doi:10.1016/j.jcis.2011.12.035

microgel suspension by micropipette at the rate of 0.5 mL/min. For both methods, the mixtures were equilibrated for 24 h at room temperature with mixing, after which the suspension was centrifuged at 50,000 rpm. The unbound PVAm was removed by several cycles of centrifugation. The PVAm content of the combined supernatants was measured by conductometric titration.

2.2.3. Microgel characterization

Electrophoretic mobility values were measured with a ZetaPlus Analyzer (Brookhaven Instruments Corp.) operating with the phase analysis light scattering (PALS) model. Samples were redispersed in 1 mM NaCl, and the pH values were adjusted with NaOH and HCl. Results were the average of 10 runs with each run containing 15 cycles.

Particle sizing was performed by dynamic light scattering (DLS) with a scattering angle of 90° using a Melles Griot HeNe 632.8 nm laser as the light source. Correlation data were analyzed by the software 9kdlsw32, version 3.34 (Brookhaven Instruments Corp.) using the cumulants method. Samples were prepared as described before for surface charge analysis. The scattering intensity was controlled between 100 and 250 kilocounts/s. Each reported particle size was the average of three measurements.

Potentiometric and conductometric titrations were carried out simultaneously by a Burivar-I2 automatic buret (ManTech Associates). The carboxyl content of microgels and the amine content of PVAm were determined by titrating 50 mg dry samples dissolved in 50 ml 5 mM NaCl and the initial pH was lowered to 3 with 0.1 M HCl. The mixture was titrated with 0.1 M NaOH with 2 min equilibration time between injections. Conductometric titration was used to measure the normality of PVAm stock solutions and to measure the concentration of unbound PVAm in the microgel binding experiments.

2.2.4. Quartz crystal microbalance (QCM) measurements

The QCM measurements were made with a QCM-D E4 instrument (Q-sense, Gothenburg, Sweden). The QCM crystals with silicon dioxide coatings (Q-sense, QSX 303, Gothenburg, Sweden) were exposed to ultraviolet (UV)/ozone for 10 min and soaked in 2 wt% SDS solution for 30 min to remove organic contaminants. The clean sensors were rinsed with deionized water and dried with a stream of nitrogen gas. Finally, the sensors were exposed to UV/ozone again for 10 min before use.

The QCM sensors were first soaked in 0.5 g/L PVAm 340 kDa (pH = 7) for 30 min and then soaked in 1 mM NaCl (pH = 7) for 30 min to remove weakly attached PVAm. The sensors were then placed on the vacuum chuck of a spin coater (SPIN 150-NPP) and spun at 3000 rpm for 60 s. 40 μL of 4 g/L VAA–NIPAM microgels dispersion (pH = 7) was added to the center region of the sensor during spin coating. The microgel-coated sensors were soaked in 1 mM NaCl (pH = 7) for 30 min to remove unabsorbed microgels. The coated sensors were dried by N_2 gas and then placed in the QCM flow cell.

1 mM NaCl (pH = 7) was first introduced into the flow cell chamber for about 4 h until the resistance and frequency responses were stable. Then 10 mg/L or 100 mg/L PVAm 10 kDa (pH = 7) were introduced into the different flow cell chambers for about 10 min and then switched to 1 mM NaCl (pH = 7) for about 10 min. Finally, the sensor originally exposed to 10 mg/L PVAm was further exposed to 100 mg/L PVAm, followed by rinsing with electrolyte.

2.2.5. SEM measurements

SEM images of dried QCM sensors were obtained with JEOL 7000F SEM instrument.

3. Results

Two microgel types were prepared and characterized. VAA–NIPAM was a copolymer of N-isopropylacrylamide (NIPAM) and vinylacetic acid (VA). VAA–NIPAM microgels are water swollen uniform spheres with carboxyl groups mainly present at polymer chain ends on the gel surface. By contrast, the carboxyl groups in the MAA–NIPAM microgels, a copolymer of NIPAM and methacrylic acid, were concentrated in the interior of the microgel particles. The carboxyl content of VAA–NIPAM microgels, measured by conductometric titration [20], was 0.25 mmol/g, whereas the carboxyl content of MAA–NIPAM microgels at 0.4 mmol/g was nearly twice as high.

The properties of the three PVAm stock solutions are summarized in Table 1. The molecular weights were provided by BASF. PVAm is prepared by the hydrolysis of poly(N-vinylformamide) homopolymer. The degree of hydrolysis values given in Table 1 was measured in our laboratory by NMR – see examples in Supporting information. Because freeze dried PVAm contains an unknown amount of bound salt, it is necessary to measure stock solution concentrations by conductometric titration. These results are expressed as equivalent weights (mass of polymer/mole of titratable amine) in Table 1.

PVAm solutions were added to the microgels and after mixing for 12 h, the PVAm contents of the washed microgels were measured. Fig. 1 shows the PVAm content of the microgels as functions of the PVAm solution concentrations. Although these results are plotted as adsorption isotherms, we present a case in the discussion section that polymer binding is irreversible and that every point shown in Fig. 1 corresponds to microgels saturated with bound PVAm.

The top graph in Fig. 1 shows results for PVAm binding to VAA–NIPAM microgels. The PVAm content of the microgels was a slowly increasing function of PVAm solution concentrations up to about 100 mg/L, after which the microgel compositions were constant. The literature contains many examples of polymer adsorption onto solid surfaces. In most cases, the surface is saturated when the equilibrium concentration of polymer in solution is very low. For example, Widmaier and coworkers reported that the adsorption of PVAm on glass beads, and the minimum solution concentration giving a saturated adsorbed monolayer, was about 1 mg/L, two orders of magnitude less than the behaviors in Fig. 1 [21]. PVAm adsorption onto cellulose is another example, where essentially all the added polymer is adsorbed until the surface is saturated [22].

PVAm molecular weight influences the extent of PVAm binding to anionic microgels. The trends with changing molecular weight depend upon the location of the carboxyl groups in the microgels. The PVAm loading of VAA–NIPAM microgels increased with PVAm molecular weight – see top of Fig. 1. This behavior is analogs to polymer adsorption on a solid, non-porous surface. By contrast, the lowest molecular weight PVAm gave the highest loading of the MAA–NIPAM microgels whose charges are more concentrated in the center of the gel particles [23].

In view of the unusual behaviors of the binding curves shown Fig. 1, we came to suspect that the extent of binding was very sensitive to how the PVAm was mixed with the microgels. For the results in Fig. 1, concentrated (typically 4000 mg/L) microgels

Table 1
PVAm properties. The polymers were cleaned by dialysis, and the equivalent weight depends on degree of ionization during freeze drying.

Molecular weight/kDa	10	45	340
Degree of hydrolysis (%)	73	75	91
Equivalent weight/Da	100	76.9	83.3

Please cite this article in press as: Q. Wen et al., J. Colloid Interface Sci. (2012), doi:10.1016/j.jcis.2011.12.035

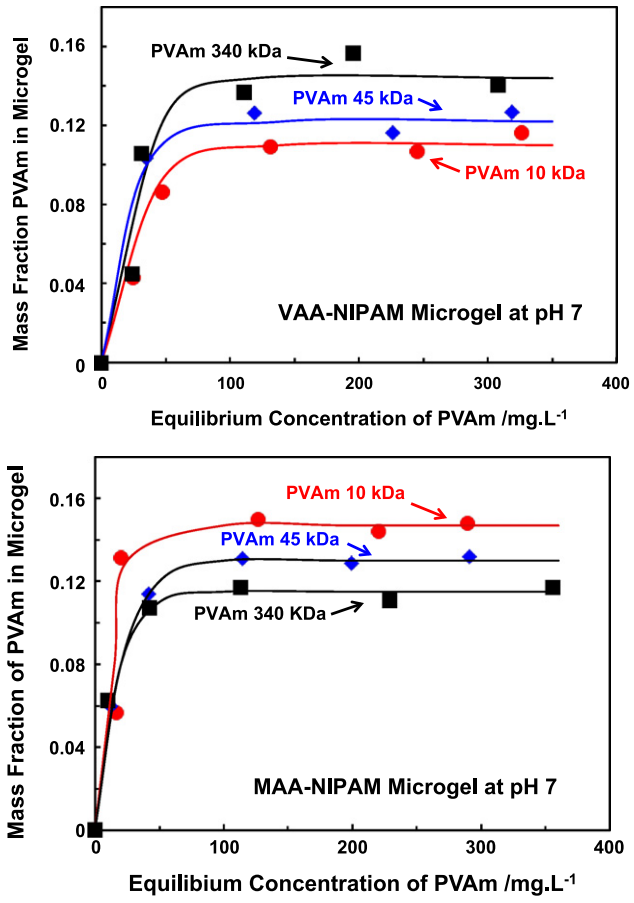

Fig. 1. Influence of PVAm molecular weight on the binding isotherms to VAA–NIPAM microgels with surface localized charges and to MAA–NIPAM microgels with core localized charges. Microgels were added to PVAm solutions.

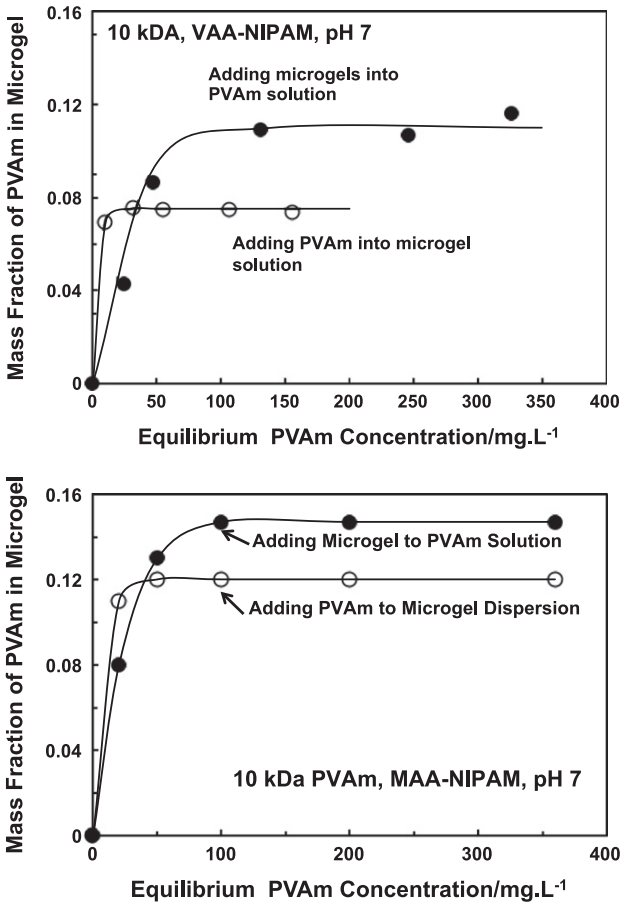

Fig. 2. Comparing isotherms obtained by slowly adding microgels to concentrated PVAm solutions to those obtained by adding PVAm to microgel suspensions. The added NaCl concentration was 1 mM.

were added to PVAm solution over about 20 min. A series of binding experiments was performed, in which about 10 mL of concentrated PVAm solution (50 to 400 mg/L) was added to 70 mL of 571 mg/L microgel dispersion. The results for the two experimental approaches are compared in Fig. 2. For both types of microgels, the maximum amount of bound PVAm and the corresponding minimum equilibrium PVAm concentration were dependent on the method of preparation – see Fig. 2. Adding PVAm to microgels gave about 20% less PVAm binding. However, the corresponding unadsorbed PVAm concentration was about an order of magnitude less than when adding microgels to PVAm. It is significant that both types of microgels displayed this behavior because with the MAA–NIPAM microgels, the PVAm molecules had to enter the microgel, whereas the PVAm would have been restricted to the surface.

The kinetically controlled extent of PVAm binding to microgels was further illustrated by quartz crystal microbalance (QCM-D) studies. A saturated layer of VAA–NIPAM was spun coated on a silica-coated crystal with an adsorbed layer of high molecular weight PVAm. Fig. 3 shows an SEM micrograph of the QCM-D surface at the end of an experiment. The surface appears saturated with dehydrated microgels in the size range 100–150 nm, while dynamic light scattering gave the diameter of the microgel particles to be around 200 nm to 250 nm.

Fig. 4 compares the frequency change for two initial PVAm solution concentrations, 10 and 100 mg/L. Like the previous adsorption experiments, the higher initial PVAm concentration gave greater adsorption as evidenced by a greater frequency change. Subsequent injections of higher PVAm concentrations did not increase the amount of PVAm binding. This is an important observation because it shows that in all cases, the surface was saturated with adsorbed PVAm after the initial exposure to PVAm solution.

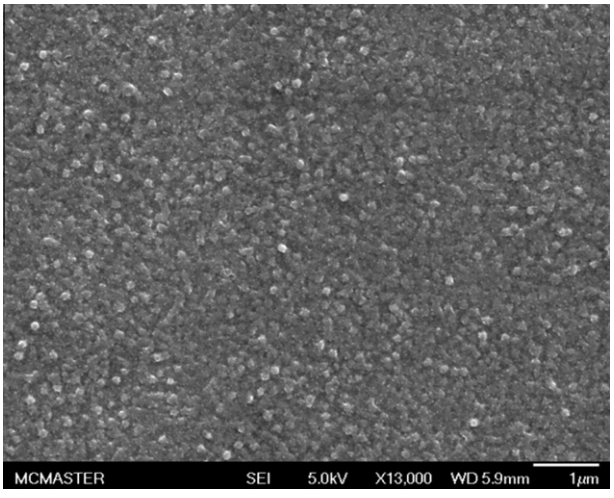

Fig. 3. SEM of a QCM-D sensor surface coated with VAA–NIPAM microgels. The particle size of the dehydrated microgels is in the range 100–150 nm, whereas in solution, the microgel diameters were 250 nm.

A major driving force for the binding of a polyelectrolyte to an oppositely charged surface or polymer is the release of

Please cite this article in press as: Q. Wen et al., J. Colloid Interface Sci. (2012), doi:10.1016/j.jcis.2011.12.035

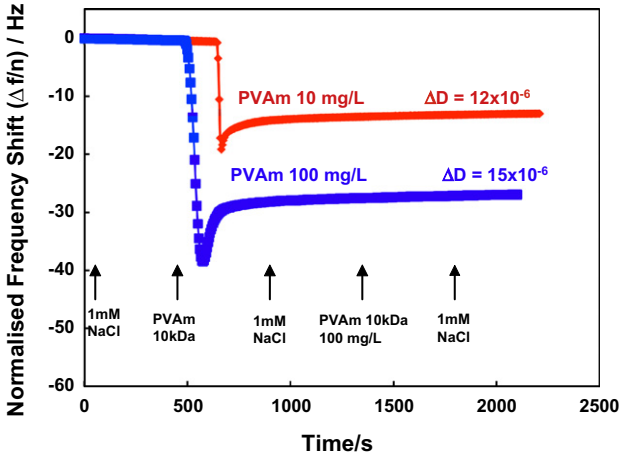

Fig. 4. Binding of 10 kDa PVAm to VAA–NIPAM microgels immobilized on a QCM-D sensor surface. The arrows indicate the time at which new solutions were introduced into the QCM-D chambers. The data sets were obtained simultaneously. The tube feeding the 10 mg/L cell was longer giving a displacement relative to the 100 mg/L on the time axis. ΔD data are the final dissipation values in each series of experiments.

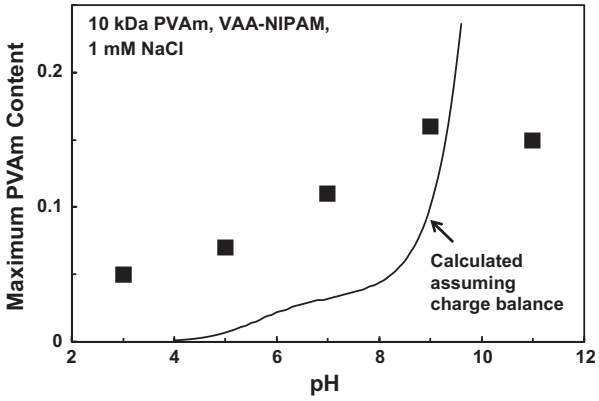

Fig. 5. The influence of pH on the maximum uptake of 10 kDa PVAm by VAA–NPAM microgels in 1 mM NaCl. Microgels were added to PVAm solutions.

counterions, giving a net entropy gain. As explained in the introduction, the degree of ionization, and thus the charge contents of both PVAm and the microgels, was strong functions of pH. Thus, we would expect the capacity of the microgels to adsorb PVAm to be a strong function of pH. Fig. 5 shows the maximum PVAm 10 K Da content of VAA–NIPAM microgels as a function of mixing pH. The points show that the experimentally determined mass fraction of PVAm increased with pH. The solid line in Fig. 5 shows the theoretical mass fraction of PVAm required to balance the ionized carboxyl groups in the microgel. This calculation was based on the assumptions that (1) the degree of ionization of microgel and PVAm did not change with complex formation; (2) the degree of PVAm ionization is given by Feng's extension of Katchalsky's model (see Eqs. (1), (2) below) [5]; and (3) the ionization behavior of the VAA–NIPAM microgels is given by Hoare's implementation of the Henderson–Hasselbalch equation – see Eq. (4)

$$pH_{pvam} = pK_{pvam} + \log\left[\frac{\alpha}{1-\alpha}\frac{(1-2\alpha+X^2)}{(\alpha-X)}\right] \quad (1)$$

$$pK_{pvam} = 8.4 + \frac{3.5I}{0.8+2I} \quad (2)$$

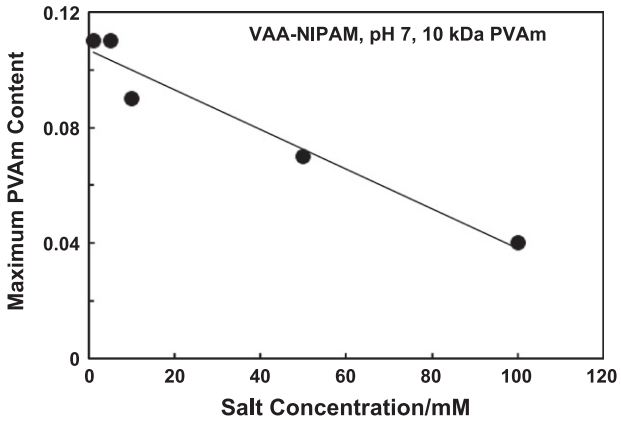

Fig. 6. The influence of NaCl concentration on the maximum uptake of 10 kDa PVAm by VAA–NIPAM microgels. The pH was 7 and microgels were added to PVAm solutions.

$$X = \frac{A(2\alpha-1) - 2\alpha + \sqrt{A^2(2\alpha-1)^2 + 4A\alpha(1-\alpha)}}{2(A-1)} \quad (3)$$

where α is the degree of ionization, A(=47) is the nearest-neighbor interaction parameter, and I(=1 mM) is the ionic strength

$$pH_{VAA}(\alpha) = 5.43 + \frac{1.16\log\alpha}{1-\alpha} \quad (4)$$

Fig. 5 shows that over most of the pH range, the PVAm content of the microgels was far in excess of that required to balance the microgel charges. Microelectrophoresis results, presented below, confirm that the treated microgels are positively charged over most of the pH range. Overcharging is a general feature of polyelectrolyte complexes and when polymers adsorb onto oppositely charge surfaces [14,24].

Fig. 6 shows the effect of ionic strength on the uptake of PVAm 10 kDa by VAA–NIPAM microgel. NaCl addition decreases PVAm binding. Similar trends have been reported for PVAm adsorption onto porous cellulose [25] and lysozyme binding to acrylic acid-co-NIPAM microgels [11].

The properties of composite microgel particles formed by adsorbing PVAm are sensitive to pH, the mass fraction of bound PVAm and the molecular weight of bound PVAm. Fig. 7 compares the results for the two types of microgels. Both types of microgels were positively charged at low pH and negatively charged at high pH. Furthermore, for both types of microgels, the mobility at low pH increased and the isoelectric pH increased with increasing mass fractions of bound PVAm 10 kDa. The swelling versus pH behavior of the surface functionalized VAA–NIPAM microgels showed large changes with pH, with the minimum swelling corresponding to the isoelectric points. By contrast, the interior functionalized MAA–NIPAM microgels showed modest changes in swelling with pH, and the results were not very sensitive to the mass fraction of bound PVAm.

Fig. 8 summarizes the influence of PVAm molecular weight on the electrophoretic mobilities and swelling characteristics of the two types of microgels. The mass fractions of bound PVAm in these experiments were approximately constant (see numbers labeling the curves). PVAm molecular weight had a dramatic effect on the colloidal properties, and both types of microgels showed similar sensitivity to molecular weight. Both the electrophoretic mobility and the swelling behaviors at low pH increased dramatically with PVAm molecular weight.

Please cite this article in press as: Q. Wen et al., J. Colloid Interface Sci. (2012), doi:10.1016/j.jcis.2011.12.035

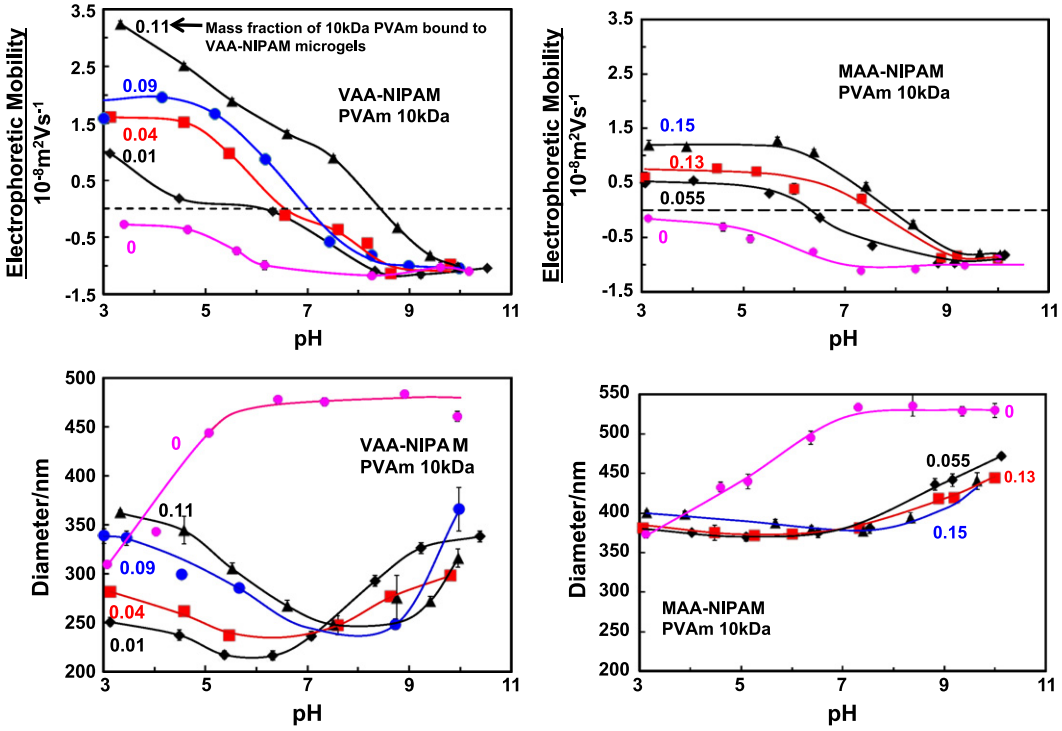

Fig. 7. The influence of the PVAm mass fraction on the pH versus diameter and electrophoretic mobility VAA–NIPAM and MAA–NIPAM microgels. The microgels were added to PVAm 10 kDa solutions at pH 7, the product was washed, and the cleaned microgels with bound PVAm were suspended in 1 mM NaCl.

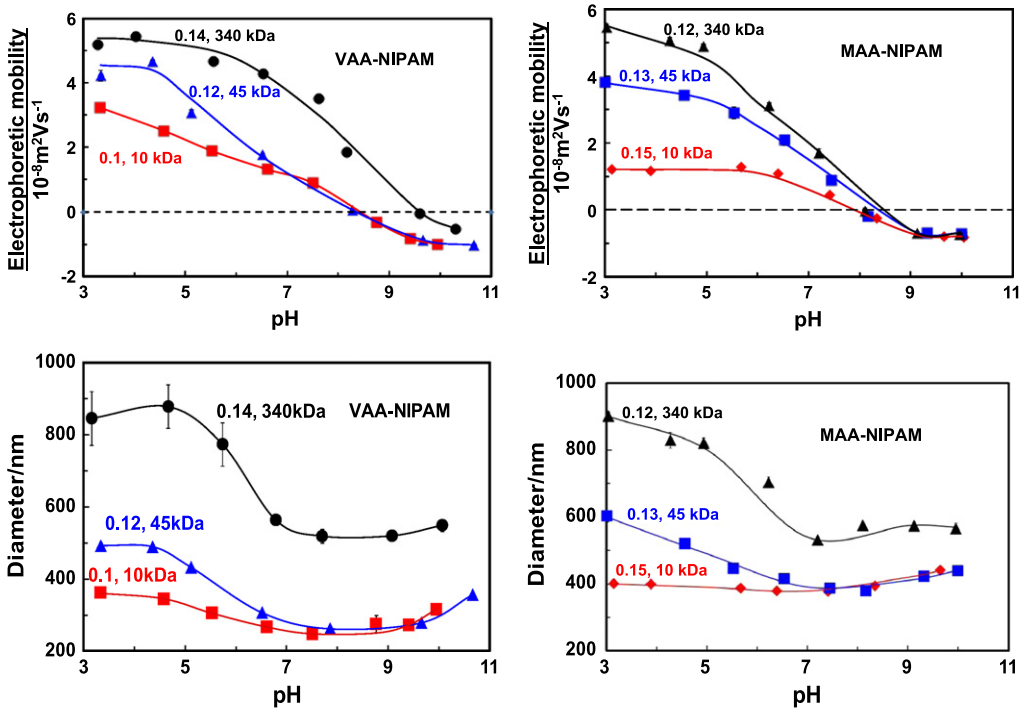

Fig. 8. The influence of PVAm molecular weight on the properties of PVAm–VAA–NIPAM and PVAm–MAA–NIPAM microgels. All measurements were made at 25 °C in 1 mM NaCl. The PVAm adsorption experiments were performed at pH 7, and the resulting microgels were washed before these experiments.

4. Discussion

The impetus for our work was to develop a commercially relevant approach to preparing colloidal sized gels with amine-rich surfaces. Simply sorbing (adsorbing and absorbing) PVAm gave colloidally stable cationic microgel that could be centrifuged, washed, and readily redispersed, even after freeze drying. Moreover, by controlling the extent of PVAm binding, it is possible to have either anionic or cationic microgels that either expand or contract with changing pH (see Figs. 7 and 8). Finally, the PVAm chains are strongly bound. We titrated the supernatant of a microgel that had been sitting for more than 4 months and less than 10% of

Please cite this article in press as: Q. Wen et al., J. Colloid Interface Sci. (2012), doi:10.1016/j.jcis.2011.12.035

PVAm had desorbed. Future publications will describe the relationships between the properties of these composite microgels and their ability to induce wet adhesion between cellulose surfaces.

In view of the existing literature summarized in the introduction, the electrokinetic and swelling properties of our microgels (see Figs. 7 and 8) displayed qualitatively predictable behaviors. For example, the maximum swelling was obtained with the highest PVAm molecular weight under conditions of maximum PVAm ionization (i.e., low pH). The microgel with surface localized charges (VAA–NIPAM) gave more dramatic effects. Richtering's work is perhaps the closest – they compared PDADMAC, a quaternary ammonium linear polymer, binding to microgels with interior or exterior charges [13]. The main difference is that the PVAm ionization is pH sensitive, whereas PDADMAC is not.

The adsorption isotherms in Fig. 1 were the most surprising aspect of our work. At first glance they look fine, displaying opposite molecular weight effects for the two types of microgels. However, closer inspection reveals that very high (50–100 mg/L) equilibrium polymer concentrations were required to reach the plateau of the binding isotherm. This observation was a challenge both technologically and scientifically. From a technological perspective, such high concentrations of unbound PVAm could interfere with microgel adsorption onto anionic surfaces. From a scientific perspective, polyelectrolyte complex formation and polyelectrolyte adsorption onto oppositely charged surfaces are usually very high affinity processes, with most of the added polymer binding before accumulating in solution. For the experiments in in Fig. 1, relatively concentrated microgel suspensions were slowly added to PVAm solutions, followed by 24 h equilibration time. When performing the experiments in the opposite way (i.e., adding concentrated PVAm to microgels), the maximum bound PVAm was a little less. However, the equilibrium PVAm concentration in solution was much lower when the binding isotherm reached a plateau value (see Fig. 2). Our QCM-D experiments (Fig. 4) confirmed that the amount of bound PVAm was a sensitive function of the initial PVAm concentration. Subsequent exposure to higher PVAm concentration solutions did not give more binding. We now propose an alternative explanation for the curves in Figs. 1, 2 and 4.

Consider, for example, the top curve in Fig. 1 (340 kDa on VAA–NIPAM microgels). The binding curve reaches a plateau value of 0.14 mass fraction of PVAm in the microgels with a corresponding PVAm solution concentration of ~100 mg/L. The conventional interpretation of such an isotherm is that the maximum coverage corresponds to saturation of the binding sites and that at half the maximum coverage, (0.07 mass fraction with ~40 mg/L PVAm in solution), half of the binding sites are unoccupied. Instead, we propose that every data point in Figs. 1 and 2 corresponds to microgels saturated with bound PVAm. That is, after 24 h equilibration in PVAm solution, there are no unoccupied binding sites. We propose that the range of PVAm-sorbed-microgel compositions in Figs. 1 and 2 reflects kinetic processes that dictate composition. The simplest, and thus most appealing explanation, is that there are two processes: (1) PVAm transport and initial binding to the microgel and (2) the reconfiguration of bound PVAm spreading across and into the microgel structure. If step 2 is much faster than step 1, the bound PVAm has time to reconfigure, occupying more binding sites and thus giving a relatively low mass of bound PVAm under saturation conditions. Alternatively, the rapid initial attachment, corresponding to high solution concentrations and low ionic strength, gives maximum PVAm binding because the binding sites are occupied before the reconfiguration is significant. The concept of competition between attachment and reconfiguration rates is not new. It has been discussed for polymer adsorption onto solids [21,22,26–33].

To summarize, we propose that the compositions of charged microgels with adsorbed polyelectrolyte are kinetically controlled. Although there has been much discussion of kinetic control in the polymer adsorption literature, we have found little mention of it in the microgel literature. Indeed, most publications do not describe the details of mixing, nor do they report the influence of mixing conditions on the extent of polyelectrolyte binding. We believe that these are kinetically frozen structures that cannot be described by thermodynamic models [11].

5. Conclusions

1. Polyvinylamine (PVAm) binding (absorption and adsorption) to carboxylated microgels gave colloidally stable, cationic microgels that can be centrifuged, washed, freeze dried, and redispersed in water with no loss in colloidal stability.
2. Because both PVAm and the carboxylated microgels are pH sensitive, changes in microgel swelling and electrophoretic mobility in response to pH change can be positive or negative depending upon pH and the PVAm content of the microgels.
3. The steady-state saturated content of bound PVAm in the microgels varied by a factor of four in our experiments and was kinetically controlled by the balance between the rate of PVAm attachment and reconfiguration rate of bound PVAm. We argue that this is a general feature of polyelectrolyte binding to microgels and that mixing conditions must be carefully controlled in these types of experiments.
4. PVAm binding to two types of PNIPAM microgels shows general features recently reported for other polyelectrolyte types. Specifically: (1) for surface localized anionic charges on the microgels, the mass fraction of bound PVAm increased with PVAm molecular weight and *vice versa*; (2) in virtually all conditions, the quantity of adsorbed cationic ammonium groups is much greater than the carboxylate content of the microgel; and (3) sodium chloride addition lowers the mass fraction of bound PVAm.

Acknowledgments

The authors thank the Natural Sciences and Engineering Research Council of Canada for funding this work through a cooperative research grant with BASF Canada. The authors acknowledge many stimulating conversations with Drs. Esser, Kroener, Mijolovic, and Stährfeldt all from BASF in Europe. The authors also thank the Canada Foundation for Innovation for support of this work. RP holds the Canada Research Chair in Interfacial Technologies.

Appendix A. Supplementary material

Supplementary data associated with this article can be found, in the online version, at doi:10.1016/j.jcis.2011.12.035.

References

[1] G.J. Fleer, M.A. Cohen Stuart, J.M.H.M. Scheutjens, T. Cosgrove, B. Vincent, Polymers at Interfaces, Chapman & Hall, London, 1993.
[2] R. Hogg, T.W. Healy, D.W. Fuerstenau, Trans. Faraday Soc. 62 (1966) 1638–1651.
[3] M.L. Heermann, S.R. Welter, M.A. Hubbe, Tappi J. 5 (2006) 9–14.
[4] X. Feng, K. Pouw, V. Leung, R. Pelton, Biomacromolecules 8 (2007) 2161–2166.
[5] X. Feng, R. Pelton, M. Leduc, S. Champ, Langmuir 23 (2007) 2970–2976.
[6] L. Gardlund, L. Wagberg, R. Gernandt, Colloids Surfaces A 218 (2003) 137–149.
[7] G. Decher, J.B. Schlenoff, Multilayer Thin Films: Sequential Assembly of Nanocomposite Materials, Wiley-VCH, Weinheim, 2002.
[8] C. Miao, X. Chen, R. Pelton, Ind. Eng. Chem. Res. 46 (2007) 6486–6493.
[9] C. Miao, M. Leduc, R. Pelton, J. Pulp. Paper Sci. 34 (2008) 69–75.
[10] C.W. Miao, R. Pelton, X.N. Chen, M. Leduc, Appita J. 60 (2007) 465–468.
[11] C. Johansson, J. Gernandt, M. Bradley, B. Vincent, P. Hansson, J. Colloid Interface Sci. 347 (2010) 241–251.
[12] H. Bysell, M. Malmsten, Langmuir 22 (2006) 5476–5484.

Please cite this article in press as: Q. Wen et al., J. Colloid Interface Sci. (2012), doi:10.1016/j.jcis.2011.12.035

[13] J. Kleinen, A. Klee, W. Richtering, Langmuir 26 (2010) 11258–11265.
[14] J. Kleinen, W. Richtering, Colloid Polym. Sci. 289 (2011) 739–749.
[15] H. Bysell, P. Hansson, M. Malmsten, J. Phys. Chem. B 114 (2010) 7207–7215.
[16] H. Bysell, M. Malmsten, Langmuir 25 (2009) 522–528.
[17] H. Bysell, A. Schmidtchen, M. Malmsten, Biomacromolecules 10 (2009) 2162–2168.
[18] T. Hoare, R. Pelton, Macromolecules 37 (2004) 2544–2550.
[19] A. Katchalsky, J. Mazur, P. Spitnik, J. Polym. Sci. 23 (1957) 513–532.
[20] T. Hoare, R. Pelton, Langmuir 20 (2004) 2123–2133.
[21] J. Widmaier, A. Shulga, E. Pefferkorn, S. Champ, H. Auweter, J. Colloid Interface Sci. 264 (2003) 277–283.
[22] A. Shulga, J. Widmaier, E. Pefferkorn, S. Champ, H. Auweter, J. Colloid Interface Sci. 258 (2003) 228–234.
[23] T. Hoare, R. Pelton, J. Colloid Interface Sci. 303 (2006) 109–116.
[24] G. Gillies, W. Lin, M. Borkovec, J. Phys. Chem. B 111 (2007) 8626–8633.
[25] C. Geffroy, M.P. Labeau, K. Wong, B. Cabane, M.A. Cohen Stuart, Colloids Surf. Physicochem. Eng. Aspects 172 (2000) 47.
[26] O. Oulanti, J. Widmaier, E. Pefferkorn, S. Champ, H. Auweter, J. Colloid Interface Sci. 291 (2005) 98–104.
[27] O. Oulanti, E. Pefferkorn, S. Champ, H. Auweter, J. Colloid Interface Sci. 291 (2005) 112–119.
[28] O. Oulanti, E. Pefferkorn, S. Champ, H. Auweter, J. Colloid Interface Sci. 291 (2005) 105–111.
[29] M.C.P. Van Eijk, M.A. Cohen Stuart, Langmuir 13 (1997) 5447–5450.
[30] H.M. Schneider, P. Frantz, S. Granick, Langmuir 12 (1996) 994–996.
[31] J.C. Dijt, M.a.C. Stuart, G.J. Fleer, Adv. Colloid Interface Sci. 50 (1994) 79–101.
[32] M. Einarson, R. Aksberg, L. Dberg, J.C. Berg, Colloids Surf. 53 (1991) 183–191.
[33] L. Wagberg, L. Odberg, Nordic Pulp. Paper Res. J. 4 (1989) 135–140.

Please cite this article in press as: Q. Wen et al., J. Colloid Interface Sci. (2012), doi:10.1016/j.jcis.2011.12.035

Appendix

1. Conductometric titration of microgels

To determine the carboxyl content of microgels, 120mg MAA-NIPAM MG and 120 mg VAA-NIPAM MG were dissolved in 50 ml 5mM NaCl solution titrated by 0.1 M NaOH. The NaOH consumed by MAA-NIPAM MG is 0.48 ml and by VAA-NIPAM MG is 0.3 ml. The amount of NaOH (mol) consumed by MG is equal to the amount of carboxyl groups of MG. So the carboxyl content of MAA-NIPAM MG was 0.4 mmol/g and VAA-NIPAM MG was 0.25mmol/g.

2. Titration of PVAm

To determine the equivalent weight of PVAm, PVAm with different MW was dissolved in 5mM NaCl and titrated by 0.1M NaOH. The figure below showed an example titration curve of PVAm 10KDa. The volume of NaOH consumed by 8 mg PVAm is 0.8 ml. Thus the amine content of PVAm 10KDa is 10mmol/g and the equivalent weight of PVAm 10KDa is 100g/mol.

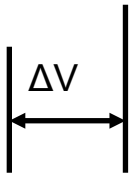

3. ^{1}H NMR of partially hydrolyzed PVAm

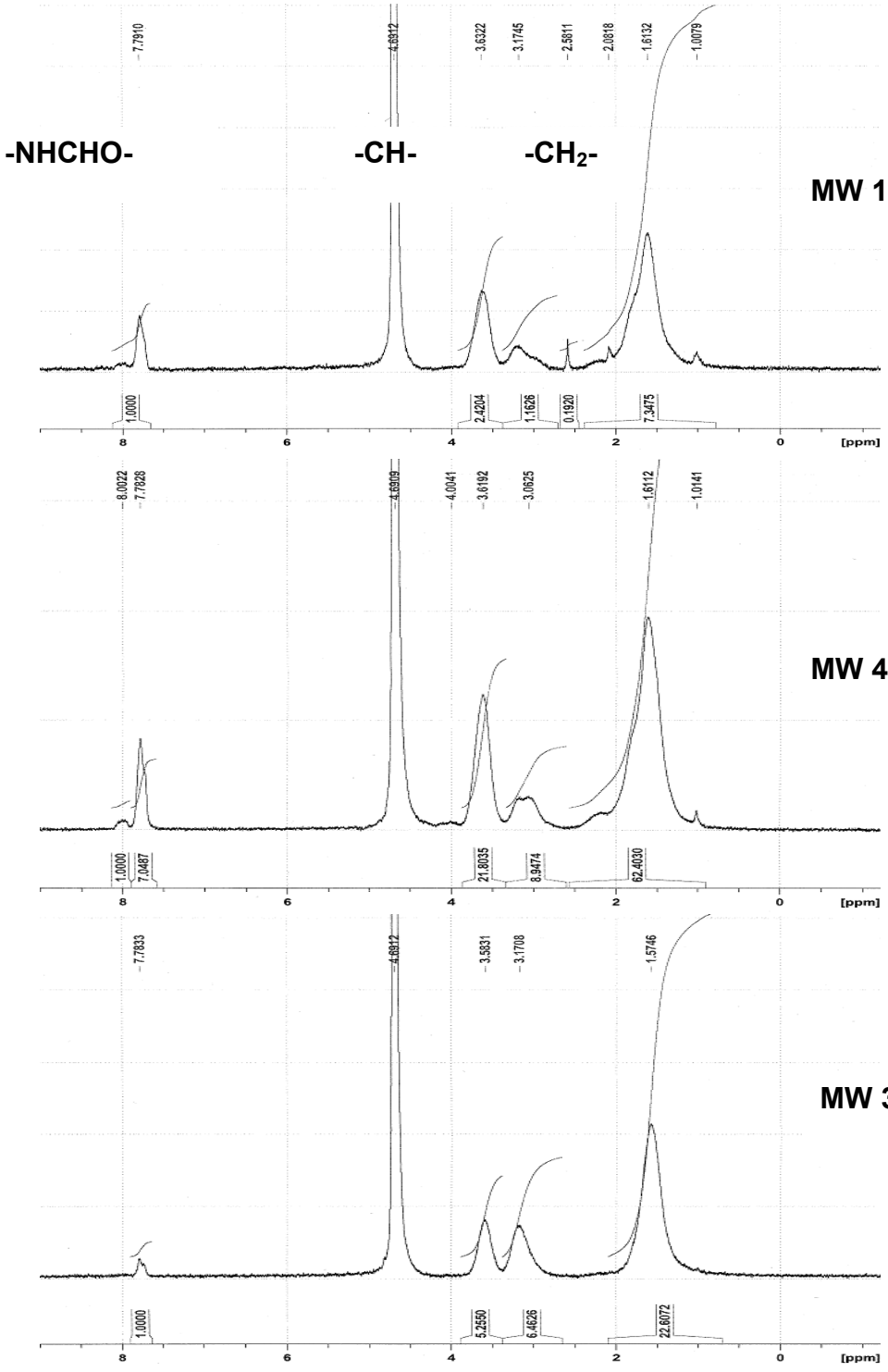

The hydrolysis degree of PVAm was determined by proton nuclear magnetic resonance spectroscopy (1H NMR) and the spectrum were shown in Fig. S1. The chemical shift of

amide group is around 8ppm and the chemical shift of CH_2 is around 1.5ppm. When the hydrolysis of PVAm was carried on, the amide groups decreased. Thus, the hydrolysis degree of PVAm is defined below:

$$HD = 1 - \frac{2 \times amide.group.peak.area}{CH_2 peak.area}$$

4. The permittivity of microgels

Objective: demonstrate equations to compare the mesh size of microgels with the gyration radius of PVAm at certain pH and thus the permittivity of microgels.

Modeling Rg of Polyvinylamine as function of MW(pH=0)

$m_o := 44\frac{gm}{mol}$ Molecular weight of a monomeric unit

$n(MW) := \frac{MW}{m_o}$ Number of monomeric unit

$L_o := 0.255nm$ Length of monomeric unit

$C_{inf} := 0.50$ Characteristic ratio(Dennis J. NaGy 1996)

$R_c(MW) := \left(C_{inf} \cdot n(MW)\right)^{0.6} \cdot L_o$ Root mean square end to end chain dimension

$r_g(MW) := \sqrt{\frac{R_c(MW)^2}{6.3}}$ Good solvent

Modeling mesh size of microgels

$n_{NIPAM} := 1.24 \cdot 10^{-2} mol$ $n_{MBA} := 6.5 \cdot 10^{-4} mol$ $n_{FM} := 3.49 \cdot 10^{-3} mol$

$x := 1$ Crosslinking coefficient

$N_x := \frac{\left[n_{NIPAM} + (1 - x) \cdot n_{MBA} + n_{FM}\right]}{x \cdot n_{MBA}}$ Average number of monomer units between crosslinking points

$N_x = 24.446$

$\xi := b_0 \cdot N_x$ ξ is the average mesh size

$b_0 := 2.55 \cdot 10^{-10} m$

thus, $\xi = 6.234 \cdot nm$

Compare the mesh size of microgels with the gyration radius of PVAm

$$\lambda(MW) := 2 \cdot \frac{r_g(MW)}{\xi}$$

Ratio of diameter of PVAm to mesh size of microgels

$$MW := 1 \frac{gm}{mol}, 10 \frac{gm}{mol} .. 1000000 \frac{gm}{mol}$$

$$MW_e := \begin{pmatrix} 10^4 \\ 4.5 \cdot 10^4 \\ 3.4 \cdot 10^5 \end{pmatrix} \cdot \frac{gm}{mol}$$

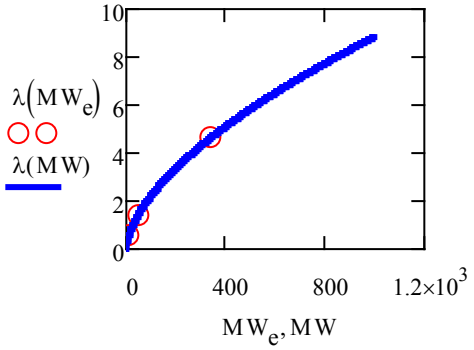

5. The charge ratio between amine to carboxyl in PVAm-abs-MGs

Objective: demonstrate equations which predict the charge ratio between primary amine groups from PVAm to carboxylic acid groups from microgels at different pH.

Modeling ionization behaviours of PVAm

$\alpha := 0.9$

Degree of ionization of PVAm

$$pK_{pvam}(I) := \left(8.4 + \frac{3.5 \cdot \frac{I}{\frac{mol}{L}}}{0.8 + 2 \cdot \frac{I}{\frac{mol}{L}}} \right)$$

The intrinsic equilibrium constant as a function of ionic strength. We derived this empirically by fitting Katchalsky's experimental data - only valid for 1:1 salt from 0 to 1 M

$A := 47$

Nearest neighbor interaction energy which is not sensitive to ionic strength

$$x(\alpha) := \frac{A \cdot (2 \cdot \alpha - 1) - 2 \cdot \alpha + \left[A^2 \cdot (2 \cdot \alpha - 1)^2 + 4 \cdot A \cdot \alpha \cdot (1 - \alpha) \right]^{0.5}}{2 \cdot (A - 1)}$$

$$pH_{pvam}(\alpha, I) := pK_{pvam}(I) + \log\left[\frac{\alpha}{1-\alpha}\cdot\frac{(1-2\cdot\alpha+x(\alpha))^2}{(\alpha-x(\alpha))^2}\right]$$

$$\alpha_{pvam}(pH, I) := \text{root}\left(pH_{pvam}(\alpha, I) - pH, \alpha\right)$$

Modeling ionization behaviours of microgels

$$pH = pKa + n\cdot\log\left(\frac{\alpha}{1-\alpha}\right)$$

Extended Henderson-Hasselbalch equation

$$pH_{maa.e} := \begin{pmatrix} 3.948 \\ 4.52 \\ 4.8775 \\ 5.378 \\ 5.95 \\ 6.4505 \\ 7.0225 \\ 7.4515 \\ 8.095 \\ 8.5955 \end{pmatrix} \qquad \alpha_{maa.e} := \begin{pmatrix} 0.032 \\ 0.0929 \\ 0.1311 \\ 0.2188 \\ 0.3708 \\ 0.5217 \\ 0.71304 \\ 0.8424 \\ 0.95923 \\ 0.99739 \end{pmatrix}$$

$$pH_{vaa.e} := \begin{pmatrix} 4.0195 \\ 4.45 \\ 4.906 \\ 5.14 \\ 5.5618 \\ 5.97 \\ 6.426 \\ 6.958 \\ 7.49 \\ 8.0026 \end{pmatrix} \qquad \alpha_{vaa.e} := \begin{pmatrix} 0.0371 \\ 0.1392 \\ 0.3031 \\ 0.4285 \\ 0.5808 \\ 0.7704 \\ 0.9135 \\ 0.9604 \\ 0.9799 \\ 0.9873 \end{pmatrix}$$

$$\text{lnfit}\left(\frac{\alpha_{maa.e}}{1-\alpha_{maa.e}}, pH_{maa.e}\right) = \begin{pmatrix} 0.541 \\ 6.099 \end{pmatrix} \qquad \text{lnfit}\left(\frac{\alpha_{vaa.e}}{1-\alpha_{vaa.e}}, pH_{vaa.e}\right) = \begin{pmatrix} 0.516 \\ 5.421 \end{pmatrix}$$

Finding slope of semilog plots:

$$\ln(10)\cdot 0.541 = 1.246$$

$$\ln(10)\cdot 0.516 = 1.188$$

Fitted slopes were used to give empirical fitting equation below:

For MAA-NIPAm microgels

$$pH_{maa}(\alpha) := 6.099 + 1.246\log\left(\frac{\alpha}{1-\alpha}\right)$$

$$\alpha_{maa}(pH) := \frac{10^{\frac{pH-6.099}{1.246}}}{10^{\frac{pH-6.099}{1.246}} + 1}$$

For VAA-NIPAM microgels

$$pH_{vaa}(\alpha) := 5.421 + 1.188 \log\left(\frac{\alpha}{1-\alpha}\right)$$

$$\alpha_{vaa}(pH) := \frac{10^{\frac{pH-5.421}{1.188}}}{10^{\frac{pH-5.421}{1.188}} + 1}$$

$pH := 4, 4.1 .. 12$

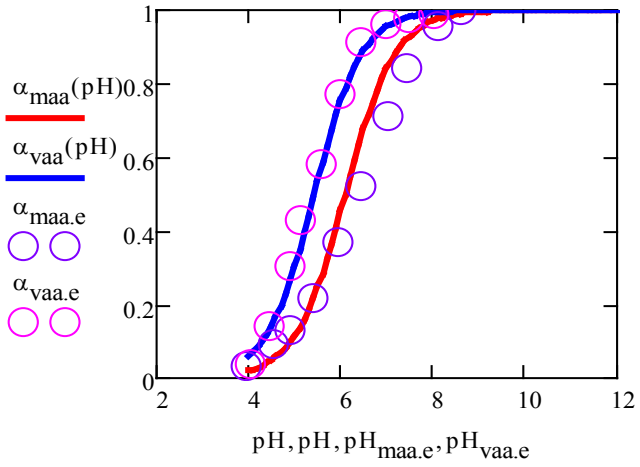

Modeling the charge ratios of amine groups to carboxyl groups

$$\Gamma = \frac{m_{pvam}}{m_{pvam} + m_{mg}}$$ mass ratio of adsorbed PVAm onto microgels

$EW_{pvam} := 1.2 \cdot 10^{-2} \frac{mol}{gm}$ $EW_{vaa} := 0.2 \cdot 10^{-3} \frac{mol}{gm}$ $EW_{maa} := 0.6 \cdot 10^{-3} \frac{mol}{gm}$ equivalent weights

$$\beta = \frac{EW_{pvam} \cdot \alpha_{pvam} \cdot m_{pvam}}{EW_{mg} \cdot \alpha_{mg} \cdot m_{mg}}$$ Defining charge ratio

$$\beta = \frac{EW_{pvam} \cdot \alpha_{pvam}}{EW_{mg} \cdot \alpha_{mg}} \cdot \frac{\Gamma}{1-\Gamma}$$

For VAA-NIPAM microgel

From experimental binding isotherms

$\Gamma_{vaa10KDa} := 0.11$ $\Gamma_{vaa45KDa} := 0.12$ $\Gamma_{vaa340KDa} := 0.14$

$$\beta_{vaa}(pH, I, \Gamma) := \frac{EW_{pvam} \cdot \alpha_{pvam}(pH, I)}{EW_{vaa} \cdot \alpha_{vaa}(pH)} \cdot \left(\frac{\Gamma}{1-\Gamma}\right)$$

$pHH := 4, 4.1 .. 10$

$\beta_{vaa}\left(pHH, 10^{-3}\frac{mol}{L}, \Gamma_{vaa10KDa}\right)$

$\beta_{vaa}\left(pHH, 10^{-3}\frac{mol}{L}, \Gamma_{vaa45KDa}\right)$

$\beta_{vaa}\left(pHH, 10^{-3}\frac{mol}{L}, \Gamma_{vaa340KDa}\right)$

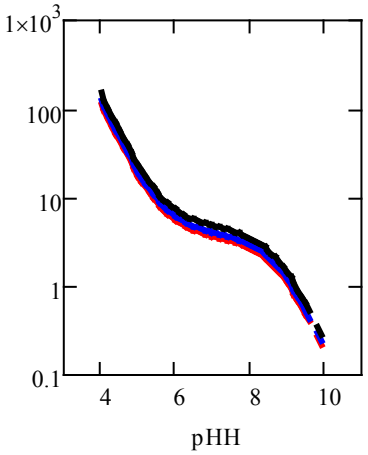

For MAA-NIPAm microgels

$\Gamma_{maa10KDa} := 0.15$ $\Gamma_{maa45KDa} := 0.13$ $\Gamma_{maa340KDa} := 0.11$

$$\beta_{maa}(pH, I, \Gamma) := \frac{EW_{pvam}\cdot\alpha_{pvam}(pH, I)}{EW_{maa}\cdot\alpha_{maa}(pH)}\left(\frac{\Gamma}{1-\Gamma}\right)$$

$\beta_{maa}\left(pHH, 10^{-3}\frac{mol}{L}, \Gamma_{maa10KDa}\right)$

$\beta_{maa}\left(pHH, 10^{-3}\frac{mol}{L}, \Gamma_{maa45KDa}\right)$

$\beta_{maa}\left(pHH, 10^{-3}\frac{mol}{L}, \Gamma_{maa340KDa}\right)$

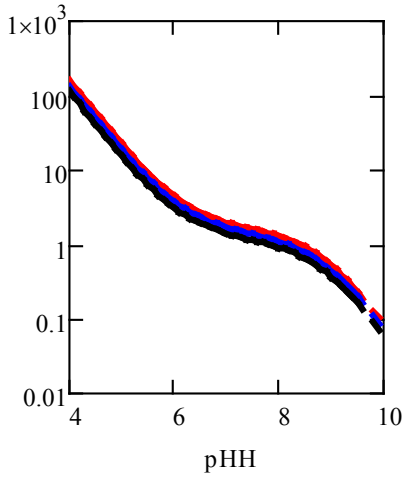

6. Modeling isoelectric point of PVAm-abs-MG

Objective: calculate the isoelectric point of PVAm-abs-MG as the function of the composition of microgels.

At the isoelectric points

$$\alpha_{pvam}\cdot EW_{pvam}\cdot m_{pvam} = \alpha_{mg}\cdot EW_{mg}\cdot m_{mg}$$

Thus, $$\frac{EW_{pvam}\cdot m_{pvam}}{EW_{mg}\cdot m_{mg}} = \frac{\alpha_{mg}}{\alpha_{pvam}}$$

$$\gamma = \frac{EW_{pvam} \cdot m_{pvam}}{EW_{pvam} \cdot m_{pvam} + EW_{mg} \cdot m_{mg}}$$

defining fractions of amine in microgels

$$\frac{EW_{pvam} \cdot m_{pvam}}{EW_{mg} \cdot m_{mg} + EW_{pvam} \cdot m_{pvam}} = \frac{\alpha_{mg}}{\alpha_{pvam} + \alpha_{mg}}$$

Thus, $\gamma = \frac{\alpha_{mg}}{\alpha_{pvam} + \alpha_{mg}}$

Since $\frac{1}{\Gamma} - 1 = \frac{m_{mg}}{m_{pvam}}$

$$\frac{1}{\gamma} - 1 = \frac{EW_{mg} \cdot m_{mg}}{EW_{pvam} \cdot m_{pvam}}$$

Emerging two equations

$$\frac{1}{\Gamma} - 1 = \frac{\alpha_{pvam} \cdot EW_{pvam}}{\alpha_{mg} \cdot EW_{mg}}$$

Thus, $\Gamma = \frac{1}{\left(\frac{\alpha_{pvam} \cdot EW_{pvam}}{\alpha_{mg} \cdot EW_{mg}}\right) + 1}$

For PVAm 10KDa adsorbed onto VAA-NIPAm microgels

$$I := 10^{-3} \frac{mol}{L}$$

$$\gamma_{e.vaa}(\Gamma) := \frac{EW_{pvam}}{\left(\frac{1}{\Gamma} - 1\right) EW_{vaa} + EW_{pvam}}$$

$$\gamma_{t.vaa}(pH) := \frac{\alpha_{vaa}(pH)}{\alpha_{vaa}(pH) + \alpha_{pvam}(pH, I)}$$

$$pH_{e.vaa} := \begin{pmatrix} 5.8 \\ 6.6 \\ 7.0 \\ 8.5 \end{pmatrix} \qquad \Gamma_{vaa} := \begin{pmatrix} 0.01 \\ 0.02 \\ 0.07 \\ 0.1 \end{pmatrix} \qquad \gamma_{e.vaa}(\Gamma_{vaa}) = \begin{pmatrix} 0.377 \\ 0.55 \\ 0.819 \\ 0.87 \end{pmatrix}$$

Experimental data

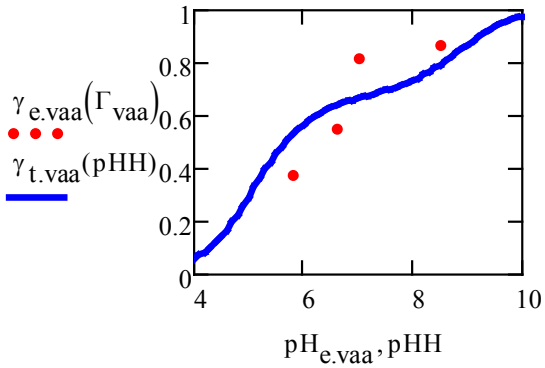

If PVAm and VAA-NIPAM MG forms complexes at the charge ratio of 1:1,

$$\Gamma_{t.vaa}(pH) := \frac{\alpha_{vaa}(pH)\cdot EW_{vaa}}{\alpha_{vaa}(pH)\cdot EW_{vaa} + \alpha_{pvam}(pH, I)\cdot EW_{pvam}}$$

$$\Gamma_{e.vaa} := \begin{pmatrix} 0.05 \\ 0.07 \\ 0.11 \\ 0.16 \\ 0.15 \end{pmatrix} \qquad pH_{e.vaa} := \begin{pmatrix} 3 \\ 5 \\ 7 \\ 9 \\ 11 \end{pmatrix}$$

Experimental data

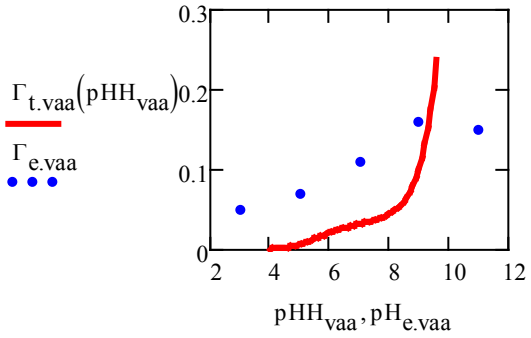

The charge ratio obtained from experimental data is larger than that from theoretical value means the PVAm content of the microgels was far in excess of that required to balance the microgel charges

For PVAm 10KDa adsorbed onto MAA-NIPAM microgles

$$\gamma_{e.maa}(\Gamma) := \frac{EW_{pvam}}{\left(\frac{1}{\Gamma} - 1\right)EW_{maa} + EW_{pvam}} \qquad \gamma_{t.maa}(pH) := \frac{\alpha_{maa}(pH)}{\alpha_{maa}(pH) + \alpha_{pvam}(pH, I)}$$

$$pH_{e.maa} := \begin{pmatrix} 6.5 \\ 7.6 \\ 8 \end{pmatrix} \qquad \Gamma_{maa} := \begin{pmatrix} 0.05 \\ 0.1 \\ 0.15 \end{pmatrix} \qquad \gamma_{e.maa}(\Gamma_{maa}) = \begin{pmatrix} 0.513 \\ 0.69 \\ 0.779 \end{pmatrix}$$

Experimental data

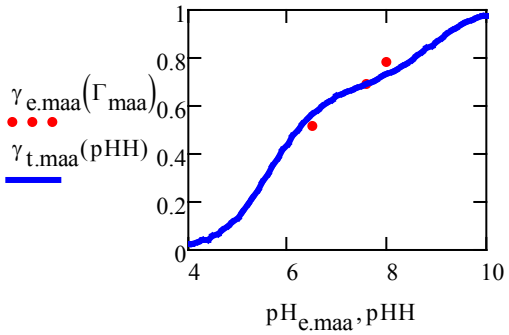

7. **Swelling behaviours of VAA-NIPAM MG and MAA-NIPAM MG after adsorbed with PVAm10kDa**

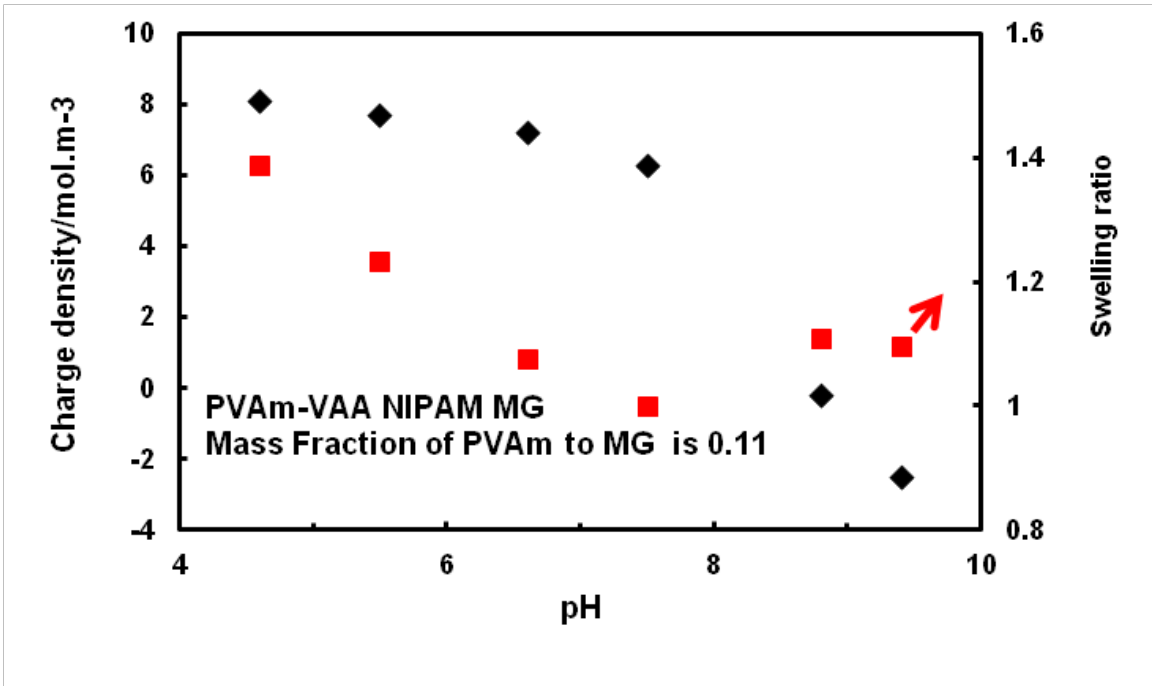

The swelling behaviour of PVAm-abs-MG is strongly influent by pH because of the charge density. For both VAA-NIPAM and MAA-NIPAM MG, PVAm binding results in particle swelling when pH is lower than 7 since the dissociation behaviour of functional groups and the positive charges provided by PVAm is higher than negative charges from MG. When pH is higher than 7, carboxyl groups is fully ionized and the quantity is larger than ionized amine groups, so the MG swells again. Thus, the swelling behaviours are actually related to the net charge density of MG.

Another factor influent the swelling behaviours is the location of functional groups. For VAA-NIPAM microgels, PVAm is adsorbed on the surface only. At low pH, PVAm stretch from loose coils to a rod like polymer which not only increases the thickness of the PVAm layer but also stretch microgels causing them to expand. However, this stretch is limited in MAA-NIPAM microgels since the functional groups spread over the microgels.

Calculation of charge density

For PVAm-VAA NIPAM MG, the maximum binding mass ratio is 0.11

$$\frac{m_{pvam}}{m_{pvam} + m_{vaa}} = 0.11 \qquad \text{Thus,} \quad \frac{m_{PVAm}}{m_{vaa}} = \frac{0.11}{0.89}$$

The number of VAA-NIPAM MG,

$$n_{vaa} = \frac{m_{vaa}}{\left(\frac{4}{3}\right)\pi\, r_{vaa.pH10}{}^{3} \cdot \rho_{mg} \cdot 0.1}$$

This number won't change after adsorption

The charge density of PVAm-VAA NIPAM MG,

$$\rho = \frac{\left(m_{pvam} \cdot \rho_{pvam} \cdot \alpha_{pvam} + m_{vaa} \cdot \rho_{vaa} \cdot \alpha_{vaa}\right)}{n_{vaa} \cdot \left(\frac{4}{3}\right)\pi \cdot r_{pvam.vaa}{}^{3}}$$

For 45mg VAA NIPAM MG,

$m_{vaa} := 0.045g$ $\qquad \rho_{vaa} := 0.25 \cdot 10^{-3} \frac{mol}{g}$

$\rho_{vaa} := 0.25 \cdot 10^{-3} \frac{mol}{g}$ $\qquad \rho_{mg} := 1000 \frac{g}{L}$

$m_{pvam} := \frac{11}{89} \cdot m_{vaa}$ $\qquad$ Thus, $m_{pvam} = 5.562 \times 10^{-3} \cdot g$

For PVAm 10KDa

$\rho_{pvam} := 0.01 \frac{mol}{g}$

Then,

$$\rho_{pvam.vaa}(pH, r_{pvam.vaa}) := \frac{m_{pvam}\cdot\rho_{pvam}\cdot\alpha_{pvam}\left(pH, 0.001\frac{mol}{L}\right) - m_{vaa}\cdot\rho_{vaa}\cdot\alpha_{vaa}(pH)}{\left[\frac{m_{vaa}}{\left(\frac{4}{3}\right)\pi\, r_{vaa.pH10}{}^{3}\rho_{mg}\cdot 0.1}\right]\cdot\left(\frac{4}{3}\right)\pi\, r_{pvam.vaa}{}^{3}}$$

From experimental data

$$pH_e := \begin{pmatrix} 4.6 \\ 5.5 \\ 6.6 \\ 7.5 \\ 8.8 \\ 9.4 \end{pmatrix} \qquad r_{pvam.vaa.e} := \begin{pmatrix} 344 \\ 306 \\ 267 \\ 248 \\ 275 \\ 272 \end{pmatrix}$$

Thus,

$$\rho_{pvam.vaa}(4.6, 344\cdot nm) = 8.075\frac{mol}{m^3} \qquad \rho_{pvam.vaa}(7.5, 248nm) = 6.258\frac{mol}{m^3}$$

$$\rho_{pvam.vaa}(5.5, 306nm) = 7.681\frac{mol}{m^3} \qquad \rho_{pvam.vaa}(8.8, 275nm) = -0.199\frac{mol}{m^3}$$

$$\rho_{pvam.vaa}(6.6, 267nm) = 7.178\frac{mol}{m^3} \qquad \rho_{pvam.vaa}(9.4, 272nm) = -2.568\frac{mol}{m^3}$$

For PVAm-MAA NIPAM MG

For 45mg MAA NIPAM MG,

$$m_{maa} := 0.045g \qquad r_{maa.pH10} := 195\cdot 10^{-9}m$$

$$\rho_{maa} := 0.4\cdot 10^{-3}\frac{mol}{g}$$

$$m_{pvam} := \frac{15}{85}\cdot m_{maa} \qquad m_{pvam} = 7.941\times 10^{-3}\cdot g$$

Then,

$$\rho_{pvam.maa}(pH, r_{pvam.maa}) := \frac{m_{pvam}\cdot\rho_{pvam}\cdot\alpha_{pvam}\left(pH, 0.001\frac{mol}{L}\right) - m_{maa}\cdot\rho_{maa}\cdot\alpha_{maa}(pH)}{\left[\frac{m_{maa}}{\left(\frac{4}{3}\right)\pi\, r_{maa.pH10}{}^{3}\rho_{mg}\cdot 0.1}\right]\cdot\left(\frac{4}{3}\right)\pi\, r_{pvam.maa}{}^{3}}$$

From experimental data

$$pH_e := \begin{pmatrix} 4.09 \\ 5.67 \\ 6.4 \\ 7.4 \\ 8.3 \\ 9.7 \end{pmatrix} \qquad r_{pvam.maa.e} := \begin{pmatrix} 398.8 \\ 387.7 \\ 379 \\ 377 \\ 393 \\ 440 \end{pmatrix}$$

Thus,

$$\rho_{pvam.maa}(4.09, 398.8nm) = 18.829 \frac{mol}{m^3} \qquad \rho_{pvam.maa}(7.5, 377nm) = 5.293 \frac{mol}{m^3}$$

$$\rho_{pvam.maa}(5.5, 387.7nm) = 13.026 \frac{mol}{m^3} \qquad \rho_{pvam.maa}(8.8, 393nm) = -0.713 \frac{mol}{m^3}$$

$$\rho_{pvam.maa}(6.6, 379nm) = 8.384 \frac{mol}{m^3} \qquad \rho_{pvam.maa}(9.4, 440nm) = -2.271 \frac{mol}{m^3}$$

Chapter 3 Microgel Adhesives for Wet Cellulose – The Role of the Polyvinylamine Coating

In chapter3, the preparation and characterization of microgels were conducted by myself. Andrew M. Vincelli who worked as a summer student helped me with some peel tests. I plotted the experimental data and Dr. Pelton helped to analyze the data. Dr. Pelton developed the spring model to simulate the peel failure of microgel adhered to wet cellulose. I wrote the first drafts and Dr. Pelton rewrote sections for the final version.

Chapter 3 Microgel Adhesives for Wet Cellulose – The Role of the Polyvinylamine Coating

Keywords: microgel, adhesion, peel mechanics, cellulose, polyvinylamine

Abstract

Nanostructured adhesive layers were prepared by adsorbing and/or grafting polyvinylamine (PVAm) onto carboxylated poly(N-isopropylacrylamide) (PNIPAM) microgels that were then assembled between layers of wet oxidized cellulose. The wet delamination force was measured as functions of PVAm content, PVAm molecular weight, coverage (mass adhesive/joint area), and the distribution of carboxyl groups in the PNIPAM microgels. The use of microgels is attractive because simple physical adsorption onto the cellulose surfaces before lamination gives much higher adhesive content and strength compared to the corresponding linear PVAm. Wet adhesion increased with PVAm content in the microgels and the quantity of microgels in the joint whereas adhesion was independent of PVAm molecular weight. Physical adsorption of the PVAm onto/into the microgels gave the same adhesion as covalently coupled PVAm. Finally, the main experimental findings were simulated by a simple model in which the microgels were treated as ideal springs.

3.1 Introduction

Moisture sensitivity is one of the major challenges inhibiting the increased use of cellulose, our most abundant renewable material. Traditional applications such as paper-based packaging or the latest composite materials containing nanocrystalline or nano-fibrillated cellulose [1] must deal with moisture sensitivity. Our research has focused on the development of new adhesive approaches for wet cellulose, a challenging substrate. Specifically we have shown that polyvinylamine (PVAm) promotes wet cellulose-cellulose adhesion if the cellulose surfaces are lightly oxidized to give a few aldehyde groups. [2] Recently, we have shown that PVAm induced wet adhesion can be improved by incorporating phenylboronic acid groups. [3, 4] Furthermore, we have shown that TEMPO mediated oxidation of cellulose can be facilitated by attaching the TEMPO catalyst to the PVAm chain giving a polymer that can oxidize and covalently couple to cellulose. [5]

In many applications, the more adhesive in the joint, the stronger is the adhesion. For example, peel force increases with adhesive thickness on pressure sensitive tapes. [6] However, with some applications controlling adhesive thickness or coverage (mass/area in joint), is difficult. For example, in papermaking strength enhancing polymers are adsorbed onto cellulose fibers before the fibers are pressed into a paper sheet. Therefore the maximum amount of adhesive in a fiber-fiber joint is the two times the polymer adsorption maximum on cellulose. For most linear, water-soluble polymers, a saturated adsorbed layer of polymer corresponds to ~ 1mg/m^2 giving a coverage in the fiber-fiber joints of ~2 mg/m^2. In other words, the maximum thickness of the dried layer of adhesive is ~2nm. We call this the limitation in adhesive coverage the "adsorption limit".

One modern approach to overcoming the adsorption limit is to coat the cellulose surfaces with a layer-by-layer assembly of alternating anionic and cationic polyelectrolytes. Wågberg's group has shown that such joints are indeed stronger compared to a single adsorbed layer. [7] A much older approach, and one inadvertently used by industry, is to form colloidal sized polyelectrolytes complexes by mixing anionic and cationic water-soluble polymers. Colloidal-sized polyelectrolyte complexes have a very much greater adsorption limit compared to the linear polymers. We studied in some detail polyelectrolyte complexes formed by mixing PVAm with carboxymethyl cellulose. Such complexes containing excess cationic PVAm adsorb onto cellulose surfaces and do promote adhesion. [8-10] However, it is difficult to control the size and properties of the colloidal product and it is particularly difficult avoid a significant quantity of excess PVAm in solution.

In an effort to enjoy the benefits of colloidal size adhesive particles without the complications of polyelectrolyte complex formation, we prepared microgels based upon polyvinylamine and compared their adhesive performance with linear polymer. [11, 12] An adsorbed monolayer of one micrometer diameter microgels puts orders of magnitude more adhesive in the fiber-fiber joint compared to linear PVAm and the results was stronger adhesion and stronger paper. Our initial work was flawed because the PVAm microgels were non-spherical and had a very broad particle size distribution, thus

inhibiting detailed modeling and analysis of the results. From a practical perspective, PVAm microgels are not ideal because the relatively expensive amine groups in the interior of the microgels may not participate in adhesion and thus were not necessary.

To circumvent our previous problems with PVAm microgels, in this work we employed very well defined, monodisperse, carboxylated poly(N-isopropylacrylamide), PNIPAM, microgels bearing a PVAm coating. The details of the microgel preparation and their loading with PVAm was recently published. [13] The goals of the work summarized herein, were to determine the influences of PVAm loading, PVAm molecular weight, and adhesive coverage on wet cellulose adhesion. In addition to experimental results, a simple model is presented in an effort understand the role of microgel properties on adhesion. Our results show that coated microgels are an elegant solution to the adsorption limit.

3.2 Experiments

PVAm: Three polyvinylamine (PVAm) solutions were provided by BASF (Ludwigshafen, Germany) with molecule weights of 10 KDa, 45KDa, 340 KDa respectively. These polymers were purified by dialysis and freeze dried. The degree of hydrolysis (MW/DH) was determined by 1H NMR (10KDa/73%, 45KDa/75%, 340KDa/91%) and the equivalent weight of freeze dried PVAm(MW/EW) was measured by conductometric titration (10KDa/100g/mol, 45KDa/113g/mol, 340KDa/112g/mol).

Microgels: Two microgels types were employed in this work: 1) VAA MG was a copolymer of vinylacetic acid and NIPAM, and; 2) MAA MG was copolymer of methacrylic acid and NIPAM. With VAA MG, most of the carboxyl groups are located near the surface on the ends of PNIPAM chains whereas the carboxyl groups are more concentrated in the center of the MAA MG.[14] Microgel properties are summarized in Table 1 and a detailed study of PVAm binding to these microgels was recently published.[13]

Preparation of PVAm-g-microgels: VAA MG (0.15 g) and PVAm (0.16 g) were redispersed in 20ml water separately. EDC (N-Ethyl-N′-(3-dimethylaminopropyl)carbodiimide hydrochloride, Aldrich), (0.07g) and Sulfo-NHS (N-hydroxysulfosuccinimide sodium salt, 98.5%, Aldrich), (0.08g) were added to microgel solution with pH adjustment to 6 for 30 min with NaOH (0.1 N). Then PVAm solution was added drop-wise and the pH was controlled at 7 for 4 h followed by several cycles of centrifugation.

Preparation of BBA-g-microgels: VAA MG (0.15g) and 1,4-bis(aminomethyl)benzene (BBA, 99%, Aldrich), (0.1g) were dissolved in 40 ml water overnight. EDC (0.12g) /Sulfo-NHS (0.13g) were added to microgel solution and pH was adjusted to 6 with HCl (0.1 N). The mixture was stirred for 4 h with pH adjustment to 6. Microgels were cleaned by several cycles of centrifugation and freeze dried for future use.

Preparation of PVAm-abs-microgels: Microgel solution and PVAm solution were adjusted to pH 7 with HCl (0.1N) and NaOH (0.1N). 5 mL microgel solution was then

added dropwise (1mL/min) into 75 mL PVAm solution with magnetic stirring. The adsorption continued for at least 24h with continuous agitation via a magnetic stir bar. Unabsorbed PVAm was removed by several cycles of centrifugation.

Microgel Characterization: The electrophoretic mobility of the microgels was measured with a ZetaPlus analyzer (Brookhaven Instruments Corp.) operating in phase analysis light scattering (PALS) model. Samples were redispersed in 1 mM NaCl and the pH values were adjusted with NaOH and HCl. Each sample was test by 10 runs (each contained 15 cycles).

Particle sizing was performance by dynamic light scattering (DLS) with a scattering angle of 90 ° using a Melles Griot HeNe 632.8 nm laser as light source. Correlation data were analyzed by the software 9kdlsw32, version 3.34 (Brookhaven Instruments Corp.) using the cumulants method. Samples were prepared as described before for surface charge analysis. The scattering intensity was controlled between 100 and 250 kilocounts/s. Each reported particle size was the average of 3 measurements.

Potentiometric and conductometric titration were carried out simultaneously by a Burivar-I2 automatic buret (ManTech Associates). The carboxyl content of microgels were determined by titrating 50 mg microgels dissolved in 50 ml 5mM NaCl while amine content of PVAm-VAA-NIPAM microgels were measured by titrating 20 ml centrifugation solution mixed with 30 ml 5mM NaCl. Data were collected using base-into-acid titration method with interval injection of 2 min to ensure complete equilibration.

Cellulose Membranes: Regenerated cellulose membranes were oxidized, laminated by with PVAm or PVAm-loaded microgels, and the delamination force of the wet laminates was determined by 90 degree peeling. Regenerated cellulose membrane (Spectra/Por®2, 12KDa MWCO, Spectrum Laboratories, Inc.) was cut into rectangular dimensions (top membrane 6 cm x 2c m, bottom membrane 6 cm x 3 cm) and boiled in deionized water for one hour to remove preservatives. In previous work we showed that the water contents of the cleaned membranes were 5% w/w at 23 °, 50% relative humidity, and the membranes swelled to approximately 50% w/w in water. The membranes had an average roughness value of 5 nm dry and 50 nm wet [15].

The cellulose membranes were oxidized with 2,2,6,6-tetramethyl-1-piperidinyoxy radical (TEMPO), sodium bromide (NaBr), and sodium hypochlorite (NaClO) following Kitaoka et al.'s method[16]. The concentration of ingredients were TEMPO 0.034 g/L, NaBr 0.34 g/L, and NaClO 2.8 wt% based on dry cellulose. The oxidation reaction was carried out at 23 °C under stirring. The pH was monitored at 10.5 by NaOH for 20 min, and the oxidation was stopped by adding ethanol. Then the cellulose membranes were removed and rinsed repeatedly with deionized water. Finally, the oxidized membranes were stored in deionized water with a small quantity of methanol at 4°C.

Laminate Preparation: A top membrane and a bottom membrane were laid onto a stainless steel disk and excess water was removed with tissue. A strip of Teflon tape (1 cm × 4 cm, G. F. Thompson Co. Ltd.) was placed along one end of the bottom membrane

to facilitate separation after lamination. 15 µL polymer solution was applied by a 20 µL micropipette (Eppendorf) onto the bottom membrane near the Teflon. Then the top membrane was progressively placed over the bottom membranes. The laminates were pressed between blotting paper on a Hot Plate (Carver, Wabash, IN) at 18.5 MPa and at room temperature for 30 min. Then the laminates were conditioned at 23 °C and 50% relative humidity overnight.

Delamination Force: The laminates were soaked in 1mM NaCl for 30 min. After removing excess water by pressing (2.4 kg hand roller) between blotting paper, the laminates were mounted onto the freely rotating aluminum wheel with a double side adhesive tape (3M Polyethylene Medical Double Coated Tape). The wheel was fixed to the bottom of an Instron 4411 universal testing system (Instron Corp., Norwood, MA) where the top membrane was peeled off at 90° at a crosshead rate of 20 mm/min. The data was recognized as peel force vs. displacement and the adhesion force was an average of steady-state peel forces. At least four replicates were carried out for each sample.

3.3 Results

The goal of this work was to determine the influences of PVAm coated, carboxylated NIPAM microgels on the adhesion between wet regenerated cellulose films. Two types of carboxylated PNIPAM microgels were employed. Those formed by copolymerization with vinylacetic acid (PNIPAM-co-VAA) that display most of the carboxyl groups on the end of surface hairs.[17] At the other extreme, microgels formed with methacrylic acid (PNIPAM-co-MAA) have a majority of carboxylate groups in the gel interior. [14] Some properties of the microgels are summarized in Table 1.

Table 1 Microgel properties. VAA MG was a copolymer of N-isopropylacrylamide (NIPAM) and vinylacetic acid (VAA) whereas MAA MG was a copolymer of methacrylic acid (MAA) and NIPAM. of the two types of microgels before PVAm binding.

	Carboxyl Content	**Diameter***	**Mass Fraction Water***	**Electrophoretic Mobility***
	mmol/g	**nm**		$10^{-8}m^2Vs^{-1}$
VAA MG	0.5	400nm	0.99	-1.5
MAA MG	0.4	450nm	0.95	-1.1

* pH 7, 1 mM NaCl, 25 °C

For most of our experiments, PVAm coated microgels were prepared by simply adsorbing PVAm onto, and into, the microgels. The resulting microgels were colloidally stable by virtue of excess ionized amine groups. The microgels were robust – they could be centrifuged and redispersed for cleaning and they easily redispersed after freeze drying.

We recently published a detailed description of the factors controlling PVAm uptake by the two types of PNIPAM microgels. [13]

Initially, we assumed that PVAm must be grafted to the microgel to give maximum adhesion – we will show that this was incorrect. NIPAM-co-VAA microgel with grafted 10 kDa PVAm was prepared by adsorbing PVAm in the presence of carbodiimide coupling agents. Figure 1 compares swelling and electrokinetic properties of PVAm grafted microgels with the corresponding microgels with adsorbed PVAm. The two types of microgels showed similar colloidal behaviors that are dominated by pH dependent ionization of polyvinylamine. Although our laboratory has had significant experience with carbodiimide mediated coupling to carboxylated microgels, [18, 19] an obvious explanation of the similarity of grafted versus adsorbed gels in Figure 1 was that the coupling chemistry failed. PNIPAM microgels have many amide groups so NMR did not provide conclusive evidence for amide formation between PVAm and carboxyls on the microgel because of the high background amide content. In order to indirectly verify our coupling chemistry under similar conditions we reacted 1,4-bis(aminomethyl)benzene with NIPAM-co-VAA microgels. The presence of aromatic substituents on the modified VAA MG was confirmed by NMR.

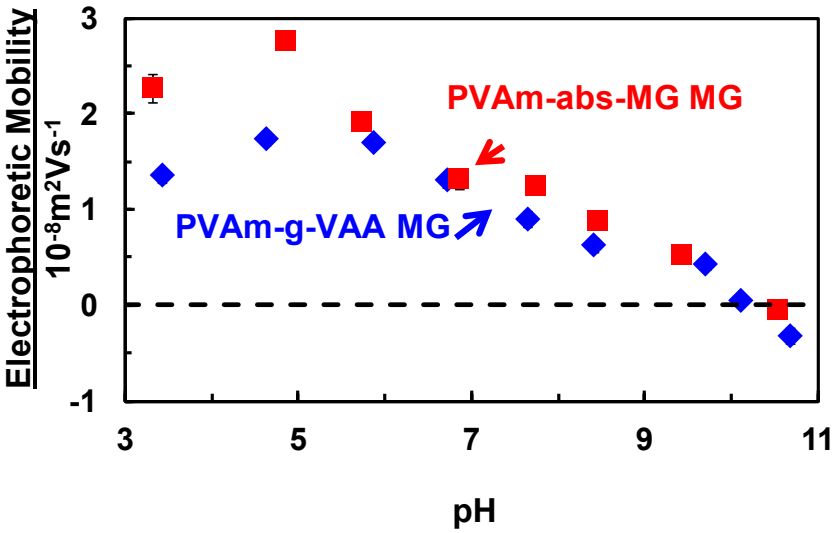

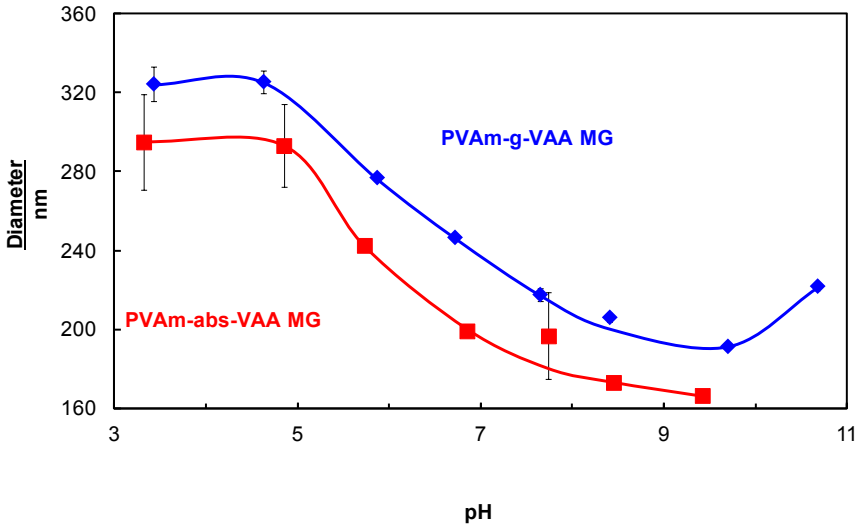

Figure 1 Comparing the pH dependent swelling and mobility of NIPAM-co-VAA microgels with adsorbed 10 kDa PVAm to the same gels with chemically grafted PVAm. The mass fraction of PVAm in the dried microgels was ~10%.

The ability of the microgels to promote adhesion between wet cellulose surfaces was measured by a wet delamination procedure developed at McMaster University. [2, 4, 20] In this test, regenerated cellulose films are slightly oxidized by TEMPO mediated oxidation and two cellulose strips are pressed together with a thin film of the microgels forming an adhesive layer between the cellulose films. The pressed laminates are dried, rewetted and the force required to separate the wet laminate was measured by a ninety-degree peel test.

The experimental section describes the many experimental parameters in this procedure including reaction times, pressing pressures, peel rates, temperatures, pH values, ionic strengths, etc. Most of these parameters were held constant. The primary variables probed in this work were the coverage of adhesive expressed as mg per square meter of cellulose-cellulose joint in the laminate and the properties of the adhesive (i.e. the type of microgel and the mass fraction of bound PVAm).

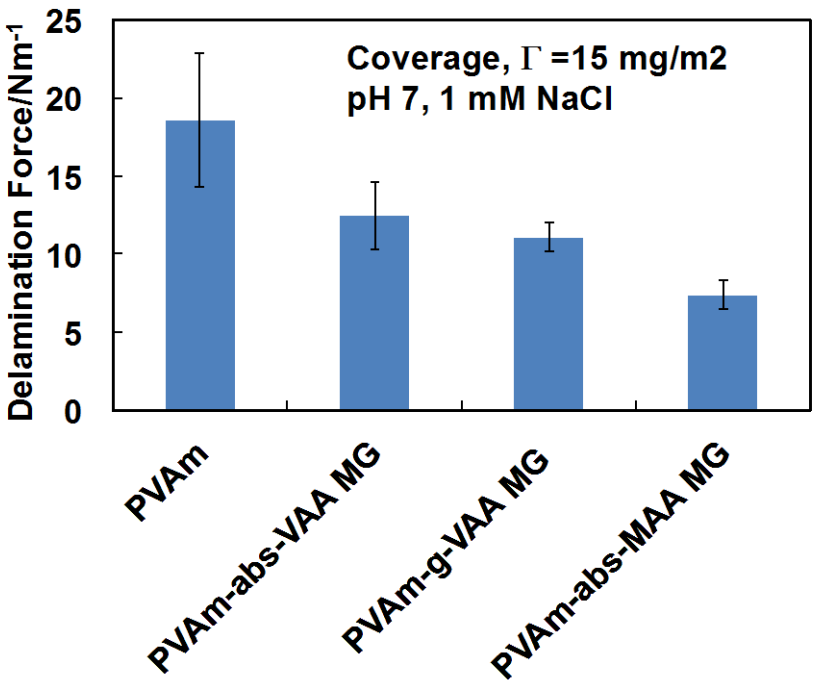

Figure 2 The influence of linear 10 kDa PVAm and three microgel types on the force required to separate wet cellulose film laminates. The coverage of each adhesive in cellulose-cellulose joints was 15 mg/m2. The MW of PVAm used to treat the microgels was 10 KDa. The error bars represent the standard deviation of the mean based on 3 measurements.

Figure 2 compares the adhesion promoting characteristics of PVAm grafted microgel (PVAm-g-VAA MG) with PVAm adsorbed on the same microgels (PVAm-abs-VAA MG). There is no significant difference between the two suggesting that there is no need for chemical grafting of PVAm onto the microgel surfaces. The other type of microgel (MAA MG) gave slightly lower adhesion possibly because some of the bound PVAm was associated with the carboxyl groups on the interior of the microgel where the cationic polymer could not contribute to adhesion.

Finally, the greatest wet adhesion in Figure 2 was obtained with PVAm alone, no microgels. Why are we working with microgels if linear polymer alone is more effective? The laminates prepared for the results in in Figure 2 were prepared by directly adding polymer solution to the cellulose films before lamination giving in this case a high adhesive coverage of 15 mg/m2. However, as explained in the introduction, the maximum amount of polymer adhesive that can be applied when using adsorption from solution for linear PVAm is two times the adsorption maximum on the fiber surfaces, typically 2 mg/m^2. [21] The role of coverage (i.e. the quantity of polymer per area in the adhesive joint) is further illustrated as follows

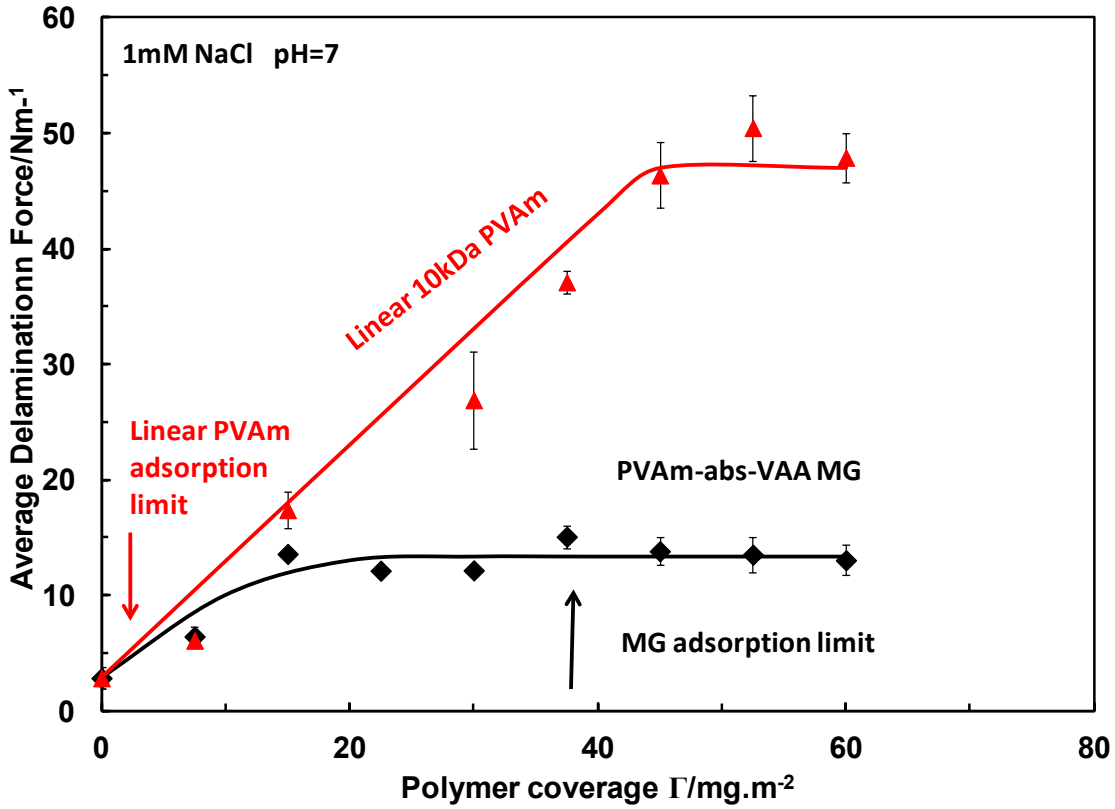

Figure 3 The influence of adhesive coverage (adhesive mass/joint area) on the delamination force. The arrows indicate estimates of the maximum coverage of linear PVAm or microgels when adsorption is used to apply the polymers. The PVAm 10 kDa content of the VAA MG was **10 w%** .

Figure 3 shows wet adhesion versus coverage of PVAm-abs-VAA MG and 10 kDa linear PVAm. Adhesion increased with coverage of both linear PVAm and the coated microgels. In these experiments we directly applied the adhesive layers to vary the coverage. The estimated maximum attainable coverage (saturation) obtainable by adsorption for microgels and linear polymer are also indicated on the graph. For the

linear PVAm the estimate, Γ_{sat} = 2 mg/m^2, is based on adsorption measurements in the literature. [21]

For the microgels we estimated the maximum coverage by the following expression that is based upon the packing of uniform spheres on a surface where D is swollen diameter, ρ is the density of polymer in the swollen microgel, and λ_m is the maximum packing fraction.

$$\Gamma_{sat} = 2\left(\frac{2}{3} D\rho\lambda_m\right) = 38\frac{mg}{m^2} \qquad 1$$

For our work, ρ was 175 kg/m^3, D was 200 nm, and we used λ_m =0.82, the value for random packing of uniform, non-overlapping circles. [22] These estimates, shown as arrows in Figure 3, reveal that using microgels brings approximately 20 times more polymer (dry mass) to the adhesive joint compared to using linear PVAm. The coverage values in Figure 3 (i.e. the X axis) correspond to the total mass of adhesive in the cellulose-adhesive-cellulose joints. However, the microgel-based adhesive only contained about 10 % PVAm. The role of PVAm content in the microgels is further illustrated in Figure 4 that shows delamination force as a function of PVAm content in the microgels. Note the total adhesive coverage was constant in this series. The delamination force increased with PVAm content. The important practical aspects of this results are: 1) low loadings of relatively expensive PVAm are quite effective; and, 2) the slope of the curve is not too great suggesting a range of microgel compositions could be tolerated in an application.

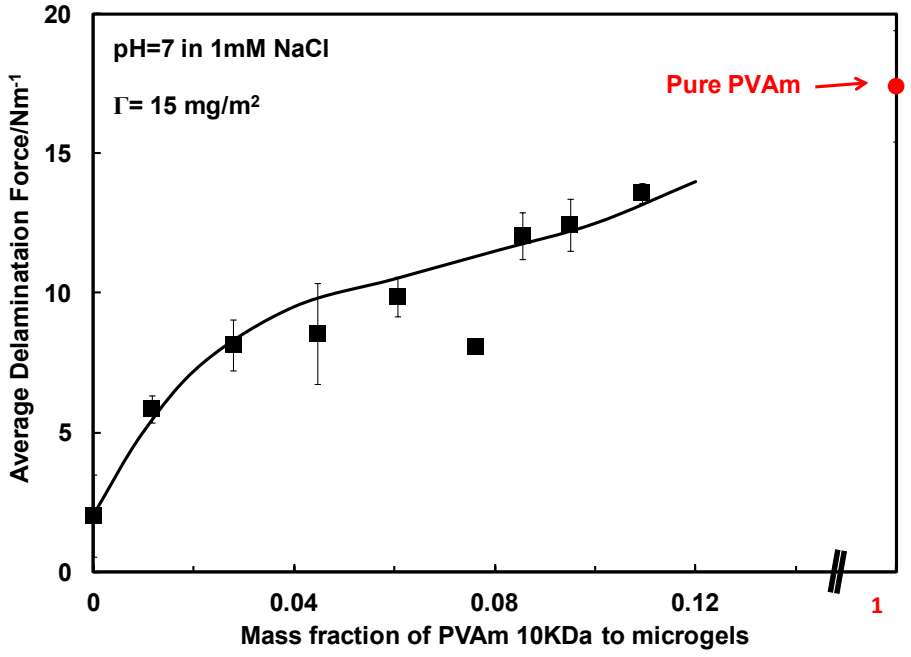

Figure 4 Influence of PVAm content in PVAm-abs-VAA MG on wet adhesion.

Another important practical aspect is PVAm molecular weight because in many cases lower molecular weight polymers are more convenient to handle. Three molecular weight PVAm samples were compared and the results are summarized in Table 2. The adhesion was approximately independent of PVAm molecular weight over the range 10 to 340 kDa. The higher adhesion was from the highest molecular with PVAm, however, this microgel also had a slightly higher PVAm content. PVAm molecular weight does not appear to be a critical variable.

Table 2 The influence of PVAm molecular weight on adhesion of PVAm-ab-VAA MG. The polymer coverage was 15 mg/m2, the pH was 7 and the NaCl concentration was 1 mM in the delamination experiments.

Mw of PVAm adsorbed KDa	PVAm Mass Fraction	Average Delamination Force Nm^{-1}
10KDa	0.11	12.4±1.4
45KDa	0.12	13.0±1.1
340KDa	0.14	16.7±1.7

From the growing body of wet adhesion measurement with PVAm, the content of primary amines is an important parameter. With linear PVAm, the amine content is determined by the degree of hydrolysis of the linear poly(N-vinylformamide). [23] Years ago we showed that wet adhesion increased with the amine content (i.e. the degree of hydrolysis). [2] In the present work,

Figure 3 shows that we can vary amine content in the microgel, which in turn varies the amine content in the adhesive joint. Figure 5 compares our old data where we varied the degree of hydrolysis of linear PVAm with our current data where we varied the PVAm content of the microgel. To facilitate this comparison, the X-axis gives coverage of primary amine groups per area of adhesive joint for the two systems. The poly(N-vinylformamide-co-vinylamine) linear copolymers and the VAA MG with adsorbed PVAm gave similar trends, however, the microgels gave slightly higher adhesion compared at the same effective amine contents.

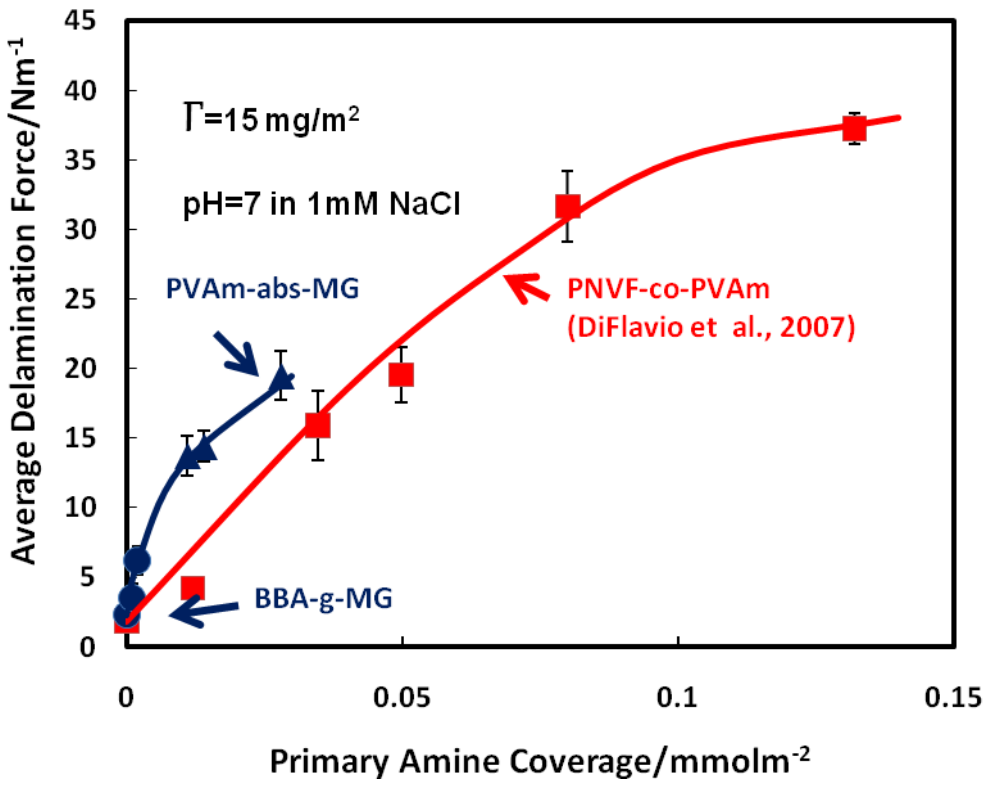

Figure 5 Wet adhesion of PVAm supported microgels and PVAm

A fundamental issue in any adhesion is the locus of failure – what breaks? The adhesive coverages in our work are very low compared to typical adhesion experiments with pressure sensitive adhesives. [6, 24] With thin adhesive layers it is often difficult to distinguish between adhesive failure, at an interface, and cohesive failure within the cellulose or the adhesive film. Sharpe's essay makes the compelling argument that interfacial forces often drive the formation of an adhesive joint by the development of an interphase, avoiding the whole issue of adhesive vs. cohesive failure. [25] We performed a few measurements with fluorescently labeled microgels where delaminated surfaces were examined by fluorescent microscopy. Figure 6 shows laser scanning confocal micrographs of cellulose surfaces after two delamination experiments. For both experiments, most of the microgels remained on the bottom cellulose membrane after peeling. However, there was some fluorescence on the top membranes suggesting failure occurred mainly at the cellulose/microgel interfaces with minor failure at the microgel/microgel interfaces.

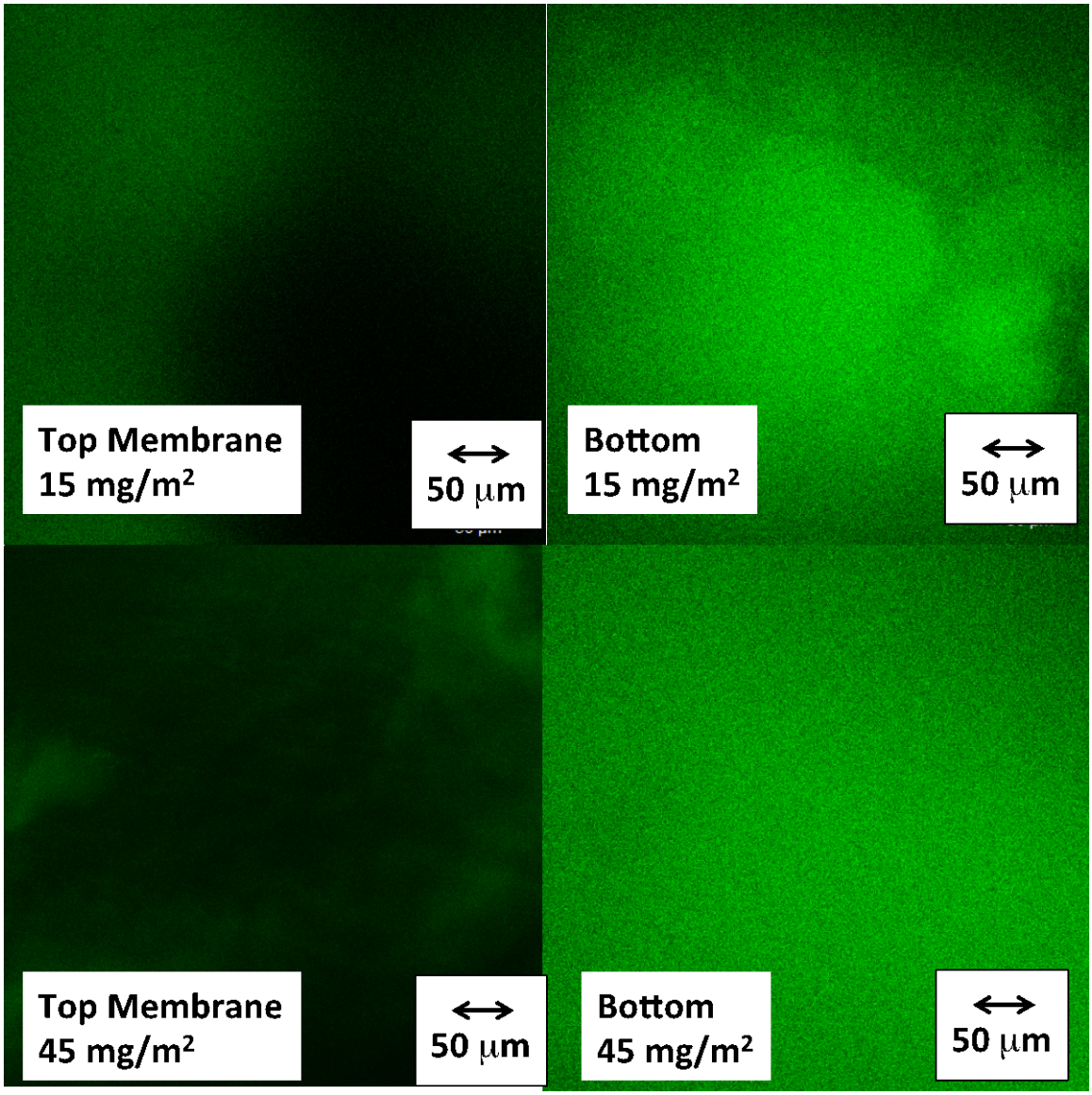

Figure 6 CLSM images of delaminated cellulose membranes. The microgels coverage for membranes (a) is 15 mg/m^2 and for membranes (b) is 45 mg/m^2. MGs were labeled with FITC

3.4 Discussion

The diameter of our PVAm loaded microgels was ~200nm whereas 2 Rg of 10 kDa PVAm is ~8 nm. Figure 7 illustrates our view of the delaminating peel front for a laminate with two layers of microgels (i.e. Γ = 38 mg/m^2 = 2 Γ_{sat}). We propose the role of the small PVAm chains is to couple the microgels to the wet cellulose films and to other microgel particles. In previous work we have summarized much evidence supporting the view that PVAm to cellulose adhesion is due to covalent bond formation (imines and aminals) between PVAm and aldehyde groups on the oxidized cellulose. [15]

Most of the results herein involved microgels with adsorbed PVAm chains; in these cases physical interactions are the sole adhesion mechanism between PVAm and the carboxylated microgels.

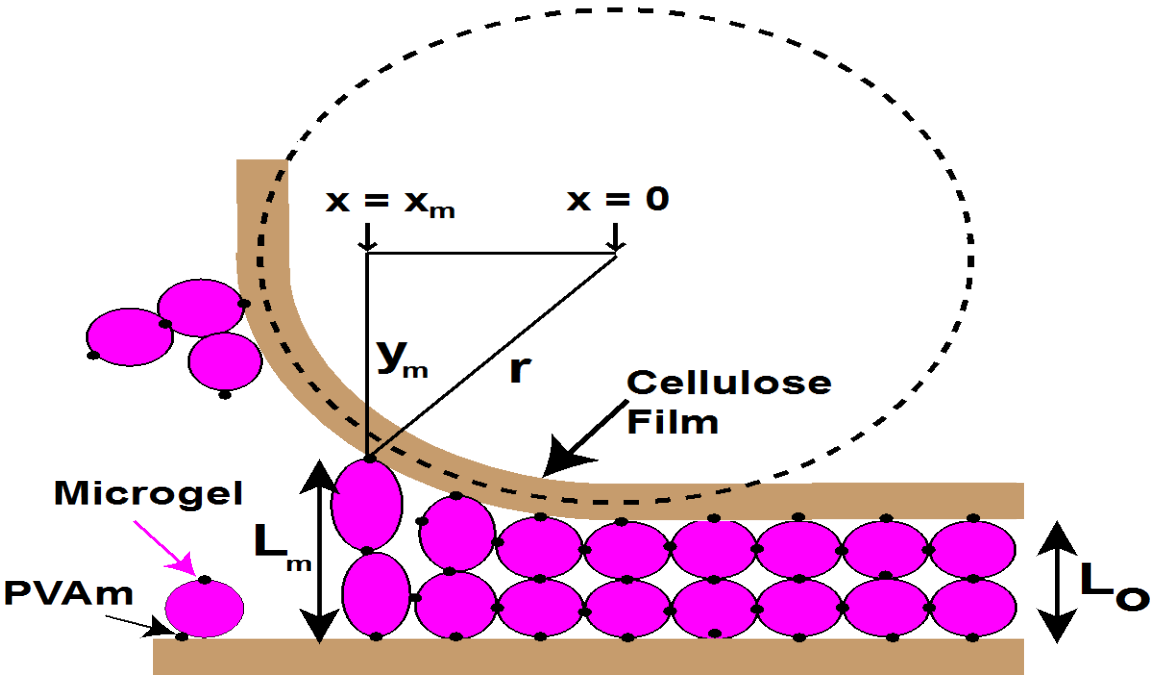

Figure 7 A schematic illustration of the peel front in our delamination experiments. The microgels are treated as ideal springs and the PVAm as stickers that fail at a critical stress.

We now describe a simple model for our delamination experiments with a view to predicting the influence of microgel properties on adhesion. Peel mechanics is a complex subject, which has been much discussed in the pressure sensitive adhesive literature.[26, 27] Our simplistic approach is to consider each microgel particle as a spring and the PVAm chains as stickers that fail at a critical stress. We further assume that the peel geometry is circular with a characteristic radius, r. Photographs of our peel delamination experiments suggest $r \sim 2$ mm. The overall peel force per unit width is assumed to be the sum of the contributions of load bearing microgels from x=0 to $x = x_m$ where x_m (see Figure 7) is the position along the peel crack where the stickers fail.

Individual springs (microgels) are assumed to obey Hooke's law (eq 2), where f is the force, k (N)vis the spring constant and ε is the elongation. A Hookean spring does not break. Bond failure is modeled by assuming that every microgel spring detaches at a critical elongation, ε_m. This is a fitting parameter for our model.

$$f = k\varepsilon \quad \text{for } \varepsilon < \varepsilon_m$$
$$f = 0 \quad \text{for } \varepsilon \geq \varepsilon_m \qquad 2$$

The total force per width in the peel zone, F(N/m), is the sum of the contributions of all the springs from $x = 0$ to $x = x_m$, and is given by the following expression where n is the number of springs (microgels) in contact with one square meter of cellulose film. ε(x)is the position dependent value of the strain.

$$F = kn\int_0^{x_m} \varepsilon(x)dx \qquad 3$$

The strain on microgel is defined as a function of the initial length (diameter) L_0 and the extended length, L – see Figure 7. Based on the circular peel geometry ε is related to r and x by following expression.

$$\varepsilon = \frac{L - L_0}{L_0} = \frac{r - \sqrt{r^2 - x^2}}{L_0} \qquad 4$$

Similarly, ε_m and x_m are also related by 4.

Dividing the spring constant, k, by area occupied by a spherical microgel on the cellulose surface gives the modulus E where D is the unstrained microgel diameter

$$k = E\frac{\pi}{4}D^2 \qquad 5$$

Substituting equations 4 and 5 into 3 gives:

$$F = \frac{nE}{L_o}\frac{\pi}{4}D^2\int_0^{x_m} r - \sqrt{r^2 - x^2}\,dx \qquad 6$$

One goal of our modeling was to calculate the peel delamination force, F, as a function of coverage for comparison with the experimental results in

Figure 3. For this a number of parameters in eq 6 had to be assigned.

The number of microgels per area on one of the cellulose surfaces in the joint, n, is related to the microgel coverage.

Figure 8 shows four cases illustrating microgel packing in the adhesive zone and the corresponding values of n, L_0 and Γ. The maximum value, n_{max}, is simply related to assumed maximum microgel packing fraction, λ_m.

$$n_{\max} = \frac{4}{\pi D^2}\lambda_m \qquad 7$$

We have chosen coverage, Γ, as primary descriptor for the microgel adhesive layers. Inspection of

Figure 8 and the definitions of n and Γ gives the following.

$$n = 2\frac{\Gamma}{\Gamma_{sat}} n_{\max} = \frac{\Gamma}{\Gamma_{sat}} \frac{8}{\pi D^2} \lambda_m \qquad \text{for } \Gamma/\Gamma_{sat} < 0.5 \qquad 8$$

$$n = n_{\max} = \frac{4}{\pi D^2} \lambda_m \qquad \text{for } \Gamma/\Gamma_{sat} \geq 0.5$$

Defining values for L_0, the unstrained spring length is problematic. Three of the four cases in

Figure 8 show full layers of microgels between the cellulose films. For these three discrete cases, eq 9 gives the relationship between L_0 and D. We assume that the same relation holds for intermediate coverages, which is an approximation.

$$L_0 = 2D\frac{\Gamma}{\Gamma_{sat}} \qquad 9$$

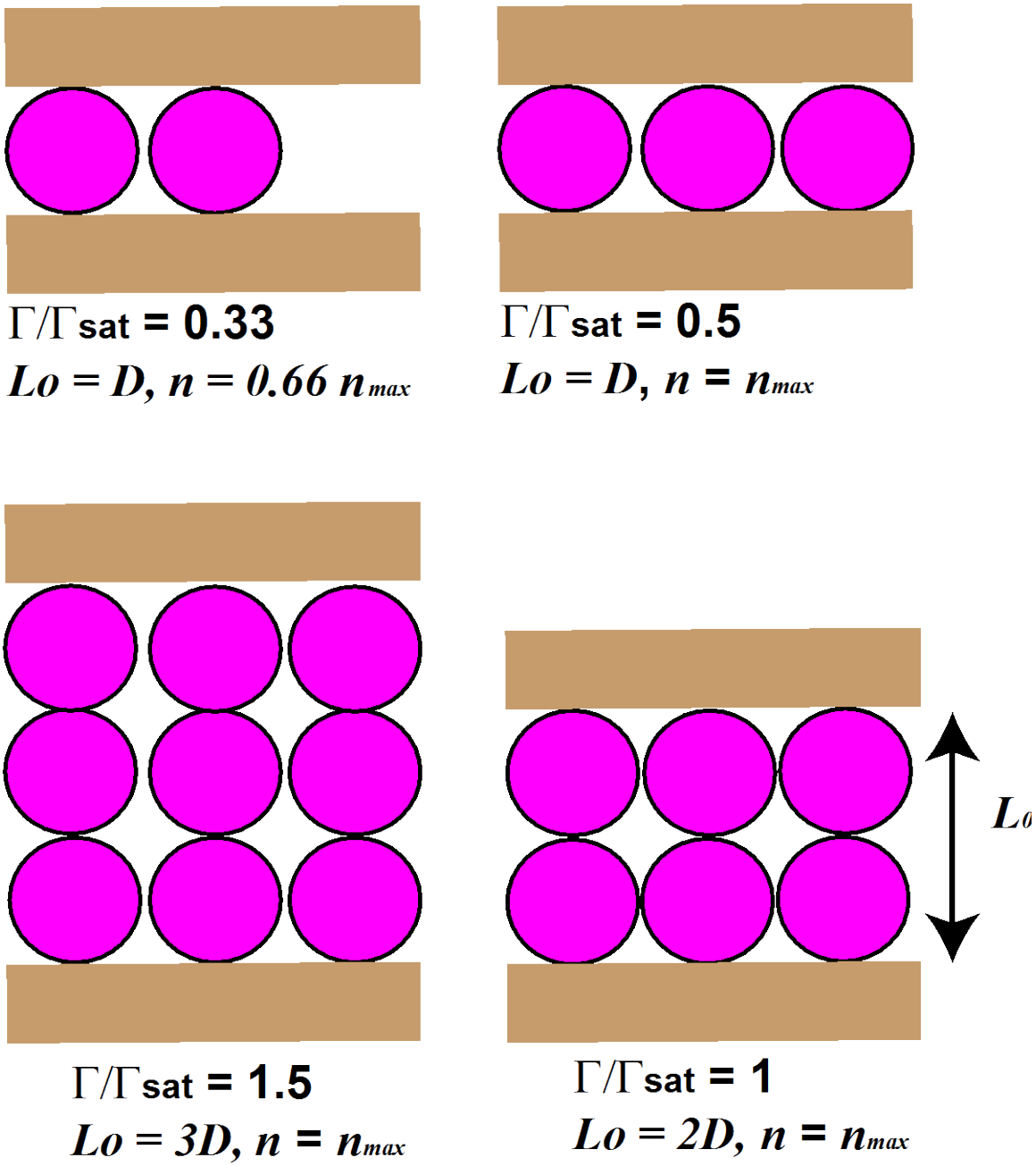

Figure 8 Illustrating the relationship between microgel coverage, Γ, and un-extended spring (microgel) length, L_0

Most of the microgel properties are embedded in the terms in front of the integral in eq 6. Substituting eqs 7 and 8 into the pre-integral term yields the following expressions.

$$\frac{nE}{L_o}\frac{\pi}{4}D^2 = \frac{E\lambda_m}{D} \qquad \text{for } \Gamma/\Gamma_{sat} \leq 0.5 \qquad 10$$

$$\frac{nE}{L_o}\frac{\pi}{4}D^2 = \frac{E\lambda_m}{2D\dfrac{\Gamma}{\Gamma_{sat}}} \quad \text{for } \Gamma/\Gamma_{sat} > 0.5$$

Based on the pre-integral terms (i.e. eq 10), delamination force is linear with elastic modulus and inversely related to microgel diameter. However, the microgel properties are also buried in x_m, the upper limit of the integral in eq 6. x_m is an important parameter – the larger it is, the more microgels contribute to the delamination force (see Figure 7. Rearranging eq 4 for the case $\varepsilon = \varepsilon_m$, $x = x_m$ and substituting for L_0 from eq 9 yields the following.

$$x_m = \sqrt{r^2 - \left(r - \varepsilon_m 2D\frac{\Gamma}{\Gamma_{sat}}\right)^2} \qquad 11$$

For the base case conditions (see Figure 9) and cellulose surfaces saturated with adsorbed microgels ($\Gamma = \Gamma_{sat}$), x_m corresponds to 89 μm, which is equivalent to a line of 447 microgels bearing the load across the peel front.

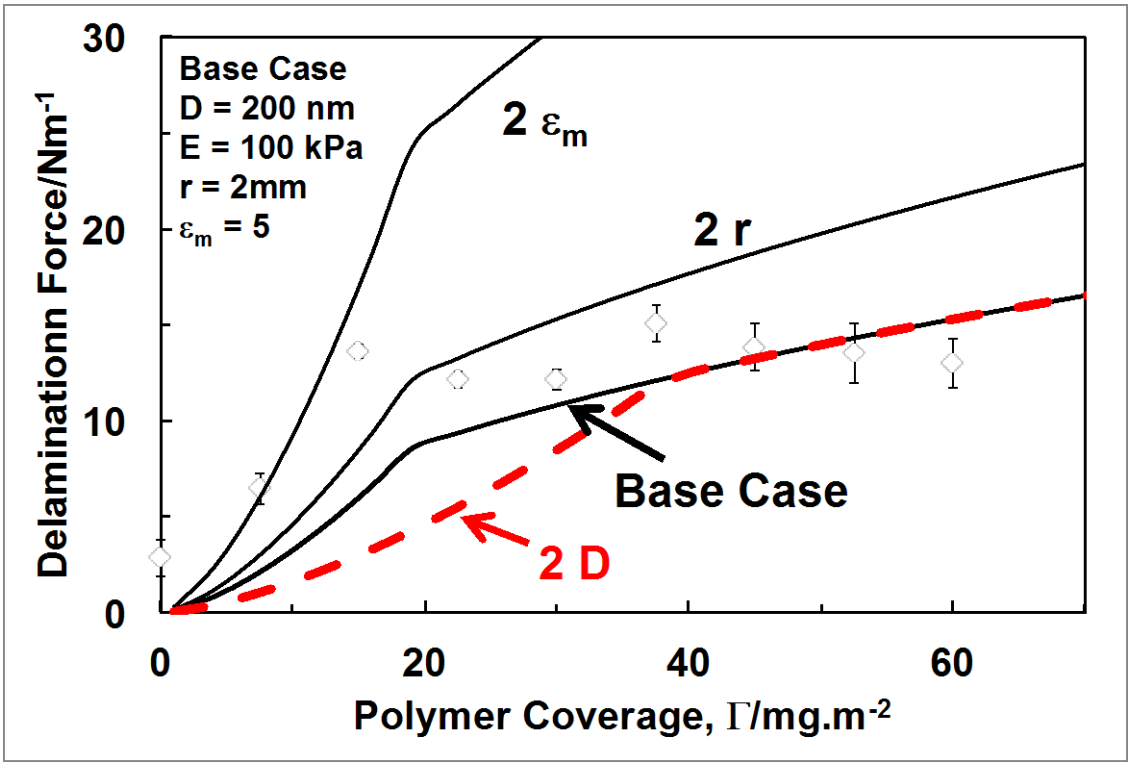

Figure 9 Comparing the predictions of the delamination model with experimental results

Microgel diameter, coverage and the strain at failure all influence x_m. The delamination peel force was calculated as functions of microgel coverage, Γ, and the calculations are

compared with experimental data in Figure 9. The calculations were performed with MathCad 14. The base case parameters are given in the figure caption. Before discussing the modeling results, we comment on our choices for the least known parameters E, the microgel extensional modulus, and ε_m, the strain at which a microgel detaches from the cellulose surface.

There have been a few experimental determinations of the modulus, E, of individual PNIPAM microgels and typically values range from <10 kPa for swollen microgels to 80 kPa for shrunken gels. [28] For our base case we set E = 100 kPa, which is at the high end because PVAm binding to our microgels caused them to shrink from 400 nm at pH 7 for the starting microgel to 200 nm for the PVAm-abs-VAA MG.

Failure most likely occurs by PVAm detaching from the cellulose or from the microgels. We found that assigning $\varepsilon_m = 5$ gave reasonable agreement between the model and our experiments. The literature has many examples of microgel diameter changing by more than a factor of 2 in response to environmental changes. Therefore, a microgel strain of 5 is somewhat high. In future work we plan to measure directly the elastic properties our microgels.

The base case prediction is close to the experimental results. All of the curves in Figure 9 feature a change of trend at point where the isolated cellulose surfaces are half covered with microgels ($\Gamma = \Gamma_{sat}/2$ and $n = n_{max}$). At higher coverages we assume no microgel-free, bare spots in the laminated joint. Mathematically, the discontinuity arises from the conditional form of eq 8.

The larger the radius of peel front, r, the greater the peel force because more microgels are load bearing in the peel front. The curvature of the cellulose membrane during peeling is function of the interfacial adhesion and membrane properties including thickness, modulus, and elasticity.[6] We have treated r as measured input parameter and we make the approximation that r is constant over the r.

The dependence on microgel diameter in Figure 9 is more complex. With larger microgels the coverage corresponding saturation the cellulose surface (i.e. $n = n_{max}$ and $\Gamma = \Gamma_{sat}/2$) increases linearly with D (see eq 1). However above monolayer coverage, the peel force is independent of microgel diameter.

The properties of the supporting microgels can be varied over a broad range. Microgel modulus can range from very light crosslinking to hard, glassy latex particles. We applied the model to predict the role of microgel elasticity, E. However, we now argue it is not appropriate to simply vary E and keep all other parameters constant. The force required to detach an individual spring, f_r, is given by the following function of E.

$$f_r = k\varepsilon_m = E\frac{\pi}{4}D^2\varepsilon_m \qquad 12$$

It seems reasonable to propose that the rupture force, f_r, is mainly dependent upon PVAm and its interaction with cellulose and the microgels. By contrast, the microgel elastic modulus, E, is dominated by microgel crosslinking and swelling. Therefore, to predict

the effects of microgel modulus (crosslinking) on adhesion at constant microgel diameter, we propose that based on eq 12, the product E.ε_m should be constant. If we double *E*, we should halve ε_m to keep the rupture force constant. Figure 10 shows the predict delamination forces as function of microgel modulus. The stiffer the microgels, the lower the adhesion force because stiffer gels result in fewer load bearing microgels at the peel front. The role of the supporting microgel properties will be explored in more detail in future work.

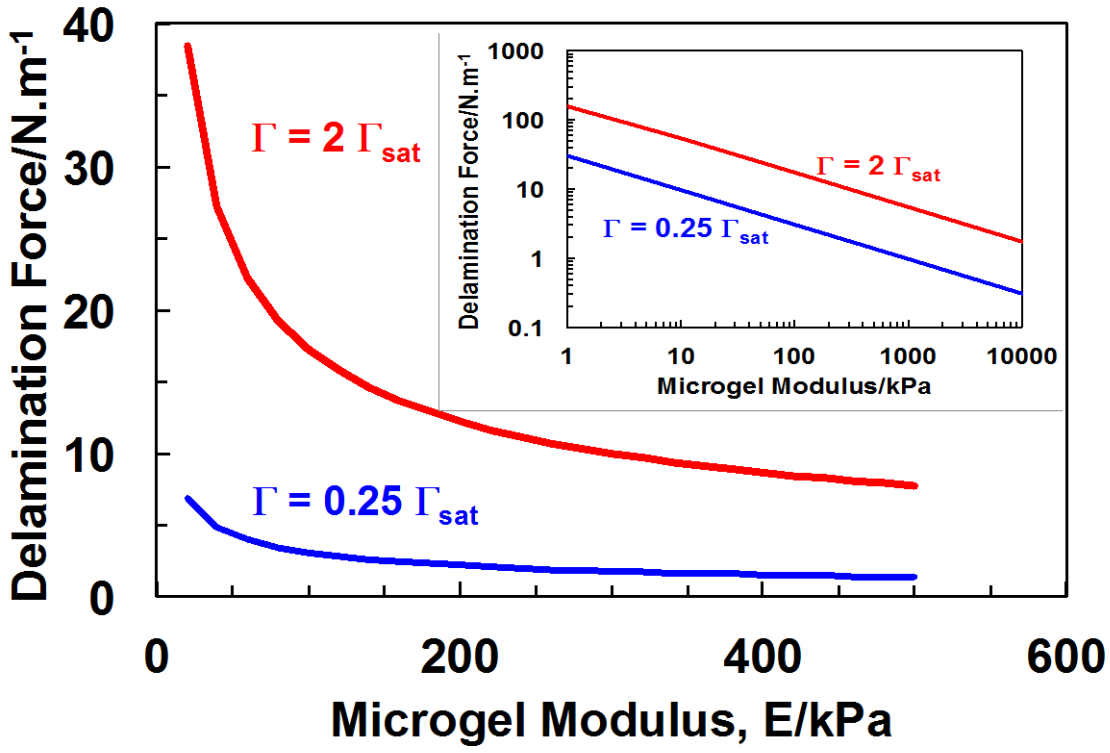

Figure 10 The influence of microgel elasticity on adhesion. The spring rupture force (eq 12) was held constant by maintaining a constant value of the product *E*.ε_m. Adhesion increased with decreasing *E* because the corresponding increase in ε_m resulted in more load bearing microgels (i.e. ε_m increases with decrease *E*).

3.5 Conclusions

1. The adhesion of wet cellulose films laminated with an adsorbed layer of PVAm-coated microgels is 5 to 10 times greater those laminated with PVAm alone. This is the major technological opportunity; microgels are a route to getting much more adhesive into fiber-fiber joints during paper manufacture.
2. For both PVAm coated microgels and for polyvinylamine-co-vinylformamide linear copolymers, wet adhesion increases with amine content. When compared at

the same total adhesive coverage and primary amine content, coated microgels and linear copolymer gave similar wet adhesion.

3. There is no adhesion advantage in covalently coupling PVAm to microgels – physical adsorption is sufficient.
4. Over the range 10 kDa to 340 kDa, the molecular weight of PVAm adsorbed onto microgels does not influence wet adhesion.
5. A simple peeling model predicts the influence of microgel elasticity, diameter and coverage on the delamination force. The microgels are treated as ideal springs and the PVAm surface polymers are stickers that detach upon failure.

Acknowledgements

The authors thank the Natural Sciences and Engineering Research Council of Canada for funding this work through a cooperative research grant with BASF Canada. The authors acknowledge many stimulating conversations with Drs. Esser, Kroener, Mijolovic, and Stährfeldt all from BASF in Europe and with Prof. Boxin Zhao, University of Waterloo. The authors also thank the Canada Foundation for Innovation for support of this work. RP holds the Canada Research Chair in Interfacial Technologies

3.6 References

1. Klemm, D.; Kramer, F.; Moritz, S.; Lindström, T.; Ankerfors, M.; Gray, D.; Dorris, A., Nanocelluloses: A New Family of Nature-Based Materials. *Angewandte Chemie International Edition* **2011,** *50*, 5438-5466.

2. Diflavio, J. L.; Bertoia, R.; Pelton, R.; Leduc, M., The Mechanism of Polyvinylamine Wet-Strengthening. In *Advances in Paper Science and Technology: Transactions of the 13th Fundamental Research Symposium*, SJ, I. A., Ed. Pulp & Paper Fundamental Research Society: Cambridge, UK, 2005; Vol. 1, pp 1293-1316.

3. Notley, S.; Chen, W.; Pelton, R., The Extraordinary Adhesion of Phenylboronic Acid Derivatives of Polyvinylamine to Wet Cellulose – a Colloidal Probe Microscopy Investigation. *Langmuir* **2009,** *25*, 6898–6904.

4. Chen, W.; Leung, V.; Kroener, H.; Pelton, R., Polyvinylamine-Phenylboronic Acid Adhesion to Cellulose Hydrogel. *Langmuir* **2009,** *25*, 6863–6868.

5. Pelton, R.; Ren, P. R.; Liu, J.; Mijolovic, D., Polyvinylamine-Graft-Tempo Adsorbs onto, Oxidizes and Covalently Bonds to Wet Cellulose. *Biomacromolecules* **2011,** *12*, 942–948.

6. Satas, D., Peel. In *Handbook of Pressure Sensitive Adhesive Technology*, 2nd Edition ed.; Satas, D., Ed. Van Nostrand Reinhold: New York, 1989.

7. Wagberg, L.; Forsberg, S.; Johansson, A.; Juntti, P., Engineering of Fibre Surface Properties by Application of the Polyelectrolyte Multilayer Concept. Part I: Modification of Paper Strength. *J. Pulp Paper Sci.* **2002,** *28*, 222-228.

8. Feng, X.; Pouw, K.; Leung, V.; Pelton, R., Adhesion of Colloidal Polyelectrolyte Complexes to Wet Cellulose. *Biomacromolecules* **2007,** *8*, 2161-2166.

9. Feng, X.; Pelton, R.; Leduc, M.; Champ, S., Colloidal Complexes from Poly(Vinyl Amine) and Carboxymethyl Cellulose Mixtures. *Langmuir* **2007,** *23*, 2970-2976.

10. Feng, X.; Pelton, R., Carboxymethyl Cellulose:Polyvinylamine Complex Hydrogel Swelling. *Macromolecules* **2007,** *40*, 1624-1630.

11. Miao, C. W.; Pelton, R.; Chen, X. N.; Leduc, M., Microgels Versus Linear Polymers for Paper Wet Strength - Size Does Matter. *Appita J.* **2007,** *60*, 465-468.

12. Miao, C.; Chen, X.; Pelton, R., Adhesion of Poly(Vinylamine) Microgels to Wet Cellulose. *Ind. Eng. Chem. Res.* **2007,** *46*, 6486-6493.

13. Wen, Q.; Vincelli, A. M.; Pelton, R., Cationic Polyvinylamine Binding to Anionic Microgels Yields Kinetically Controlled Structures. *J. Colloid Interface Sci.* **2012,** *to appear*.

14. Hoare, T.; Pelton, R., Characterizing Charge and Crosslinker Distributions in Polyelectrolyte Microgels. *Curr. Opin. Colloid Interface Sci.* **2008,** *13*, 413–428.

15. Diflavio, J. L.; Pelton, R.; Leduc, M.; Champ, S.; Essig, M.; Frechen, T., The Role of Mild Tempo-Nabr-Naclo Oxidation on the Wet Adhesion of Regenerated Cellulose Membranes with Polyvinylamine. *Cellulose* **2007,** *14*, 257-268.

16. Kitaoka, T.; Isogai, A.; Onabe, F., Chemical Modification of Pulp Fibers by Tempo-Mediated Oxidation *Nordic Pulp & Paper Reserach Journal* **1999,** *14*, 279-284.

17. Hoare, T.; Pelton, R., Highly Ph and Temperature Responsive Microgels Functionalized with Vinylacetic Acid. *Macromolecules* **2004,** *37*, 2544-2550.

18. Xu, Y.; Pharand, L.; Wen, Q.; Gonzaga, F.; Li, Y.; Ali, M. M.; Filipe, C. D. M.; Pelton, R., Controlling Biotinylation of Microgels and Modeling Streptavidin Uptake Running Title: Microgel Biotinylation. *Colloid & Polymer Science* **2011,** *289*, 659–666.

19. Su, S.; Ali, M. M.; Filipe, C. D. M.; Li, Y.; Pelton, R., Microgel-Based Inks for Paper-Supported Biosensing Applications. *Biomacromolecules* **2008,** *9*, 935-941.

20. Kurosu, K.; Pelton, R., Simple Lysine-Containing Polypeptide and Polyvinylamine Adhesives for Wet Cellulose. *J. Pulp Paper Sci.* **2004,** *30*, 228-232.

21. Geffroy, C.; Labeau, M. P.; Wong, K.; Cabane, B.; Cohen Stuart, M. a. C., Kinetics of Adsorption of Polyvinylamine onto Cellulose. *Colloids Surfaces A* **2000,** *172*, 47-56.

22. Kausch, H. H.; Fesko, D. G.; Tschoegl, N. W., The Random Packing of Circles in a Plane. *J. Colloid Interface Sci.* **1971,** *37*, 603-611.

23. Pinschmidt, R. K.; Renz, W. L.; Carroll, W. E.; Yacoub, K.; Drescher, J.; Nordquist, A. F.; Chen, N., N-Vinylformamide - Building Block for Novel Polymer Structures. *Journal of Macromolecular Science-Pure and Applied Chemistry* **1997,** *A34*, 1885-1905.

24. Kendall, K., *Molecular Adhesion and Its Applications - the Sticky Universe*. Plenum London, 2001.

25. Sharpe, L. H., Some Fundamental Issues in Adhesion: A Conceptual View. *J. Adhesion* **1998,** *67*, 277-289.

26. Kaelble, D. H., Peel Adhesion: Influence of Surface Energies and Adhesive Rheology. *J. Adhesion* **1969,** *1*, 102-123.

27. Williams, J. A.; Kauzlarich, J. J., The Influence of Peel Angle on the Mechanics of Peeling Flexible Adherends with Arbitrary Load-Extension Characteristics. *Tribology International* **2005,** *38*, 951-958.

28. Hashmi, S. M.; Dufresne, E. R., Mechanical Properties of Individual Microgel Particles through the Deswelling Transition. *Soft Matter* **2009,** *5*, 3682-3688.

3.7 Appendix

Spring Model for Peeling

Objective: gain insight into the influence of polymer properties on adhesion

Single Spring

$f = ks \cdot \varepsilon$ Hook's law - force

$\varepsilon = \frac{L - L_o}{L_o}$ Spring elongation
L - total spring length, Lo length where f =0

$L - L_o = L_o \cdot \varepsilon = \delta$ distance spring is moved

Work to extend one spring

$$W(\varepsilon) = \int_0^{\delta} f \, d\delta = \int_0^{\varepsilon} ks \cdot \varepsilon \, dL_o \cdot \varepsilon = \int_0^{\varepsilon} ks \cdot \varepsilon \cdot L_o \, d\varepsilon = \frac{1}{2} \cdot ks \cdot L_o \cdot \varepsilon^2$$

General work spring specific

$\frac{1}{2} \cdot ks \cdot L_o \cdot \varepsilon_m^2$ work to break one spring

Collection of Springs Making a Joint

Parameters

$\varepsilon_m := 2$ The maximum elongation at which spring breaks

$n := \frac{0.05}{nm^2}$ number of springs per unit area in joint

$\omega := 10mm$ Peel sample width

$L_o := 50nm$ Unextended polymer length

$MW_s := 10kDa$ MWs of polymer - not independent of Lo

$ks := 10^{-10} \cdot N$ Spring constant

$x_m := 10\mu m$ Length of peel zone

Derived quantities

$\omega \cdot x_m = 1 \times 10^{-7} m^2$ Load bearing area

$n \cdot \omega \cdot x_m = 5 \times 10^9$ total number of load bearing chains

$$\Gamma_c := n \cdot \frac{MW_s}{N_{av}} \qquad \Gamma_c = 0.8303\,m^{-2} \cdot mg$$

Case 1 Pulling straight up or shearing - all elongations equal

$F_{smax} := n \cdot ks \cdot \varepsilon_m$ Maximum force required to shear joint to failure per area of joint

$F_{smax} = 1 \times 10^{7}\,m^{-2} \cdot N$

$W_{smax} := \frac{n}{2} \cdot ks \cdot L_o \cdot \varepsilon_m^{\,2}$ Corresponding work to break joint per area of joint

$W_{smax} = 0.5\,m^{-1} \cdot N$ $W_{smax} = 0.5\,m^{-2} \cdot J$

Case 2 Peeling a stiff film

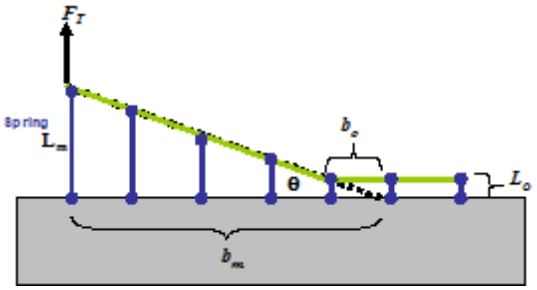

Here we assume a linear peel geometry

$\theta := 10deg$ Assumed peel angle

$L - L_o = x \cdot Tan(\theta)$ $x := nm$

$\varepsilon_{sf}(x, L_o, \theta) := \frac{x}{L_o} \cdot \tan(\theta)$ $\varepsilon_{sf}(x, L_o, \theta) = 3.5265 \times 10^{-3}$

$x_{msf}(L_o, \theta, \varepsilon_m) := \varepsilon_m \cdot \frac{L_o}{\tan(\theta)}$ $x_{msf}(L_o, \theta, \varepsilon_m) = 567.1282 \cdot nm$

$\theta\theta := 1deg, 2deg .. 89deg$

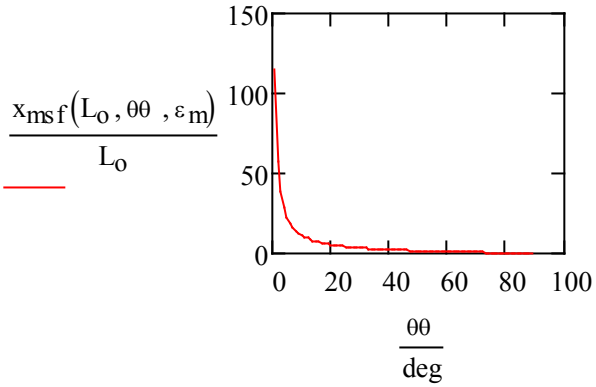

$n \cdot \omega \cdot dx$ number of springs per incremental area

Total force to lift film

$$F = \int_{0m}^{x_{msf}} n \cdot \omega \cdot ks \cdot \frac{\tan(\theta)}{L_o} \cdot x \, dx = n \cdot \omega \cdot ks \cdot \frac{\tan(\theta)}{L_o \cdot 2} \cdot x_{msf}^{2} = n \cdot \omega \cdot ks \cdot \frac{\tan(\theta)}{L_o \cdot 2} \cdot \left(\varepsilon_m \cdot \frac{L_o}{\tan(\theta)} \right)^2$$

Force per width

$$F_{sf}(L_o, \theta, \varepsilon_m) := \frac{n \cdot ks}{2} \cdot \frac{L_o}{\tan(\theta)} \cdot \varepsilon_m^{2} \qquad F_{sf}(L_o, \theta, \varepsilon_m) = 2.8356\, m^{-1} \cdot N$$

$\varepsilon\varepsilon := 0.05, 0.1 .. 10$

$\theta\theta := deg, 2deg .. 80deg$

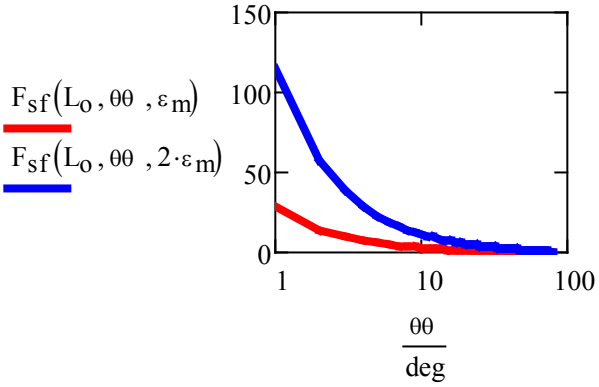

Low peeling angle has many more load bearing chains so force is high.

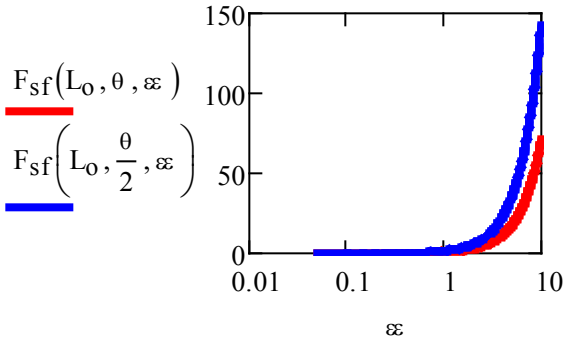

Peel force increases with square of maximum elongation

Case 3 Circular Peel Front

Microgel Properties

$\rho := 175\frac{kg}{m^3}$ Polymer density in swollen microgel

$E := 100kPa$ Elastic modulus of microgel

$D := 200nm$ Microgel diameter

$\sigma_m := 2$ Strain at break

$f_m := 0.82$ Maximum microgel packing fraction - random circles

Peel Geometry

$r := 0.5cm$ Radius of curvature of peel front

Part A - a slab of adhesive

$L_o := 500nm$ Slab thickness

$n = 5 \times 10^{16} m^{-2}$ Spring density

$y = \sqrt{r^2 - x^2}$ From equation of circle

$L - L_o = r - y$ L is the spring length, Lo is the unstrained length

$\sigma_{cir}(L_o, r, x) := \frac{r - \sqrt{r^2 - x^2}}{L_o}$ Strain as a function of x

$\sigma_{cir}(L_o, r, 0m) = 0$

$xx := 0.001r, 0.002r .. 0.1r$

$\sigma_{cir}(L_o, r, xx)$

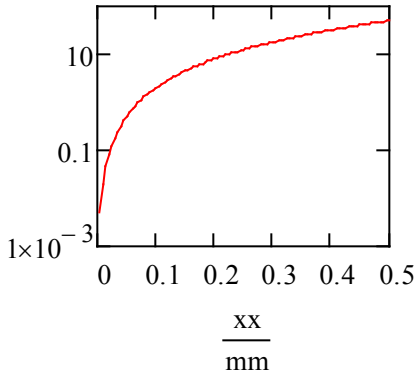

Determining the maximum x as a function of σ m

$$\sigma_m = \frac{r - \sqrt{r^2 - x_m^2}}{L_o}$$

$$x_m = \sqrt{r^2 - (r - \sigma_m \cdot L_o)^2}$$

$$x_{cirm}(L_o, r, \sigma_m) := \sqrt{r^2 - (r - \sigma_m \cdot L_o)^2}$$

checking

This is the x value corresponding to the maximum elongation

$\sigma_{cir}(L_o, r, x_{cirm}(L_o, r, \varepsilon_m)) = 2$ $\sigma_m = 2$

$x_{cirm}(L_o, r, \varepsilon_m) = 9.9995 \times 10^{-5}\,m$

$$F_{cir}(L_o, r, \sigma_m) := \int_{0m}^{x_{cirm}(L_o, r, \sigma_m)} n \cdot ks \cdot \frac{r - \sqrt{r^2 - x^2}}{L_o}$$

Total force required to extend all springs per unit width

$II := 0, 1 .. 5$

$rr := 1\mu m, 2\mu m .. cm$

$L_o = 5 \times 10^{-7}\,m$

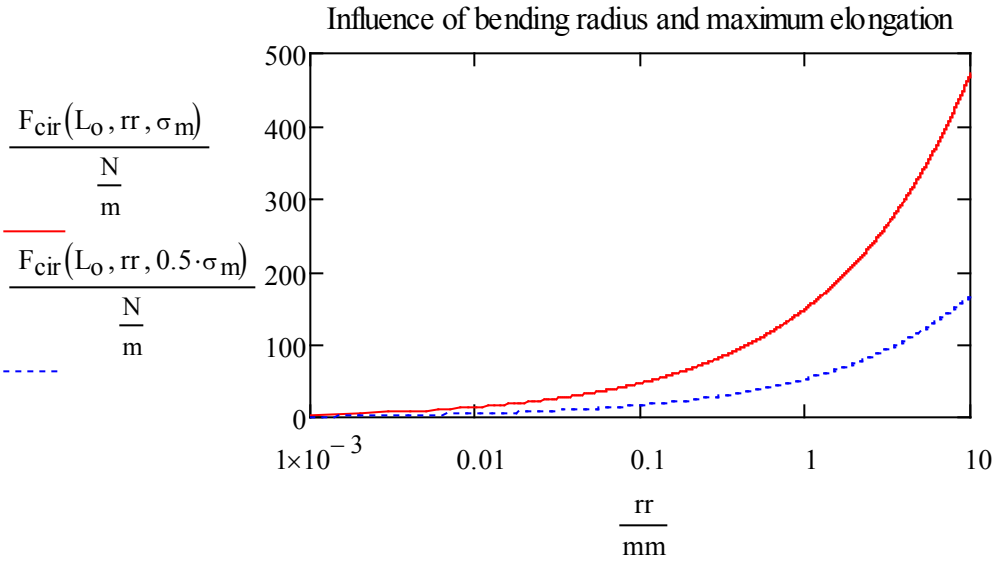

$\sigma\sigma := 0.05, 0.1 .. 10$

$r := 2mm$

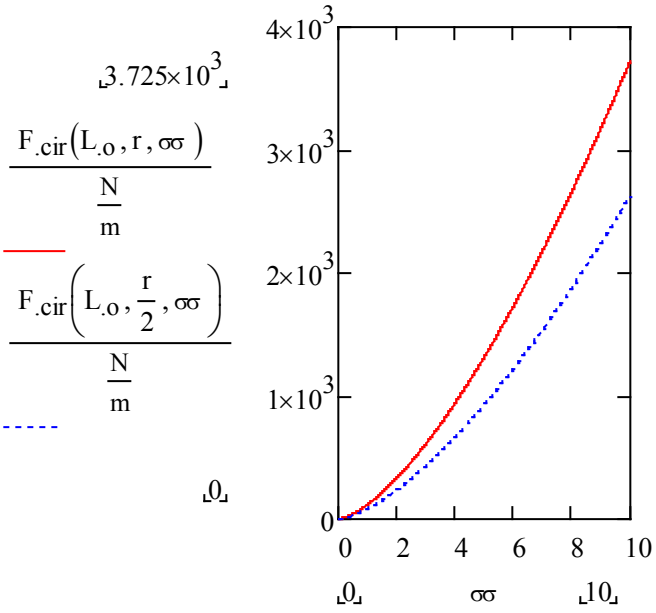

Smaller r, lower peel force, fewer springs bearing load

$LL := nm, 2nm .. 1000nm$

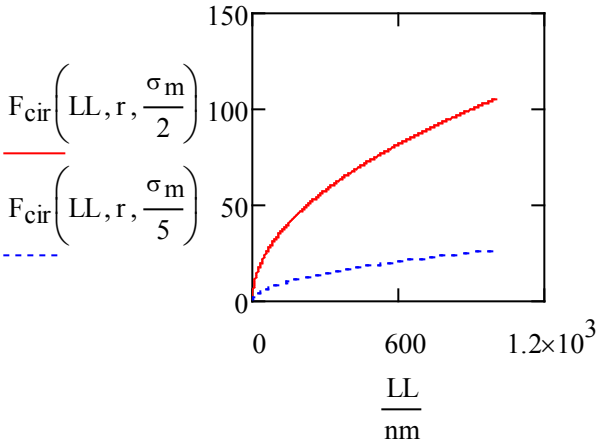

$r = 2\cdot mm$

$\varepsilon_m = 2$

LL the length of the surface chains is proportional to coverage and to MW in the case of an adsorbed monolayer

Part B - Circular peel front with microgels

$\Gamma_m(D) := \frac{2}{3}\cdot D\cdot\rho\cdot f_m$ monolayer coverage as function of microgel properties

concentration of microgels in contact with cellulose surfaces in joint

$$n_{mg}(D,\Gamma) := \left[\left(\frac{\Gamma}{\Gamma_m(D)} < 1\right)\cdot\frac{\Gamma}{\Gamma_m(D)} + \left(\frac{\Gamma}{\Gamma_m(D)} \geq 1\right)\right]\cdot\frac{f_m}{\pi\cdot\left(\frac{D}{2}\right)^2}$$

$n_{mg}\left(D,\Gamma_m(D)\right) = 2.6101\times10^{13}\,m^{-2}$

$xx := 0\cdot\Gamma_m(D), 0.05\cdot\Gamma_m(D)\,..\,2\cdot\Gamma_m(D)$

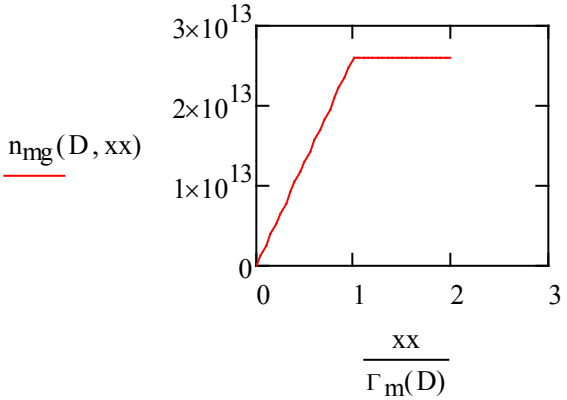

The unstrained chain length

$$L_{omg}(D,\Gamma) := 2D\cdot\frac{\Gamma}{\Gamma_m(D)}$$

Microgel elastic properties

$$k_{mg}(E,D) := E\cdot\pi\cdot\left(\frac{D}{2}\right)^2$$

k_{mg} is the Hooke's law constant for one microgel

$$k_{mg}(10kPa, 200nm) = 3.1416\times 10^{-10}\,kg\cdot s^{-2}\cdot m$$

Maximum x value

$$x_{mgm}(D,\Gamma,r,\sigma_m) := \sqrt{r^2-\left(r-\sigma_m\cdot L_{omg}(D,\Gamma)\right)^2}$$

$$x_{mgm}\left(D, 10\frac{mg}{m^2}, r, \sigma_m\right) = 0.0409\cdot mm$$

Integrating for all of the springs

$$F_{mg}(D,\Gamma,r,\sigma_m,E) := \frac{n_{mg}(D,\Gamma)\cdot k_{mg}(E,D)}{L_{omg}(D,\Gamma)}\cdot\int_{0m}^{x_{mgm}(D,\Gamma,r,\sigma_m)} r-\sqrt{r^2-x^2}\ dx$$

$$F_{mg}\left(D, 20\frac{mg}{m^2}, r, \sigma_m, E\right) = 3.1611\cdot\frac{N}{m}$$

$$\frac{F_{mg}(D, \Gamma\Gamma, r, \sigma_m, E)}{\frac{N}{m}}$$

$$\frac{F_{mg}(D, \Gamma\Gamma, r, 1 \cdot \sigma_m, E \cdot 2)}{\frac{N}{m}}$$

$$\frac{F_{mg}(D, \Gamma\Gamma, r, \sigma_m \cdot 2, E \cdot 1)}{\frac{N}{m}}$$

$$\frac{F_{mg}\left(D, \Gamma\Gamma, r, \frac{\sigma_m}{2}, E \cdot 2\right)}{\frac{N}{m}}$$

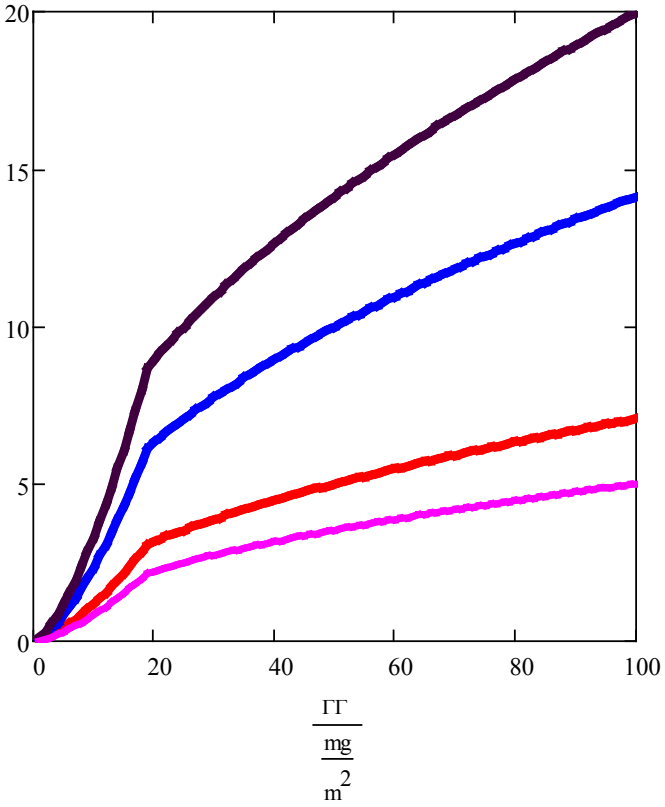

$r = 2 \cdot mm$ $\sigma_m = 2$

$D = 200 \cdot nm$ $E = 100 \cdot kPa$

$\Gamma_m(D) = 19.1333\, m^{-2} \cdot mg$

$\sigma\sigma := 0.1\sigma_m, 0.2\sigma_m .. 2\sigma_m$

$$\frac{F_{mg}(D, \Gamma_m(D) \cdot 0.5, r, \sigma\sigma, E)}{\frac{N}{m}}$$

$$\frac{F_{mg}(D, \Gamma_m(D) \cdot 2, r, \sigma\sigma, E)}{\frac{N}{m}}$$

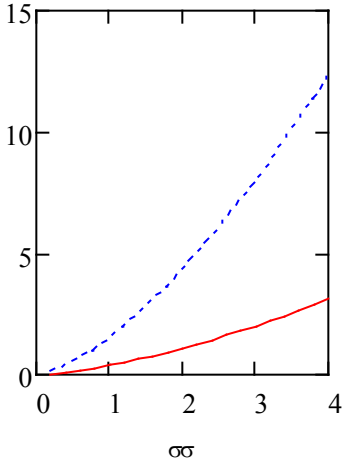

Force approximate linear with failure strain

$EE := 0.1E, 0.2E .. 5E$

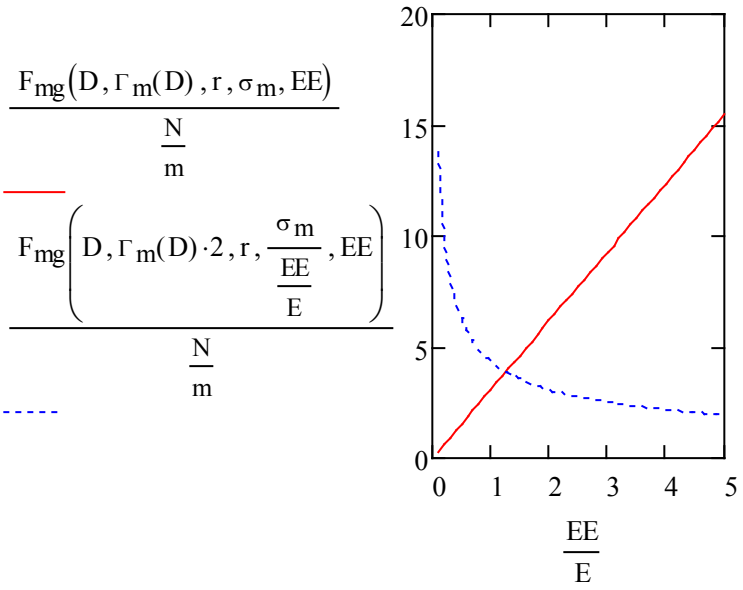

The failure force for a spring is σ mE Therefore to change E at constant failure force we must also change σ m

Chapter 4 Influence of Microgel Stiffness and Sizes on Wet Adhesion with Cellulose

In chapter4, the preparation and characterization of microgels were conducted by me with the help of Antonyos Fahmy. I prepared the cellulose model films and performed the wet adhesion tests. Dr. Pelton gave many helpful suggestions on both experiments and data analysis. I wrote the first draft and Dr. Pelton revised it.

Chapter 4 Influence of Microgel Stiffness and Sizes on Wet Adhesion with Cellulose

Abstract

Carboxylated microgels (VAA-NIPAM) were synthesized under various conditions to yield different particle sizes and crosslink densities. Carboxylated polystyrene latex was introduced as the model of highly crosslinked microgel. By physical adsorption of PVAm to carboxylated particles, PVAm coated adhesives with different sizes and stiffness were prepared. Wet adhesion measurements were carried out by using a 90° peel test of laminates consisting of two wet oxidised cellulose membranes and a layer of polymeric adhesive. Delamination force was measured as the function of the microgel stiffness, microgel sizes and cellulose roughness. The results show that the wet adhesion decreased with increasing stiffness of microgels. The size of microgels did not affect the wet adhesion of smooth cellulose films. However, for rough cellulose films, it was shown that when the diameter of microgels was comparable to the roughness of cellulose membranes, the largest wet adhesion could be achieved.The influence of temperature was studied since the NIPAM microgels are thermo-sensitive. Although PVAm-abs-MG deswelled when the temperature increased over the volume transition temperature, more PVAm-abs-MG was absorbed more onto the surface of cellulose membranes at room temperature resulting in a higher wet adhesion with cellulose.

4.1 Introduction

Our previous studies have focused on the influence of surface chemistry of microgels on wet adhesion with cellulose. By modifying the surface chemical properties of anionic carboxylated microgels (VAA-NIPAM MG), the major functional groups of microgels were transformed into primary amine groups which could form covalent bonds with aldehyde groups on cellulose. Thus, strong wet adhesion was obtained.

Compared with linear polymer, microgel based adhesives gave stronger wet adhesion with cellulose due to the large bulk volume of microgels which overcome the adsorption limit for linear polymer.[1] In addition, the thickness of an adsorbed polymeric layer is around several nanometers while for microgels, so the thickness of an adsorbed polymeric layer could reach several micrometers depending on the diameter of the microgels. Miao's work showed the advantage of PVAm microgels with regards to the wet adhesion with cellulose fibers but the polydispersity of PVAm microgels leads to difficulties when analyzing the size effect.[1] Therefore, our work prepared PVAm coated microgels based on VAA-NIPAM microgels which were monodispersed and well defined. The benefit of the size effect of microgels on wet adhesion with cellulose was studied by varying the size of VAA-NIPAM microgels.

Considering the influence of microgel structures on wet adhesion with cellulose, stiffness is another factor. The gel stiffness which is controlled by the crosslinker density will affect the mechanical properties of microgels[2]. It was known that filler particles specifically, mineral particles weakened the paper strength due to a reduced fiber-fiber bond area.[3] Even with the aid of a polymeric coating on filler particles, which promotes the filler-fiber interactions such as starch modified clay particles displays reduced paper strength.[4-5] However, the relationship between fiber-fiber bonds and stiffness of filler particles is not well defined. Thus, our strategy is to create microgels with varying stiffness and study the impact on the wet adhesion with cellulose.

The most famous property of NIPAM based microgels is thermosensitivity[6]. Aqueous colloidal PNIPAM microgels go through a reversible volume phase transition when the temperature is over certain temperature called the lower critical solution temperature (LCST). This is due to hydrophobic interactions induced by isopropyl groups that overcome the hydrophilic interactions between water molecules and amide groups causing water molecules to be expelled from the polymer network[7-9]. Since PNIPAM microgels shrink at high temperature, we expected more microgels adsorbed onto cellulose surfaces and thus a higher wet adhesion with cellulose.

It is difficult to study the wet adhesion of polymer with pulp fibres since the surface condition of wood fibres is complicated in terms of physical morphology and chemical composition. In contrast, model cellulose film provides a platform for us to study the fundamental parameters that influent the wet adhesion between polymer and cellulose. Hishiwa et. al. simply prepared rough cellulose films by cast and smooth cellulose films

by coagulation from dimethylacetamide/lithium chloride (DMAc/LiCl) cellulose solution[10]. Ultra-smooth cellulose surfaces could be prepared by Langmuir-Blodgett technique, however, it is a time consuming process and requires special equipments[11-12]. Spin-coating could also be employed to create cellulose model films and the thickness of the film is well controlled by the spin coating parameter, such as the concentration of cellulose solutions, the spin speed and the cellulose solvents[13-15]. Thus, LB deposition and spin coating are more suitable for the preparation of thin and smooth cellulose surfaces while direct casting could be applied to produce relatively thick and rough cellulose surfaces with large dimensions.

All of the techniques utilized in the preparation of cellulose model surfaces required solvents that could dissolve cellulose. The common solvents for cellulose are N-methylmorpholine N-oxide (NMMO)[16-18] and DMAc–LiCl[19-20]. The partial substitution of the hydroxyl groups of cellulose results in higher solubility. Thus, trimethylsilyl cellulose (TMSC) has been introduced as a medium for cellulose model surfaces which could be easily dissolved in most non-polar solvents such as chloroform and toluene[21]. Schaub *et al*. used TMSC to prepare cellulose model surfaces and cellulose films were recovered by a simple vapour phase acid hydrolysis[22]. However, the traditional cellulose dissolution process involved unusual solvents under harsh conditions, which cannot be recycled leading to serious environmental problems[23-24]. Recently, room temperature ionic liquid (IL) has attracted considerable interest as green solvents for cellulose[25-27]. Swatloski et. al. firstly prepared dissolved cellulose without derivation in IL and regenerated cellulose films from IL 1-butyl-3-methylimidazolium chloride by adding water, acetone and ethanol[26]. In addition, IL could be recycled by evaporation, ionic exchange, reverse osmosis and salting out[28]. Since halogen anions cause IL to be corrosive and toxic [29], 1-ethyl-3-methylimidazolium acetate (EMIMAC) is considered as a good candidate for dissolving cellulose due to low toxicity, low melting point and low viscosity[30].

Therefore, to create model cellulose films that could be used in peel tests which require films with relatively large dimensions, cast cellulose films were prepared from EMIMAC containing 5% cellulose. Different surface roughness was created by casting films through various conditions. The objective of this study was to investigate the relationship between the physical properties of microgels and the surface roughness of cellulose films on wet adhesion.

4.2 Experiments

4.2.1 Materials

N-isopropylacrylamide (NIPAM, 97%, Sigma-Aldrich) was purified by recrystallization from a 60:40 toluene:hexane mixture. N,N-Methylenebisacrylamide (MBA, 99+%, Aldrich), vinylacetic acid (VAA, 97%, Aldrich), sodium dodecyl sulfate (SDS, 98%, Aldrich), ammonium persulfate (APS, 99%, BDH), 2,2,6,6-tetramethyl-1-piperidinyloxy

(TEMPO), sodium bromide (NaBr) and sodium hypochlorite(NaClO) were purchased from Sigma-Aldrich and used as received. Carboxyl latex (4% w/v 0.2 μm) was purchased from Invitrogen and used as received. Polyvinylamine (PVAm) with a molecular weight of 10 KDa and 1-ethyl-3-methylimidazolium acetate (EMIMAC) with 5% cellulose were provided by BASF (Ludwigshafen, Germany). PVAm was purified by dialysis and freeze dried before use. The degree of hydrolysis (MW/DH) was determined by 1H NMR (10KDa/73%) and the equivalent weight was measured by conductometric titration (10KDa/100g/mol).

4.2.2 Methods

4.2.2.1 Preparation of VAA-NIPAM MG

Microgel synthesis was carried out in a 250 ml three-necked flask with continuous stirring at 200 rpm according to the recipes in Table **1**[31-33]. The dosage of VAA which provided the functional groups to microgels was the same for all of the microgels to keep the same carboxyl content in each sample. Different dosages of APS and SDS were introduced to the polymerization reaction to achieve different sizes of microgels while different dosages of MBA were added into the reactions to obtain different cross-linker density. NIPAM, MBA, SDS and VAA were dissolved in 150 ml of deionized water and heated to the polymerization temperature under the flow of nitrogen gas. After 30 min'tes' preheat, APS was dissolved in 10 ml of deionized water and added to initiate the reaction. The polymerization temperature was set to 70 °C for most of reactions. To synthesize microgels with diameter over micrometer, polymerization temperature was changed to 60°C[33] and 45-65°C respectively[32]. Following polymerization, all of the microgels were cleaned by several cycles of centrifugation (Beckman model Optima L-80 XP) until the supernatant conductivity was less than 5 μs/cm.

Table 1 VAA-NIPAM MG recipes

Sample	NIPAM g	VAA μL	MBA g	SDS g	APS g	Reaction Temperature
C03	**1.4**	**300**	**0.06**	**0.04**	**0.1**	**70°C**
C05	**1.4**	**300**	**0.1**	**0.04**	**0.1**	**70°C**
C10	**1.4**	**300**	**0.2**	**0.04**	**0.1**	**70°C**
C15	**1.4**	**300**	**0.3**	**0.04**	**0.1**	**70°C**
S02	**1.4**	**300**	**0.1**	**0.08**	**0.2**	**70°C**
S04	**1.4**	**300**	**0.1**	**0.02**	**0.05**	**70°C**
S08	**1.4**	**300**	**0.1**	**0**	**0.025**	**70°C**
S15	**1.4**	**300**	**0.1**	**0**	**0.05**	**60°C**
S25	**1.4**	**300**	**0.1**	**0**	**0.05**	**45 to 65 °C at a ramp rate of 30 °C/h. and keep on 65 °C**

4.2.2.2 Preparation of PVAm-abs-MG

VAA-NIPAM MGs were redispersed in 20 mL of 1mM NaCl at a concentration of 4g/L and PVAm was redispersed in 60 mL of 1mM NaCl at a concentration of 0.5g/L. The microgel dispersion was added into PVAm solution drop-wise and the pH was stabilized at 7 for 1h. The unabsorbed PVAm was removed by several cycles of centrifugation.

4.2.2.3 Preparation of PVAm-abs-PS

Carboxyl latex dispersion was diluted to 0.5g/L with 1mM NaCl and 5mg PVAm was dissolved in 10ml of 1mM NaCl. Then PVAm solution was added into carboxyl latex dispersion drop-wise and the pH was adjusted to 7 for 1h. The unabsorbed PVAm was removed by several cycles of centrifugation.

4.2.2.4 Colloidal particles characterization

All colloidal particles were freeze-dried and stored at 4°C before use. For characterization, colloidal particles were redispersed in 1mM NaCl at a concentration of 1g/L overnight. The electrophoretic mobility of colloidal particles was measured by a ZetaPlus analyzer (Brookhaven Instruments Corp., phase analysis light scattering model). Each sample was tested using 10 runs (each contained 15 cycles). For colloidal particles with diameter smaller than 1μm, particle sizing was determined using dynamic light scattering (Brookhaven Instruments Corporation, BIC) fitted with a Melles Griot HeNe 632.8 nm laser as the light source. For colloidal particles with a diameter larger than 1μm, the size was measured by a Mastersizer (Malvern Instruments Ltd, UK). Each reported particle size was the average of 3 measurements.

The total charge groups of colloidal particles were confirmed using Potentiometric and conductometric titration carried out simultaneously via a Burivar-I2 automatic buret (ManTech Associates). The carboxyl content was determined by titrating 50 mg colloidal particles dissolved in 50 ml of 5mM NaCl while the amine content of PVAm modified particles were measured by titrating 20 ml of centrifugation solution mixed with 30 ml 5mM NaCl. Data was collected using a base-into-acid titration method with an interval injection of 2 min to ensure complete equilibration.

4.2.2.5 Preparation of cellulose films

Cellulose membranes were prepared through the variation of cellulose solubility in water, ethanol and ionic liquid[26]. First of all, silicon wafer was fixed on a flat surface by masking tape so that the wafer did not move when the coating was applied. A glass rod (Diameter=5.9mm) with both ends surrounding the masking tape was placed at the top of substrate and an appropriate amount of ionic liquid containing cellulose was spread in front of the coating rod. The thickness of the cellulose films were determined by the thickness of the tapes that surrounded the ends of the glass rod. In this work, 10 layers of taps were applied to the glass rod and the thickness of cast cellulose films was around 0.1mm. Furthermore, the coating rod was drawn down to the end of substrate smoothly.

At last, the substrate with the coating was placed in a water bath for 24 hours so that the ionic liquid dissolved in water and cellulose membranes were precipitated from water. Following dialysis, the cellulose membranes were dried under vacuum at room temperature.

An Optical Digital Profilometer (Veeco WYKO NT1100 Optical Profiling System, DYMEK Company Ltd.) was employed to study the topography of the cellulose membrane surfaces providing line scans and three-dimensional recordings. The principles were to investigate the interference fringes displaced by the object. All of the cellulose membranes were tested in wet conditions.

4.2.2.6 Cellulose laminates preparation

The membranes were cut from cellulose films into rectangular strips according to the dimensions of 20mm×60mm and 30×60mm. Prior to polymer application the cellulose membranes were soaked in a dilute salt solution (1mM NaCl, pH7). The oxidation of the cellulose membranes was carried in TEMPO/NaBr/NaClO solution which is described elsewhere[34].

Adhesive specimens were prepared by bringing two wet cellulose membranes (top membrane: 20mm×60mm and bottom membrane: 30×60mm) together with a thin layer of polymer between them and a strip of Teflon tape (G.F. Thompson Co. Ltd, TWB480P) to act as a release point. The polymer was applied by either a direct application method or an adsorption method. In the direct application method, 15 μL of polymer solution was deposited onto the bottom cellulose membrane by a micropipette (Eppendorf) and then spread carefully by the top membrane. In the adsorption method, the top membrane was soaked in a 0.5g/L polymer solution followed with a rinsing cycle in 1mM NaCl. The cellulose laminates were then pressed between blotting paper under a constant load (20000lb unless otherwise specified) using a Carve Press for 30 min and dried at 23°C and 50%RH for at least 24 hrs.

4.2.2.7 Cellulose laminates delamination

The laminates were soaked in 1mM NaCl (pH 7) for 30min and then blotted to remove the excess water. The laminates were then fixed to a free moving aluminum wheel running on rubber sealed radial bearings (SKF 608-2RS1) by means of moisture-resistant two-sided tape (3M Polyethylene Medical Double Coated Tape 1522). The top membrane was peeled off at 90° at a crosshead rate of 20 mm/min. All testing was done using an Instron 4411 universal testing system (Instron Corporation, Canton, MA) fitted with a 50N load cell (Model 2530-437). At least four replicates were carried out for each sample.

4.2.2.8 Quartz crystal microbalance (QCM) measurement

The QCM measurements were made with a QCM-D E4 instrument (Q-sense, Gothenburg, Sweden) and cellulose-coated QCM sensors (Q-Sense, QSX 334, Gothenburg, Sweden). The sensors were allowed to swell in deionized water for at least 12 h and then oxidised

in TEMPO/NaBr/NaClO solutions for 30 min at pH=10.5 before use. The oxidation recipe was the same as that for cellulose membranes. After the sensors were placed into the flow cell of QCM, 1mM NaCl was pumped into the flow cell for at least 4h to achieve a stable baseline. In this study, data was plotted from a frequency shift and dissipation change in the third overtone because the resonator is less impacted by the mechanical forces that resulted from mounting the resonator[35].

The adsorption of PVAm-abs-MG to cellulose at different temperatures was studied by QCM. Firstly, 1mM NaCl solution (pH=7) was pumped into two modules in the flow cell chamber for at least 4hr to achieve a stable baseline and the temperature was set to 25°C. The flow cell chamber was then heated to 45°C. After the temperature was stable for 30min, 1g/L PVAm-abs-MG dispersion (pH=7) was introduced into the first module of QCM for 30min and then switched to 1mM NaCl solution (pH=7) for 30min to remove unadsorbed microgels. The temperature was lowered to 25°C subsequently. At last, 1g/L PVAm-abs-MG dispersion (pH=7) was pumped into the second module for 30 min followed with a 30 min' wash of 1mM NaCl solution.

The swelling behaviours of PVAm-abs-MG on cellulose were monitored with QCM as well. Firstly, 1g/L PVAm-abs-MG dispersion (pH=7) was introduced into the flow cell for 30min and switched to 1mM NaCl (pH=7) for 30min. Then 1mM NaCl (pH=4) was pumped into the flow cell and the pH was adjusted to 7 after 60min. This previous step was repeated. When the measurement was completed, the sensor was dried in a conditioned room (T=25°C, RH=50%) overnight. The sensor was then rewetted in 1mM NaCl solution (pH=7) for 12hr and placed into the QCM to monitor the swelling behaviours of PVAm-abs-MG at different pH.

4.3 Results

The major goal of this study was to investigate the influence of gel stiffness and gel size on the wet adhesion of cellulose. Therefore, VAA-NIPAM microgels with varying stiffness and diameters were prepared and the recipes are listed in Table 1. The carboxyl content of VAA-NIPAM microgels in this work was 0.5 mmol/g.

In the case of an ideal crosslinked network with no defects in terms of loose ends and intramolecular crosslinks, the elasticity of the network can be described as below:[36-37]

$$G = \frac{E}{3} = \frac{\rho RT}{M_c} \qquad \text{..... Equation 1}$$

Where G is the shear modulus(Pa), E is the Young's Modulus(Pa),ρ is the density of the elastically active crosslinks($g.cm^{-3}$), Mc is the molecular weight of crosslinker($mol.g^{-1}$),R is the gas constant and T is the temperature. Therefore, the crosslink density of microgels is proportional to the modulus of microgels and thus the stiffness of microgels.

It was shown that the Young's modulus was increased with the crosslink density of the microgel. [2]In another words, microgels become stiffer with increasing crosslink content. Therefore, the stiffness of VAA-NIPAM microgels was varied by changing crosslink dosage from 3% to 15% during synthesis. After polymeric synthesis, PVAm was coated to VAA-NIPAM MG via adsorptions and unabsorbed PVAm was removed by centrifugation. The details regarding unadsorbed PVAm removal are described elsewhere.[38] The amine content of the PVAm coated microgels was 10 w% calculated from the titration of the centrifuge supernatant.

To characterize the microgel stiffness, the swelling behaviours of microgels with different crosslink density were measured by DLS and the results are shown in Figure 1. The swelling behaviours of crosslinked network depend on the stiffness of the polymeric network, the affinity between the polymer and solvent, and the osmotic pressure caused by the counterions[39]. Higher crosslink densities within microgels create more stiffness within the polymeric network resulting in smaller swelling ratios.[40-41]Thus the swelling ratio reflects the stiffness of the microgels.

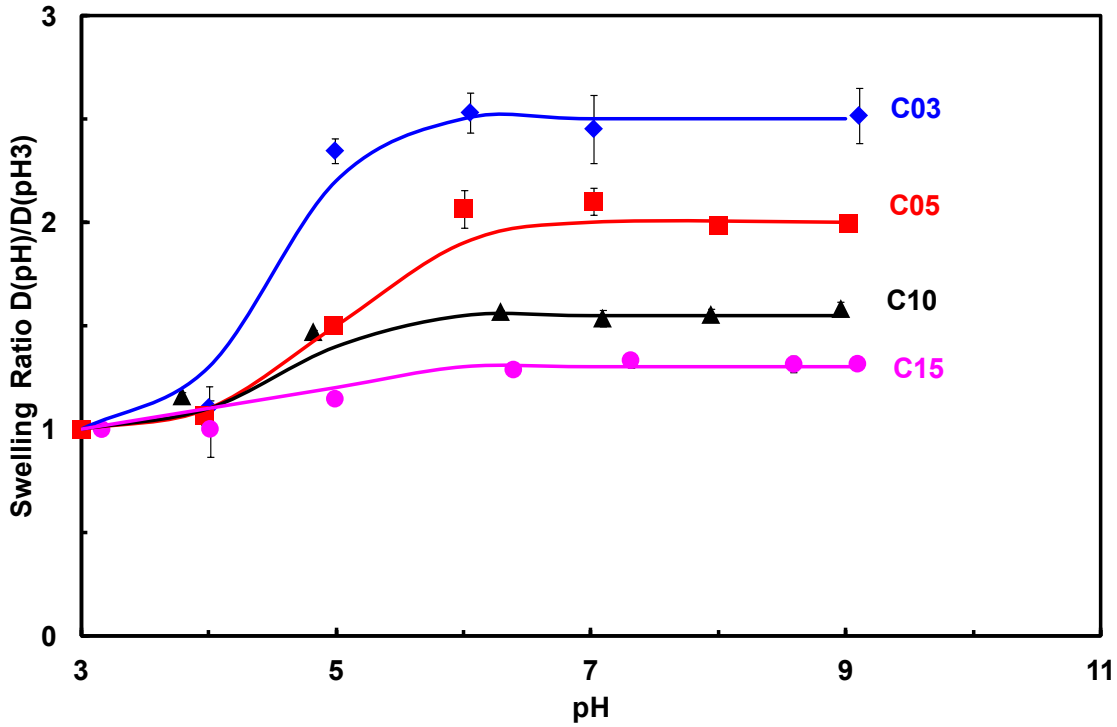

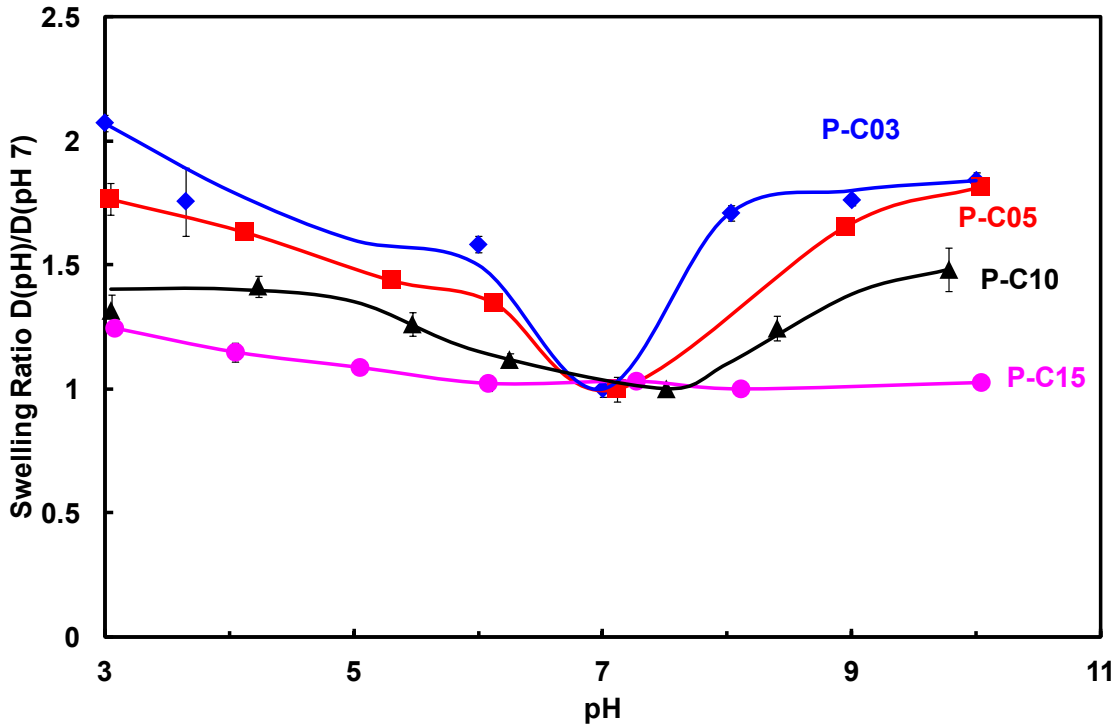

Figure 1 pH dependences of MG with different crosslink densities

As shown in Figure 1, the swelling ratio of VAA-NIPAM microgels (C03-C15) increased with pH and reached the maximum value at around pH 6. After the adsorption of PVAm, the swelling ratio of PVAm-abs-MG achieved a minimum value at around pH 7 and increased towards pH 3 and pH 10. VAA-NIPAM microgels are highly pH sensitive due to the carboxylic acid groups located on the surfaces of microgels, which start to dissociate from pH 4 causing the microgels to swell[31]. After the adsorption of PVAm to the surface of VAA-NIPAM microgels, the swelling behaviours of microgels changed since the dissociation response of PVAm is opposite with respect to microgels. The primary amine groups on PVAm are fully ionized at pH 3 and the degree of ionization reduces with increasing pH values. Thus the swelling behaviours of PVAm-abs-MG were the compromise between carboxylic acid groups and primary amine groups. In both figures, the maximum swelling ratio rises with a reduced crosslinked density of microgels indicating a decrease in microgel stiffness.

Generally, the NIPAM based microgels are synthesized at 70°C leading to the formation of gel particles with sub-micron diameters[6-7, 42]. In order to change the size of the microgels within the sub-micron range, different concentrations of surfactant SDS and initiator APS were introduced to the synthesis solution. By stabilizing the small particles, increasing SDS concentration could result in smaller microgel particles[7]. APS initiated the reaction by decomposition to form primary radicals contributing to the formation of the precursor particles[43]. Increasing the concentration of APS leads to the production of more nuclei and thus smaller microgel particles. Thus, microgels particle with a diameter lower than 500 nm (s02-s04) were prepared by varying the concentration of SDS and APS. To synthesize microgels with a diameter over a micron, temperature control is the key issue. Lower temperatures limit the decomposition of APS leading to lower concentration of nuclei[43-44]. This causes the microgels to grow to bigger sizes. However, it is possible to form coagulum when the reaction temperature is low[45]. By the introduction of a temperature ramp at the nuclei stage during the microgel synthesis, the nucleation stage is altered by the growth of the particles[32, 46]. The phase separation in the early stage avoids the formation of coagulum. Therefore, VAA-NIPAM MGs (S15-S25) with diameters over one micron were prepared by changing the reaction temperature. The adsorption of PVAm to VAA-NIPAM microgels were the same as described above and the amine content was controlled at 10w%. The pH dependences of VAA-NIPAM MGs and PVAm-abs-MGs with different sizes are shown in Figure 2. The swelling behaviours shown in Figure 2 are consistent with the results displayed in Figure 1. Thus, PVAm-abs-MGs with a diameter range from 200 nm to 2μm were successfully prepared.

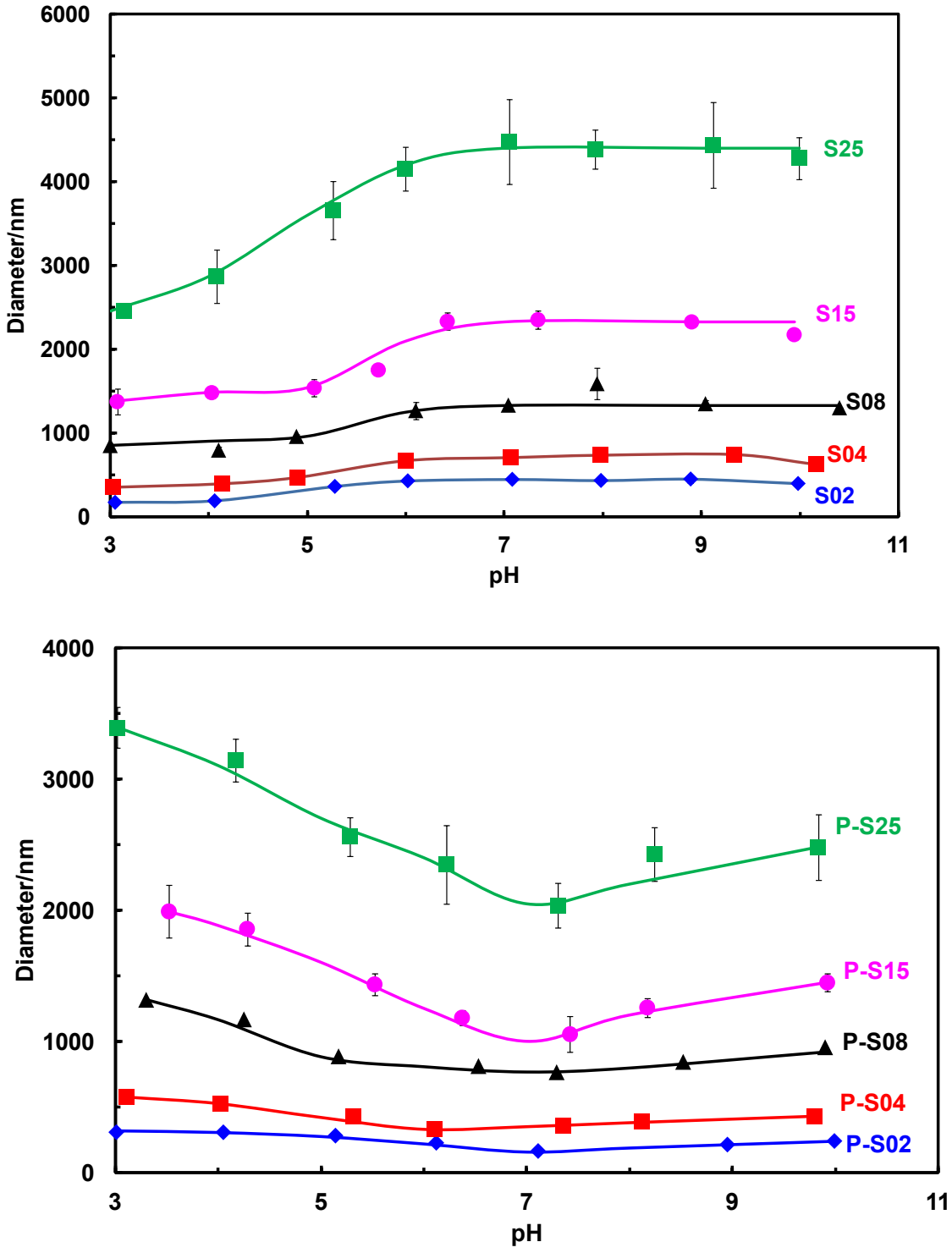

Figure 2 pH dependences of VAA-NIPAM MG and PVAm-abs-MG with different sizes

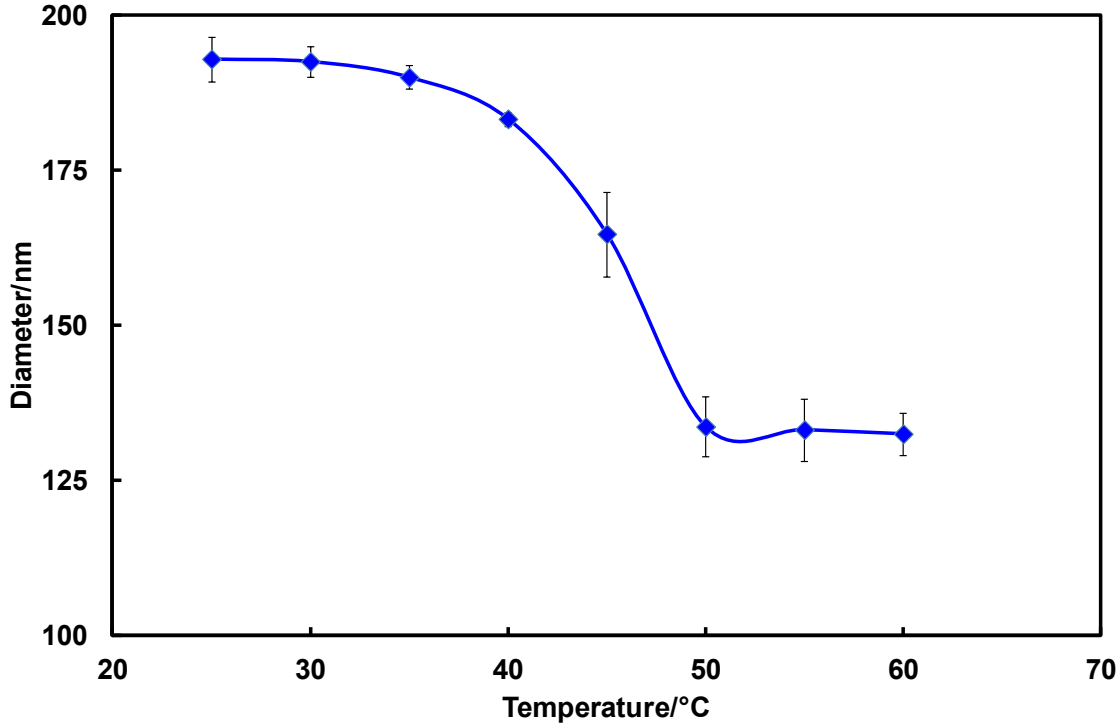

Figure 3 Temperature dependence of PVAm-abs-MG (P-S02)

Figure 3 shows the thermosensitivity of PVAm-abs-MG at pH7. After adsorbing a thin layer of PVAm onto the surface of VAA-NIPAM microgels, the PVAm-abs-MG still held the thermosensitive property. As shown in Figure 3, the diameter of PVAm-abs-MG reduced dramatically with increasing temperature indicating that the microgels went through a volume phase transition and the volume phase transition temperature was around 50°C.

Carboxylated polystyrene latex was introduced to this study as a model of highly crosslinked microgels since a high concentration of crosslinker leads to failure of particle formation during synthesis[6]. The amount of PVAm adsorbed to carboxylated latex was controlled by mixing conditions and unabsorbed PVAm was removed by centrifugation. The characterization of PVAm-abs-PS is shown in Figure 4. The diameter of PVAm-abs-PS did not change with pH since the latex was a solid particle and the surface charges altered with pH could not induce the deformation of particles. The electrophoretic mobilities of PVAm-abs-MG varied with pH values. The positive values of electrophoretic mobilities at low pH indicated positive charges of latex introduced by protonated primary amine groups of PVAm. The negative values of electrophoretic mobilities at high pH reflected the negative charges contributed by the dissociation of carboxylic acid groups originally from latex.

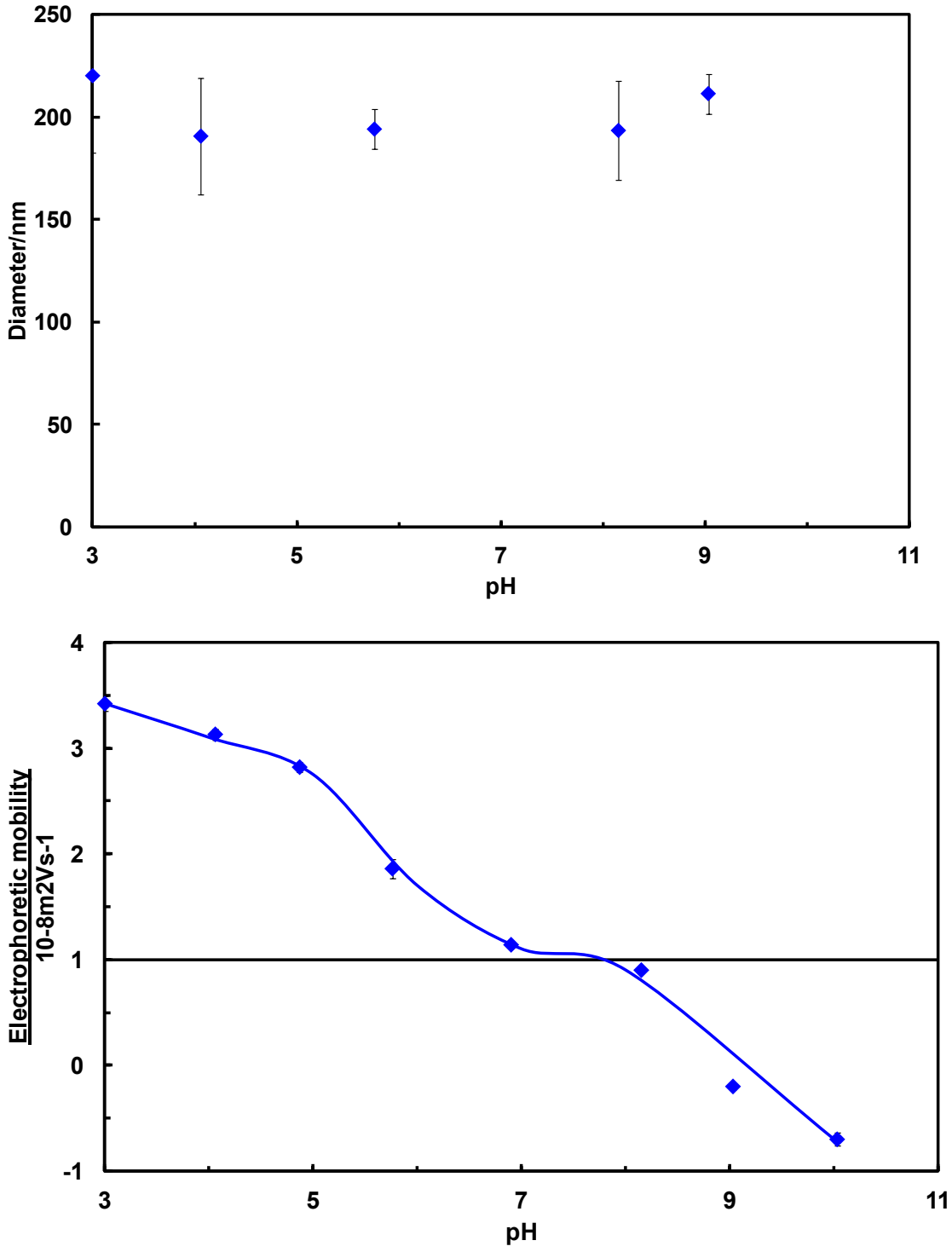

Figure 4 pH dependence of PVAm-abs-PS

To prepare cellulose films with different roughness, different precipitation conditions and substrates were tested. The cellulose films were dried in vacuum oven to get flat surfaces. The morphology of regenerated cellulose films from IL depends on the conditions in which the IL solution contacts with regenerated solvent[26]. For casting methods, the roughness of substrate supporting the regenerated cellulose films could be another factor influencing the roughness of cellulose films. Figure 5 shows the roughness measurements of cellulose films prepared under different conditions. The roughness of cellulose films was measured in wet condition. The roughness was expressed as [47]

$$R_a = \frac{1}{MN}\sum_{j=1}^{N}\sum_{i=1}^{M}\left|Z_{ij}\right| \qquad \text{Equation 2}$$

where M and N are the number of data points in X and Y respectively, and Z is the surface height relative to the mean plane.

The first film with a roughness of 27.08 nm was prepared by slowly coagulating of the IL containing cellulose under saturated water vapour overnight followed by soaking in deionized water to dissolve IL completely. The roughness of the polished silicon wafer that supported the regenerated cellulose film was around 30nm, which is close to the roughness of cast cellulose films. The second and the third film shown in Figure 5 were supported on the same polished silicon wafer but cast in different solvents. The second film was cast in water/ethanol resulting in a surface roughness of 326.89 nm, which is one order larger than the roughness of the film cast in water vapour. The third film that was cast in water had a surface roughness of 634.07nm. The result of different casting solvents led to various exchange rates of IL during film precipitation and thus numerous roughness on cellulose films. The last film shown in Figure 5 had the largest surface roughness of 1μm. This cellulose film was cast on unpolished silicon wafer resulting in roughness of 1μm.

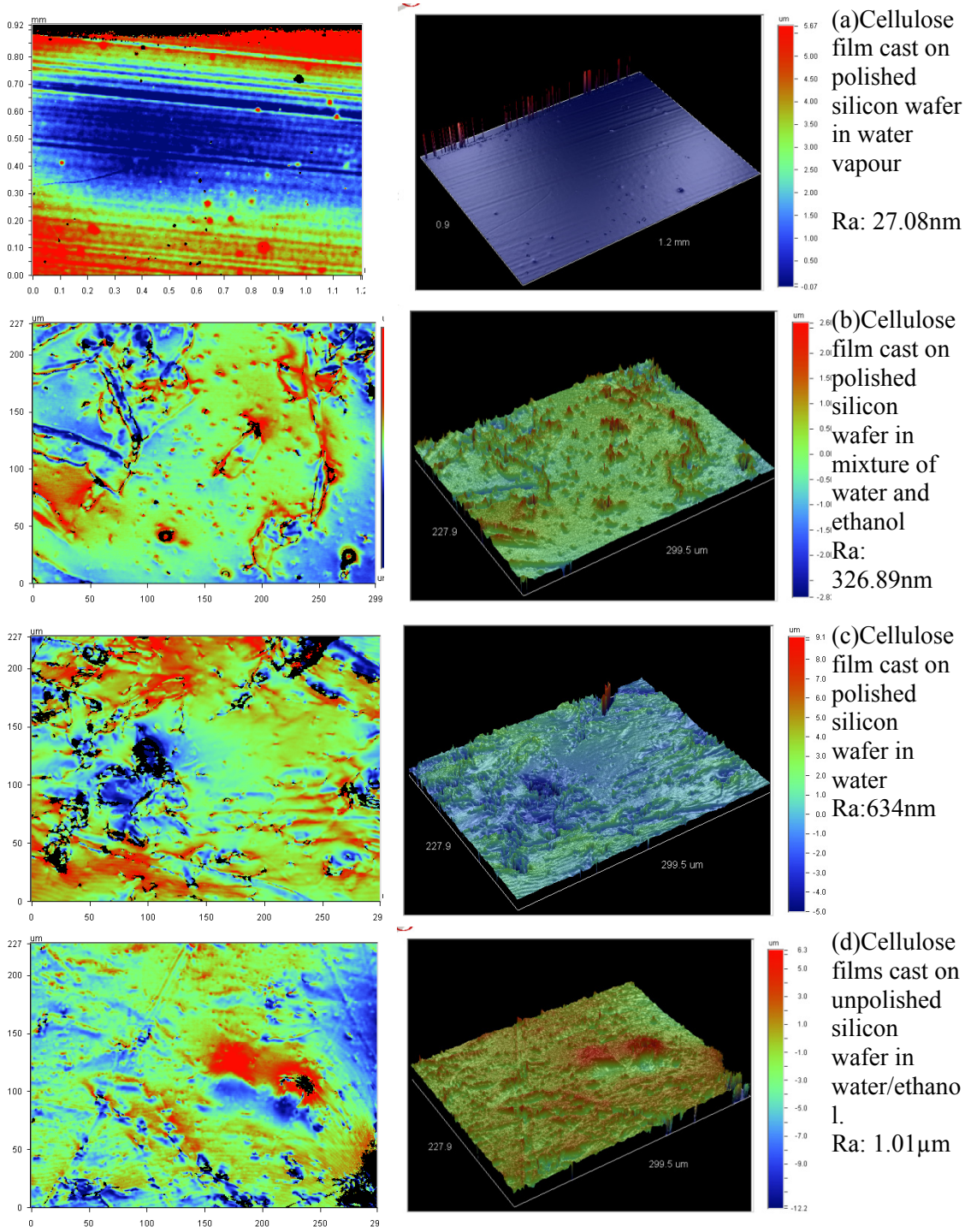

Figure 5 Profilometer generated images for surfaces roughness of wet cellulose films cast from IL

Figure 6 shows the influence of the crosslink density of microgels on wet adhesion to cellulose. The cellulose films involved in this graph have smooth surfaces (Ra=27.08nm). The different crosslink densities were achieved by varying the crosslink degree of VAA-NIPAM microgels. The highest crosslink density was obtained by the replacement of VAA-NIPAM microgel with a carboxylated latex of the similar size. The amine content was 10wt% for PVAm-abs-MG and PVAm-abs-PS. As shown in Figure 6, the delamination force only dropped 20% when the crosslink density of microgels increased from 3% to 15%. After the substitution of soft microgels to hard latex, the delamination force reduced by 50%. Thus, the wet adhesion slowly decreased with an increment in the crosslink density of polymeric adhesives.

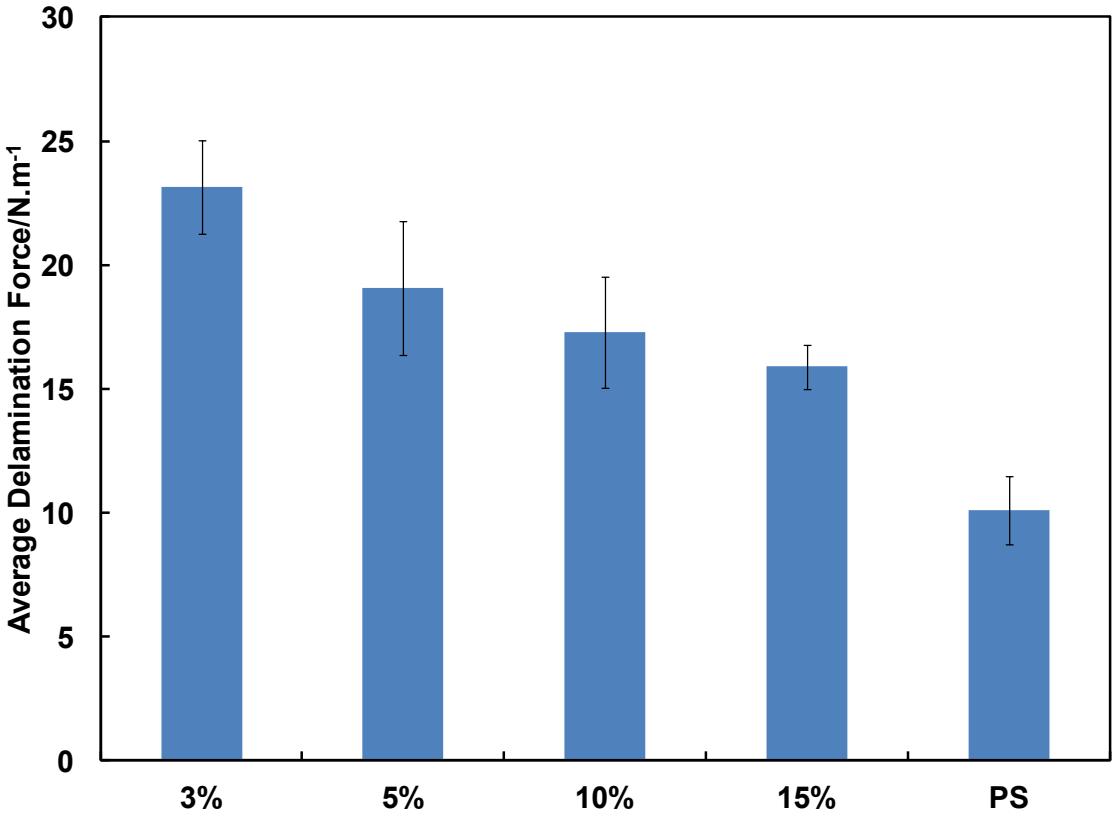

Figure 6 The effect of crosslink density of microgels on wet adhesion with smooth cellulose surfaces (Ra=27.1nm)

To study the effect of the surface roughness of a cellulose surface to wet adhesion with microgels, a series of PVAm-abs-MGs with different sizes and cellulose films with different surface roughnesses were prepared. The amine content of PVAm-abs-MGs were maintained at 10wt% while the sizes of PVAm-abs-MGs ranged from 160nm to 2050nm. Homemade cellulose films were cut into certain dimensions to fit in a 90° peel tester developed at McMaster Univesity.[48-49] Cellulose films were oxidised by

TEMPO/NaBr/NaClO before they were laminated with polymers via pipettes application. All of the cellulose laminates were dried in a conditioned room and then rewetted before peel tests. The wet adhesion measurements are shown in Figure 7. For the cellulose film with a roughness of 27.08nm, which could be considered as smooth surfaces, the wet adhesion contributed by PVAm-abs-MGs with different sizes was almost the same. In another word, the size of PVAm-abs-MGs did not influence the wet adhesion to smooth cellulose films. This result is consistent with Miao's study[50]. When the cellulose surfaces became rougher, the influence of the microgel size on wet adhesion became relevant especially for smaller particles. For microgels with a diameter of 160nm, the delamination force decreased gradually with an increased surface roughness of cellulose films while for microgel with diameters of 1000nm and 2050nm exhibited, delamination forces that did not relate to the roughness of cellulose films. Therefore, for rough cellulose surfaces, relatively larger microgels provided strong wet adhesion.

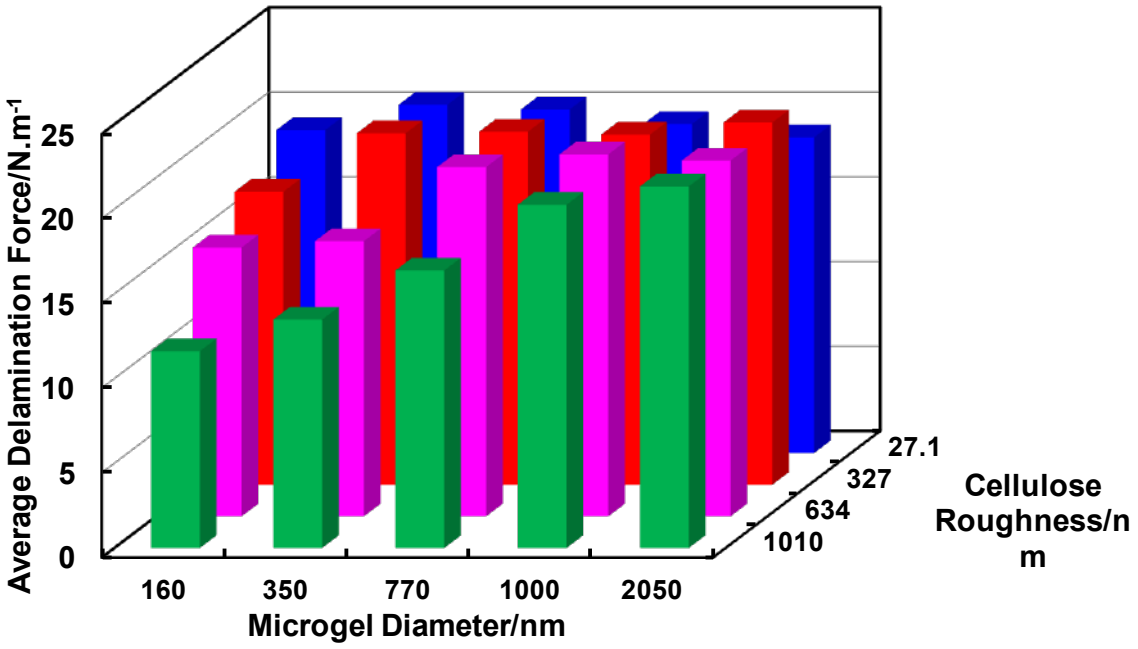

Figure 7 The influence of microgel size on wet adhesion to rough cellulose surfaces

The NIPAM based microgels were of specific interest due to their thermosensitivity. After the adsorption of PVAm to the surface of VAA-NIPAM microgels, PVAm-abs-MGs remained sensitive to temperature, which is shown in Figure 3. Cellulose laminates were prepared by adsorbing PVAm-abs-MG at 25°C and 50°C followed by washing in 1mM NaCl solutions at the same temperature as adsorption. The phase volume transition

of PVAm-abs-MG could be identified by the color change of dispersion. The wet adhesion measurements are shown in Figure 8 . The laminates prepared at 25°C achieved a higher delamination force which was twice as that obtained by laminates prepared at 50°C.

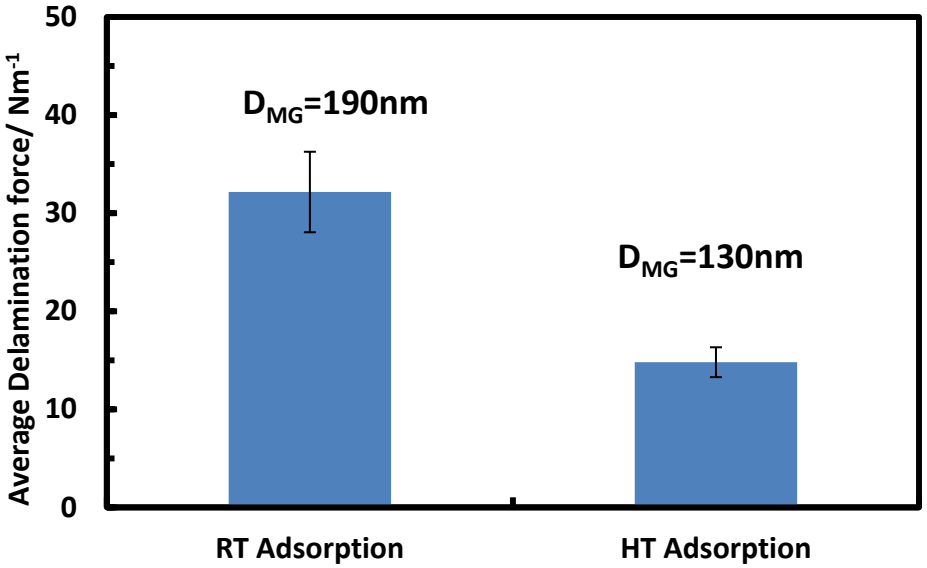

Figure 8 The effect of temperature on wet adhesion of PVAm-abs-MG with smooth cellulose surfaces

The wet adhesion with cellulose is related to the amount of adhesives deposited onto cellulose surfaces. Therefore, the temperature effect on the performance of PVAm-abs-MGs was studied by QCM as well. Aldehyde groups were introduced onto the QCM sensors by TEMPO/NaBr/NaClO oxidation. PVAm-abs-MGs were adsorbed onto QCM sensors with cellulose coatings at different temperatures. The unabsorbed microgels were washed off by 1mM NaCl solution at the same temperature. Figure 9 compares the frequency shift and dissipation change for the PVAm-abs-MG adsorbed on cellulose at different temperatures. The frequency increase with temperature initially indicated the deswelling of cellulose. PVAm-abs-MG adsorbed at 45°C resulted in a frequency that dropped by 56.3 Hz whereas PVAm-abs-MG adsorbed at 25°C resulted in a frequency that dropped by 177.58Hz. According to the Sauerbrey Equation, for rigid adsorbed layers, the change of frequency is proportional to the change of mass[51-52]:

$$\Delta f = \frac{C\Delta m}{n} \qquad \text{Equation 3}$$

where n is the overtone number, C is the mass sensitivity constant.

However, microgels loses at least 50wt% water when the temperature is over the LCST.[53] Thus for microgels adsorbed at different temperatures, the change of mass indicated by QCM was the sum of the mass change of microgels and water. To exclude the influence of water in the mass change, the sensor with microgels adsorbed at 45°C was cooled to 25°C. Compared to the frequency baseline at 25°C, the frequency change induced by microgel adsorbed at 45°C was 115.2Hz and the frequency change caused by microgel adsorbed at 25°C was 201.6Hz. Referred to Squerbrey Equation, the mass change on oxidised cellulose caused by microgel adsorption at 25°C was larger than that at 45°C by about a factor of 2. Therefore, the number of microgels adsorbed onto oxidised cellulose at 25°C was about twice of that at 45°C.

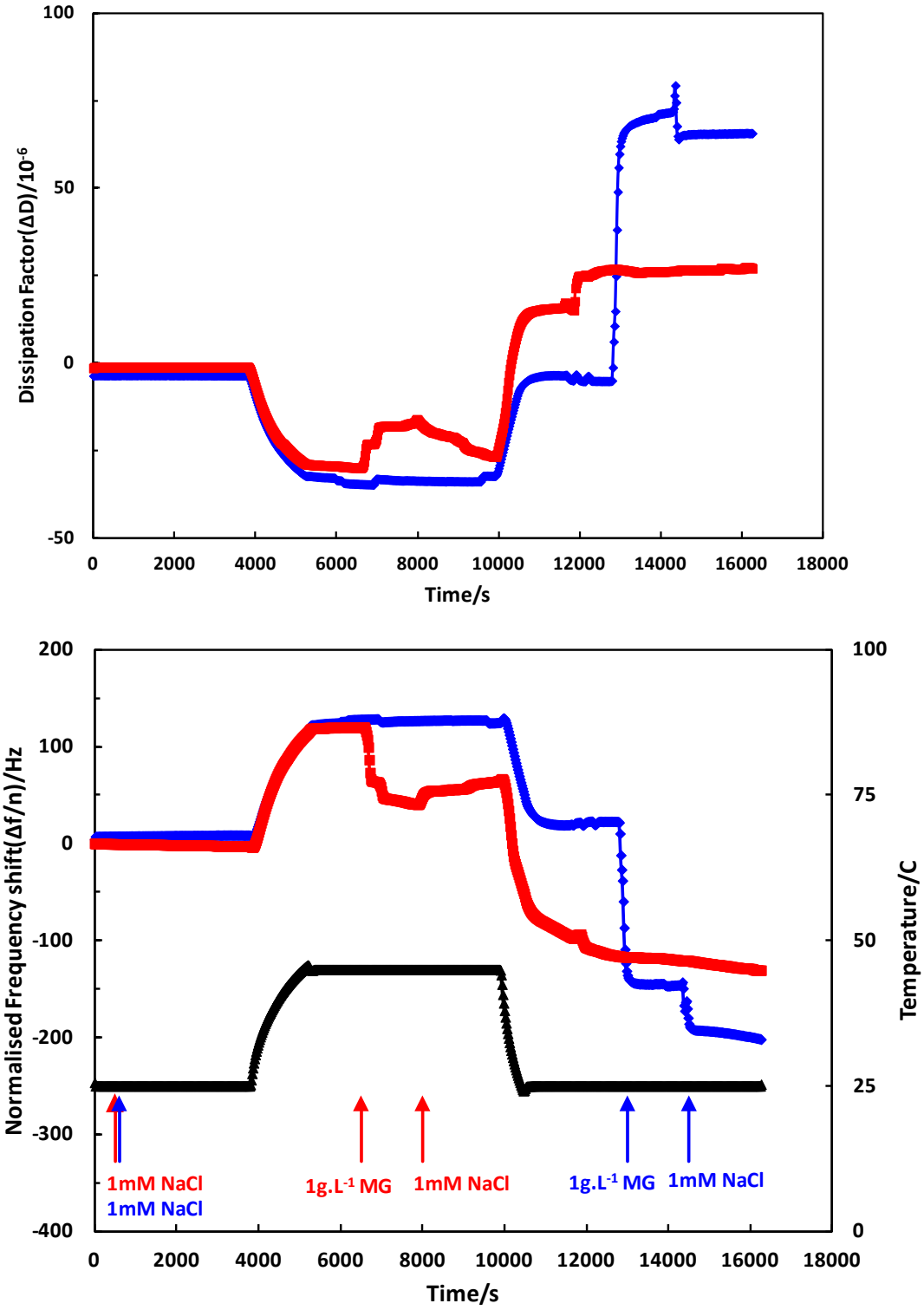

Figure 9 Adsorption of PVAm-abs-MG onto oxidised cellulose coated QCM sensors at different temperatures (1mM NaCl, pH=7)

The swelling behaviours of microgels on cellulose with covalent bonds and without covalent bonds were monitored by QCM as well. Since aldehyde groups were introduced to cellulose by oxidation, covalent bonds could form between the aldehyde groups of cellulose and the amine groups of PVAm-abs-MGs. After the adsorption of PVAm-abs-MGs onto the QCM sensor, amide bonds formed when the sensor was drying in the conditioning room. As shown in Figure 10, the frequency change induced by microgel swelling on cellulose without covalent bonds was around 70Hz and the frequency change induced by microgel swelling on cellulose with covalent bonds was the same degree. Therefore, after covalent bonding with cellulose, the ability of microgel to swell did not change.

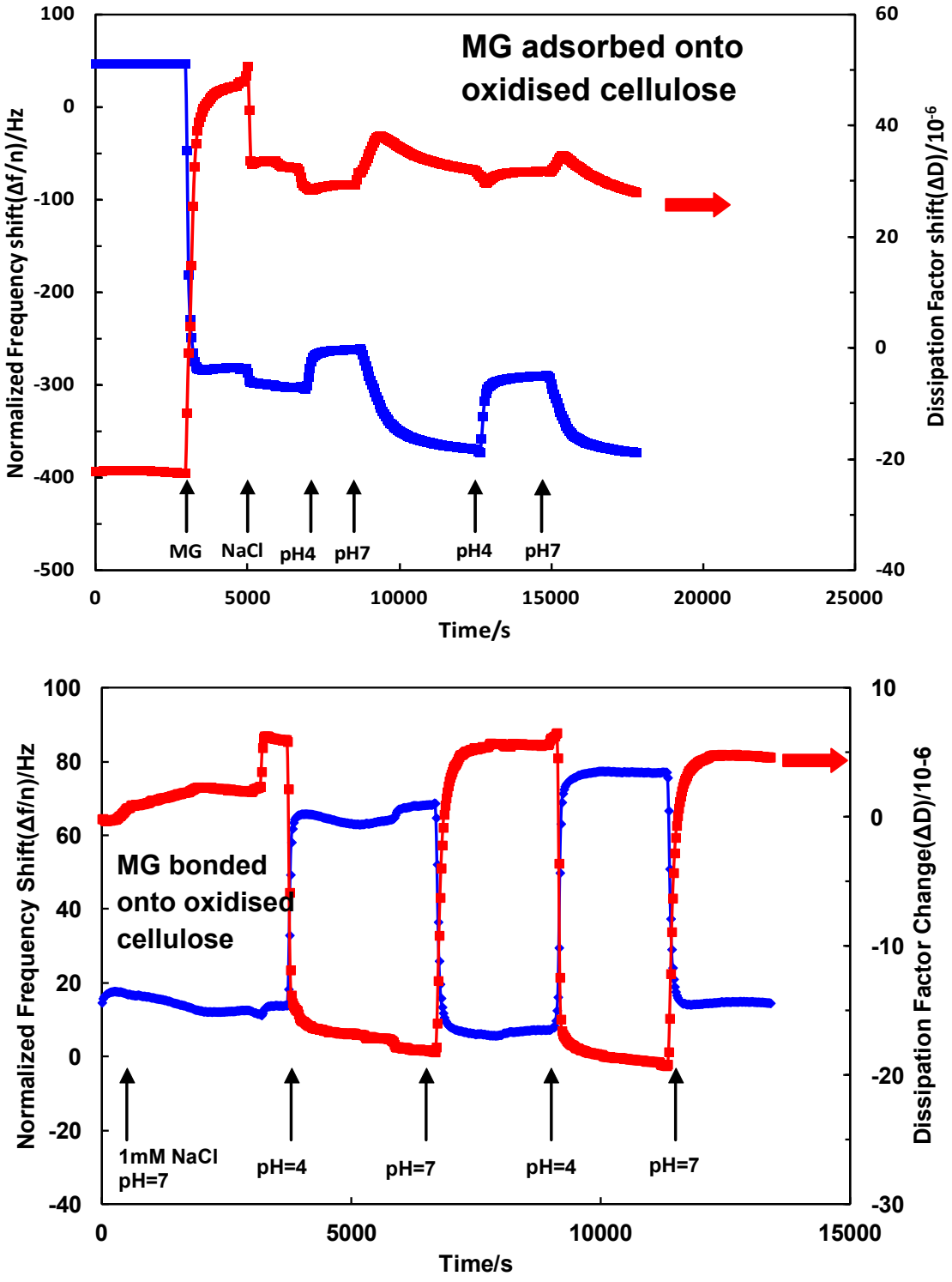

Figure 10 Swelling behaviours of PVAm-abs-MG on oxidised cellulose coated QCM sensors before and after covalent bonded with cellulose

4.4 Discussion

To understand the wet strengthening mechanism of microgels based adhesives to cellulose, the relationship between the size of microgels and the roughness of cellulose surfaces was investigated. Glen et al. delivered two simple models of strength enhancement introduced by adhesives to rough surfaces[54]. They pointed out that the strength could be provided either by pulling off adhesives from deep cylinder holes on the smooth surfaces or via a force to break the continuous layer of adhesives. Since the regenerated cellulose films were prepared by precipitation from ionic liquid, the cellulose films were closed films without pores[10, 26]. In addition, the sizes of microgels ranged from 200nm to 2000nm. Thus, it is impossible for microgels to penetrate into the cellulose film in order to contribute to wet adhesion. In this case, microgels work as adhesives by contacting both cellulose films.

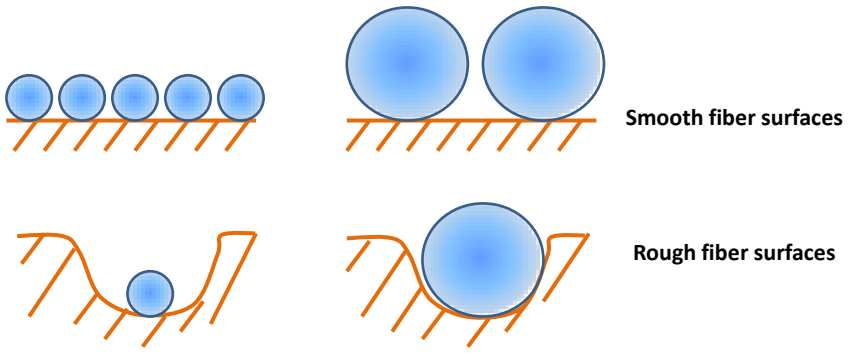

Figure 11 Microgels on cellulose membranes with different roughness

According to the study of Shahid et.al., the cleavage strength increased with the roughness of adhered surfaces due to the increment of surface area[55]. Figure 7 displays that, for small microgel particles with a diameter lower than 1μm, the peel force decreases with rougher surfaces while for microgel particles larger than 1μm, the peel force was stable over cellulose surfaces with different roughness. This result seemed to be the opposite of Shahid's study. However, considering the effective contact area between adhesives and adhered surfaces, both results are .in agreement with each other. The real

contact area between adhesives and substrates could be different from the surface area of substrates and the adhesion strength should depend on the real contact area[56]. As shown in Figure 11, when the microgels were added onto relatively smooth cellulose films, every microgel could contact effectively with cellulose films despite the size of microgels. Whereas, when small microgels were added between rough cellulose films, they were too small to contact both surfaces of the cellulose films in order to contribute to the wet adhesion. In other words, the decreased wet adhesion was due to the reduction of the effective contact area between small microgels and rough cellulose films. Therefore, if the diameter of the microgel based adhesives is smaller than the scale of the surface roughness of the cellulose films, the wet adhesion weakens by an increment with respect to the cellulose roughness; if the diameter of the microgel based adhesives is larger than the scale of the surface roughness of cellulose, the wet adhesion will not be influenced by cellulose roughness.

The stiffness of microgel based adhesives is another important property that could influence the wet adhesion to cellulose. As shown in Figure 1 and Figure 4, PVAm-abs-MG could swell with the dissociation of functional groups even with the highest crosslink density at 15%. The particle size of PVAm-abs-PS did not change with pH indicating the hardness of particles. According to Equation 1, the crosslink densities of microgels varied from 3% to 15% resulting in the stiffness of microgels increasing by 4 fold. Polystyrene latex is a solid material and the young's modulus of polystyrene is $3*10^9$ Pa, which is about 5 orders' larger than that of microgels[57-58]. Figure 6 shows that the wet adhesion was reduced by increasing the crosslink densities of microgels and when VAA-NIPAM microgels were replaced with latex, the wet adhesion with cellulose was dramatically weakened. This result is consistent with the model described in chapter 3. The stiffer the microgels, the weaker the wet adhesion with cellulose. The reason for failure most likely happened between PVAm and microgels because the covalent bonds between PVAm and cellulose were stronger than the electrostatic attraction between PVAm and microgels. The delamination force was determined by the detachment of PVAm from microgels. When the microgels become stiffer, the deformation of microgels under an external force is smaller resulting in the detachment of PVAm.

The impact of temperature on the performance of PVAm-abs-MG adhered to cellulose was opposite with respect to our hypothesis. Originally, we thought that PVAm-abs-MG shrunk at high temperatures and more microgels would adsorb onto cellulose surfaces resulting in high wet adhesion. At a glance of Figure 8 and Figure 9, the results showed that the mass of PVAm-abs-MG adsorbed onto cellulose at 45°C was about half of that at 25°C. In addition, the wet adhesion with cellulose enhanced by PVAm-abs-MG adsorbed at 45°C was around half of that at 25°C. The wet adhesion with cellulose provided by PVAm-abs-MG was proportional to the mass of the PVAm-abs-MG adsorbed onto cellulose. The adsorption density of charged microgels onto surfaces is mainly determined by the electrostatic interactions between microgels.[59-60] Microgels with the same charges are repulsive to each other and the distance between them depends on particle-particle repulsion. When the temperature is over the LCST, the volumes of microgels decrease dramatically and the charge density on the surfaces of the microgels

increased resulting in a larger repulsion between microgels. Because the distance between microgels become larger and the packing density decrease at higher temperature, the wet adhesion with cellulose decreased.

4.5 Conclusion

By varying the cellulose precipitation conditions, cellulose films with different roughness were prepared.

Increasing the stiffness of microgels weakens the wet adhesion with cellulose since the deformation of microgels under external forces becomes smaller resulting in the detachment of PVAm.

The influence of the size of microgels on wet adhesion to cellulose depends on the relative roughness of cellulose. For smooth cellulose surfaces, the wet adhesion is not sensitive to the size of microgels. For rough cellulose surfaces, larger microgels take the advantage of bulk volume that could fill the gap formed between cellulose surfaces, which contribute more to wet adhesion.

Increasing temperature reduced the amount of microgels adsorbed onto wet cellulose resulting in lower wet adhesion with cellulose.

Microgels were able to reswell after drying in the cellulose laminates.

4.6 References

1. Miao, C.; Pelton, R.; Chen, X.; Leduc, M., Microgels versus Linear Polymers for Paper Wet Strength - Size Does Matter. *Appita Journal: Journal of the Technical Association of the Australian and New Zealand Pulp and Paper Industry* 2007, *60* (6), 465.

2. Burmistrova, A.; Richter, M.; Uzum, C.; Klitzing, R., Effect of cross-linker density of P(NIPAM-co-AAc) microgels at solid surfaces on the swelling/shrinking behaviour and the Young's modulus. *Colloid & Polymer Science* 2011, *289* (5), 613-624.

3. Li, L. C., A.; Pelton, R., A new analysis of filler effects on paper strength. *J Pulp Pap Sci* 2002, *28* (8).

4. Yan, Z.; Liu, Q.; Deng, Y.; Ragauskas, A., Improvement of paper strength with starch modified clay. *J Appl Polym Sci* 2005, *97* (1), 44-50.

5. Yoon, S.-Y.; Deng, Y., Clay–starch composites and their application in papermaking. *J Appl Polym Sci* 2006, *100* (2), 1032-1038.

6. Pelton, R. H.; Chibante, P., Preparation of aqueous latices with N-isopropylacrylamide. *Colloids and surfaces* 1986, *20* (3), 247.

7. Pelton, R., Temperature-sensitive aqueous microgels. *Advances in Colloid and Interface Science* 2000, *85* (1), 1.

8. Ma, X.; Xi, J.; Zhao, X.; Tang, X., Deswelling comparison of temperature-sensitive poly(N-isopropylacrylamide) microgels containing functional □ OH groups with different hydrophilic long side chains. *Journal of Polymer Science Part B: Polymer Physics* 2005, *43* (24), 3575-3583.

9. Jones, C. D.; Lyon, L. A., Shell-Restricted Swelling and Core Compression in Poly(N-isopropylacrylamide) Core−Shell Microgels. *Macromolecules* 2003, *36* (6), 1988-1993.

10. Hishikawa, Y.; Togawa, E.; Kataoka, Y.; Kondo, T., Characterization of amorphous domains in cellulosic materials using a FTIR deuteration monitoring analysis. *Polymer* 1999, *40* (25), 7117-7124.

11. Holmberg, M.; Wigren, R.; Erlandsson, R.; Claesson, P. M., Interactions between cellulose and colloidal silica in the presence of polyelectrolytes. *Colloids and Surfaces A: Physicochemical and Engineering Aspects* 1997, *129-130* (0), 175-183.

12. Holmberg, M.; Berg, J.; Stemme, S.; Ödberg, L.; Rasmusson, J.; Claesson, P., Surface Force Studies of Langmuir–Blodgett Cellulose Films. *Journal of Colloid and Interface Science* 1997, *186* (2), 369.

13. Gunnars, S.; Wågberg, L.; Cohen Stuart, M. A., Model films of cellulose: I. Method development and initial results. *Cellulose* 2002, *9* (3), 239-249.

14. Bornside, D. E.; Brown, R. A.; Ackmann, P. W.; Frank, J. R.; Tryba, A. A.; Geyling, F. T., *The effects of gas phase convection on mass transfer in spin coating*. AIP: 1993; Vol. 73, p 585-600.

15. Kontturi, E.; Thüne, P. C.; Niemantsverdriet, J. W., Cellulose Model SurfacesSimplified Preparation by Spin Coating and Characterization by X-ray Photoelectron Spectroscopy, Infrared Spectroscopy, and Atomic Force Microscopy. *Langmuir* 2003, *19* (14), 5735-5741.

16. Chanzy, H.; Paillet, M.; Hagège, R., Spinning of cellulose from N-methyl morpholine N-oxide in the presence of additives. *Polymer* 1990, *31* (3), 400-405.

17. Paillet, M.; Peguy, A., New biodegradable films from exploded wood solutions. *J Appl Polym Sci* 1990, *40* (3-4), 427-433.

18. Chanzy, H.; Peguy, A.; Chaunis, S.; Monzie, P., Oriented cellulose films and fibers from a mesophase system. *Journal of Polymer Science: Polymer Physics Edition* 1980, *18* (5), 1137-1144.

19. Bianchi, E.; Ciferri, A.; Conio, G.; Tealdi, A., Fiber formation from liquid-crystalline precursors. II. Cellulose in N,N-dimethylacetamide-lithium chloride. *Journal of Polymer Science Part B: Polymer Physics* 1989, *27* (7), 1477-1484.

20. Focher, B.; Marzetti, A.; Conio, G.; Marsano, E.; Cosani, A.; Terbojevich, M., Fibers from DMAc-LiCl solutions of steam exploded wood. *J Appl Polym Sci* 1994, *51* (4), 583-591.

21. Kontturi, E.; Tammelin, T.; Osterberg, M., Cellulose-model films and the fundamental approach. *Chemical Society Reviews* 2006, *35* (12), 1287-1304.

22. Schaub, M.; Wenz, G.; Wegner, G.; Stein, A.; Klemm, D., Ultrathin films of cellulose on silicon wafers. *Adv Mater* 1993, *5* (12), 919-922.

23. Zhang, H.; Wu, J.; Zhang, J.; He, J., 1-Allyl-3-methylimidazolium Chloride Room Temperature Ionic Liquid: A New and Powerful Nonderivatizing Solvent for Cellulose. *Macromolecules* 2005, *38* (20), 8272-8277.

24. Wu, J.; Zhang, J.; Zhang, H.; He, J.; Ren, Q.; Guo, M., Homogeneous Acetylation of Cellulose in a New Ionic Liquid. *Biomacromolecules* 2004, *5* (2), 266-268.

25. Zhu, S.; Wu, Y.; Chen, Q.; Yu, Z.; Wang, C.; Jin, S.; Ding, Y.; Wu, G., Dissolution of cellulose with ionic liquids and its application: a mini-review. *Green Chemistry* 2006, *8* (4), 325-327.

26. Swatloski, R. P.; Spear, S. K.; Holbrey, J. D.; Rogers, R. D., Dissolution of Cellose with Ionic Liquids. *J. Am. Chem. Soc.* 2002, *124* (18), 4974-4975.

27. Barthel, S.; Heinze, T., Acylation and carbanilation of cellulose in ionic liquids. *Green Chemistry* 2006, *8* (3), 301-306.

28. Gutowski, K. E.; Broker, G. A.; Willauer, H. D.; Huddleston, J. G.; Swatloski, R. P.; Holbrey, J. D.; Rogers, R. D., Controlling the Aqueous Miscibility of Ionic Liquids: Aqueous Biphasic Systems of Water-Miscible Ionic Liquids and Water-Structuring Salts for Recycle, Metathesis, and Separations. *J. Am. Chem. Soc.* 2003, *125* (22), 6632-6633.

29. Swatloski, R. P.; Holbrey, J. D.; Memon, S. B.; Caldwell, G. A.; Caldwell, K. A.; Rogers, R. D., Using Caenorhabditis elegans to probe toxicity of 1-alkyl-3-methylimidazolium chloride based ionic liquids. *Chemical Communications* 2004, (6), 668-669.

30. Sun, N.; Rahman, M.; Qin, Y.; Maxim, M. L.; Rodriguez, H.; Rogers, R. D., Complete dissolution and partial delignification of wood in the ionic liquid 1-ethyl-3-methylimidazolium acetate. *Green Chemistry* 2009, *11* (5), 646-655.

31. Hoare, T.; Pelton, R., Highly pH and temperature responsive microgels functionalized with vinylacetic acid. *Macromolecules* 2004, *37* (7), 2544-2550.

32. Meng, Z.; Smith, M.; Lyon, L., Temperature-programmed synthesis of micron-sized multi-responsive microgels. *Colloid & Polymer Science* 2009, *287* (3), 277-285.

33. Meng, Z. Self-assembly and chemo-ligation strategies for polymeric multi-responsive microgels Ph.D Thesis, Georgia Institute of Technology, 2009.

34. Kitaoka, T.; Isogai, A.; Onabe, F., Chemical modification of pulp fibers by TEMPO-mediated oxidation *Nordic Pulp & Paper Reserach Journal* 1999, *14* (4), 279-284.

35. Bottom, V. E., *Introduction to quartz crystal unit design*. New York: Van Nostrand Reinhold, 1982.

36. Treloar, L. R. G., *The physics of rubber elasticity*. 2d ed. -- ed.; Oxford: Clarendon Press, 1958.

37. Tagit, O.; Tomczak, N.; Vancso, G. J., Probing the Morphology and Nanoscale Mechanics of Single Poly(N-isopropylacrylamide) Microgels Across the Lower-Critical-Solution Temperature by Atomic Force Microscopy. *Small* 2008, *4* (1), 119-126.

38. Wen, Q. V., A. M.; Pelton, R., Cationic Polyvinylamine Binding to Anionic Microgels Yields Kinetically Controlled Structures. *Journal of Colloid and Interface Science* 2012, accepted.

39. Shibayama, M.; Tanaka, T., Volume phase transition and related phenomena of polymer gels

Responsive Gels: Volume Transitions I. Dušek, K., Ed. Springer Berlin / Heidelberg: 1993; Vol. 109, pp 1-62.

40. Sierra-Martín, B.; Choi, Y.; Romero-Cano, M. S.; Cosgrove, T.; Vincent, B.; Fernández-Barbero, A., Microscopic Signature of a Microgel Volume Phase Transition. *Macromolecules* 2005, *38* (26), 10782-10787.

41. Varga, I.; Gilányi, T.; Mészáros, R.; Filipcsei, G.; Zrínyi, M., Effect of Cross-Link Density on the Internal Structure of Poly(N-isopropylacrylamide) Microgels. *The Journal of Physical Chemistry B* 2001, *105* (38), 9071-9076.

42. Kawaguchi, H; Kawahara, M.; Yaguchi, N.; Hoshino, F.; Ohtsuka, Y., *Hydrogel microspheres. I: Preparation of monodisperse hydrogel microspheres of submicron or micron size*. Nature Publishing Group: Avenel, NJ, ETATS-UNIS, 1988; Vol. 20.

43. Kolthoff, I. M.; Miller, I. K., The Chemistry of Persulfate. I. The Kinetics and Mechanism of the Decomposition of the Persulfate Ion in Aqueous Medium1. *J. Am. Chem. Soc.* 1951, *73* (7), 3055-3059.

44. Meng, Z.; Cho, J. K.; Debord, S.; Breedveld, V.; Lyon, L. A., Crystallization Behavior of Soft, Attractive Microgels. *The Journal of Physical Chemistry B* 2007, *111* (25), 6992-6997.

45. Downey, J. S.; McIsaac, G.; Frank, R. S.; Stöver, H. D. H., Poly(divinylbenzene) Microspheres as an Intermediate Morphology between Microgel, Macrogel, and Coagulum in Cross-Linking Precipitation Polymerization. *Macromolecules* 2001, *34* (13), 4534-4541.

46. Zhou, S.; Chu, B., Synthesis and Volume Phase Transition of Poly(methacrylic acid-co-N-isopropylacrylamide) Microgel Particles in Water. *The Journal of Physical Chemistry B* 1998, *102* (8), 1364-1371.

47. Eichenlaub, S.; Gelb, A.; Beaudoin, S., Roughness models for particle adhesion. *Journal of Colloid and Interface Science* 2004, *280* (2), 289-298.

48. Kurosu, K.; Pelton, R., Simple lysine-containing polypeptide and polyvinylamine adhesives for wet cellulose. *J Pulp Pap Sci* 2004, *30* (8), 228-232.

49. John-Louis, D.; Robert, B.; Robert, P.; Marc, L., The mechanism of polyvinylamine wet-strengthening. 2005.

50. Miao, C.; Chen, X.; Pelton, R., Adhesion of Poly(vinylamine) Microgels to Wet Cellulose. *Industrial & Engineering Chemistry Research* 2007, *46* (20), 6486-6493.

51. Sauerbrey, G., Verwendung von Schwingquarzen zur Wägung dünner Schichten und zur Mikrowägung. *Zeitschrift für Physik A Hadrons and Nuclei* 1959, *155* (2), 206-222.

52. Kontturi, K. S.; Tammelin, T.; Johansson, L.-S.; Stenius, P., Adsorption of Cationic Starch on Cellulose Studied by QCM-D. *Langmuir* 2008, *24* (9), 4743-4749.

53. Pelton, R.; Hong, J., Some properties of newsprint impregnated with polyvinylamine. *Tappi J.* 2002, *1* (10), 21.

54. Gent, A. N.; Lin, C. W., Model Studies of the Effect of Surface Roughness and Mechanical Interlocking on Adhesion. *The Journal of Adhesion* 1990, *32* (2), 113.

55. Shahid, M.; Hashim, S. A., Effect of surface roughness on the strength of cleavage joints. *International Journal of Adhesion and Adhesives* 2002, *22* (3), 235-244.

56. Kalnins, M.; Sirmacs, A.; Malers, L., On the importance of some surface and interface characteristics in the formation of the properties of adhesive joints. *International Journal of Adhesion and Adhesives* 1997, *17* (4), 365-372.

57. Bucknall, C. B.; Hall, M. M., On the size of the secondary mechanical loss peak in rubber-modified polymers. *J.Mater.Sci.* 1971, *6* (2), 95-101.

58. Barentsen, W. M.; Heikens, D., Mechanical properties of polystyrene/low density polyethylene blends. *Polymer* 1973, *14* (11), 579-583.

59. Schmidt, S.; Motschmann, H.; Hellweg, T.; von Klitzing, R., Thermoresponsive surfaces by spin-coating of PNIPAM-co-PAA microgels: A combined AFM and ellipsometry study. *Polymer* 2008, *49* (3), 749.

60. Lu, Y.; Drechsler, M., Charge-Induced Self-Assembly of 2-Dimensional Thermosensitive Microgel Particle Patterns. *Langmuir* 2009, *25* (22), 13100-13105.

Chapter 5 Influence of Microgel Based Adhesives on Wet Paper Strength

In chapter 5, the preparation and characterization of microgels were conducted by me. Andrew M. Vincelli and Steven Zecchin helped me with handsheets preparation and tensile tests. Dr. Pelton contributed valuable suggestions on both experiments and data analysis. I wrote the first draft and Dr. Pelton revised it.

Chapter 5 Influence of Microgel Based Adhesives on Wet Paper Strength

Abstract

A microgel based wet strength resin was prepared by physically adsorbing PVAm onto carboxylated PNIPAM microgels. Linear PVAm was introduced for comparison. Polymeric additives were added into unbeaten, bleached, softwood kraft pulp to form handsheets. The wet tensile strength was measured as the function of PVAm molecular weight, PVAm content in microgels, polymeric coverage on fibers, and the hardness of carboxylated particles. For linear PVAm, high molecular weight PVAm gave a higher wet strength of paper. In contrast, with regards to microgels with a PVAm coating, the wet paper strength was not sensitive to the molecular weight of PVAm. In terms of PVAm loading on the surfaces of microgels, higher PVAm content contributed more to wet paper strength and 10wt%PVAm in microgels showed comparable wet paper strength to PVAm microgels which contained 100wt% PVAm. When the carboxylated microgels were replaced by carboxylated polystyrene latex, the PVAm coating still worked better than PVAm itself. But the wet strength of paper treated with PVAm-abs-MG was larger than that treated with PVAm-abs-PS by a factor of 2.

5.1 Introduction

Generally, cellulose based paper loses 90% of its tensile strength when it comes in contact with water since pulp fibers are hydrophilic and swell resulting in the destruction of fiber-fiber joints[1]. Due to the demands for paper quality, wet strength resins most commonly water soluble polymers are added into paper pulp in order to increase water resistance [2]. The wet strength of paper depends on the bonded area which could be increased by the introduction of wet strength resins used to hold the faces together.[2-3] Urea-Formaldehyde (UF) was recognized as one of the important commercial wet strength resins since it could homo-crosslink to protect the fiber-fiber bonds[4]. But the usage of UF was limited by the papermaking industry preference of a neutral pH environment[5]. Although Polyamide-Epichlorohydrin (PAE) is commonly used as a wet strength resin due to its rapid adsorption onto cellulose fibers and chemical reactivity with carboxyl groups of cellulose, the byproduct of commercial PAE solution contains organic chlorine, which leads to paper mills releasing absorbable organic chlorine into the environment [4, 6]. Therefore, polyvinylamine (PVAm) [7-9], poly(carboxylic acids)[10-11] and aldehyde-containing polymers[12-13] have been studied as candidates for environmental friendly wet strength additives. Since PVAm is highly positively charged at a wide pH range, it could be adsorbed onto anionic cellulose fibers by electrostatic interactions, which promotes the reaction between amine groups from PVAm and aldehyde groups from cellulose[14].

Compared with linear PVAm, colloidal particles could form thicker layers on surfaces due to their larger sizes. Since linear PVAm could only form a monolayer on the surface of cellulose and the amount of adsorbed linear PVAm is around 1 mg/m^2, the amount of colloidal particles adsorbed onto cellulose could be at a realizable magnitude of two orders higher[15]. Complexes formed by PVAm/CMC could serve as wet strength resins[16]. However, the formation of complexes is difficult to control and is accompanied by excess polymer in the solution, which is a major drawback considering the cost of papermaking. Miao developed PVAm microgels and showed that the handsheets treated with PVAm microgels had triple the wet strength as that with linear PVAm[17]. But the PVAm microgel synthesis followed with hydrolysis is too complicated for industrial application and the size distribution of PVAm microgels is wide ranging from nm to μm. In our previous work, PVAm-abs-MG was prepared and added into cellulose laminates. The wet adhesion measurements were conducted by 90° peel tests. The results showed that PVAm-abs-MG gave higher wet adhesion than linear PVAm at the same amine coverage on cellulose membranes. Furthermore, the wet adhesion to cellulose membranes is not sensitive to molecular weight.

In this work we compare colloidal PVAm-abs-MG with linear PVAm as wet strength resins in paper pulp. The aim of this study is to establish the connection between the architecture of colloidal particles and their performance on strength enhancement of wet paper. Carboxylated PNIPAM microgel was chosen as the platform for microgel based adhesives since the system was well defined. In the future, PNIPAM microgels could be replaced by any anionic particles such as starch which is much cheaper and

environmental friendly. Eventually, PVAm coated particles could become commercialized wet strength resins in papermaking industry.

5.2 Experiments

5.2.1 Materials

Three polyvinylamine (PVAm) were involved in this research which was kindly provided by BASF (Ludwigshafen, Germany) and the number-average molecule weight were 10 kDa (Lupamin 1095), 45kDa (Lupamin 5095), 340 kDa (Lupamin 9095). All of the PVAm was further purified by dialysis and freeze dried before use. The details of PVAm involved in this study were shown in Table 1. N-Isopropylacrylamide (NIPAM, 97%, Sigma-Aldrich) was purified by recrystallization from a 60:40 toluene:hexane mixture. N,N-Methylenebisacrylamide (MBA, 99+%, Aldrich), vinylacetic acid (VAA, 97%, Aldrich), sodium dodecyl sulfate (SDS, 98%, Aldrich), ammonium persulfate (APS, 99%, BDH), 2,2,6,6-tetramethyl-1-piperidinyloxy (TEMPO), sodium bromide (NaBr) and sodium hypochlorite(NaClO) were purchased from Sigma-Aldrich and used as received. Carboxyl latex (4% w/v 0.2 μm) was purchased from Invitrogen and used as received.

Table 1. The properties of PVAm used in this work

Molecular weight	Degree of hydrolysis	Equivalent weight
10kDa	73%	100 g/mol
45kDa	75%	76.9 g/mol
340kDa	91%	83.3 g/mol

5.2.2 PVAm-abs-MG Preparation

Anionic microgels (VAA-NIPAM) were synthesized following Hoare's method[18]. The polymerization was carried out in 150ml deionized water containing NIPAM(1.4g), MBA(0.1g), SDS(0.05g) and VAA(0.1g) at 70°C under constant stirring. The microgels were purified via several cycles of centrifugation (50 min at 50000 rpm, Beckman model Optima L-80 XP) until supernatant conductivity was less than 5 μs/cm.

VAA-NIPAM MG was redispersed in 1mM NaCl at a concentration of 4g/L and the pH was adjusted to 7 using NaOH(0.1N). A desired amount of PVAm was dispersed in 70 ml 1mM NaCl and the pH was adjusted to 7 by HC(0.1N). Then 10 mL of microgel solution was added dropwise (1mL/min) into 70 mL of PVAm solution with constant stirring. The

mixture was left stirring for at least 2h and the unabsorbed PVAm was removed by several cycles of centrifugation.

5.2.3 PVAm-abs-PS Preparation

The carboxyl latex was diluted in 1mM NaCl to 4g/L. A desired amount of PVAm was dispersed in 70ml 1mM NaCl. 10ml latex dispersion was then added into PVAm solution dropwise (1mL/min) and the pH was stablized at 7 for 2h. The unabsorbed PVAm was removed by several cycles of centrifugation.

5.2.4 TEMPO-Mediated Oxidation of Cellulose

Unbeaten, bleached soft kraft wood pulp (Avenor, Thunder Bay Mill) was used. The dry pulp was soaked in deionized water at a concentration of 12.5g/L overnight and disintegrated (Labtech Instruments Inc. Model 500-1) for 10 minutes at 3000 RPM to achieve a consistency of 1.2% before use. All of the cellulose fibers were oxidized with TEMPO, NaBr and NaClO following Kitaoka et al.'s method[19]. The concentration of ingredients used were TEMPO 0.034 g/L, NaBr 0.34 g/L, and NaClO 2.8 wt% based on dry cellulose fibers. The oxidation reaction was carried out at 23 °C under stirring. The pH was stabilized at 10.5 using NaOH for 20 min, and the oxidation was stopped by adding ethanol. The cellulose fibers were washed repeatedly with deionized water through a Buchner Funnel.

5.2.5 Handsheet preparation

Handsheets with basis weights of 60 g/m^2 were prepared by the semi-automatic sheet machine (Labtech Instruments Inc. Model 300-1) following TAPPI method, T205 sp-95. The dispersed SKB pulp was then diluted into a concentration of 0.3 wt% and the desired amount of polymer was added into 0.5% consistency pulp with pH adjusted to 7 by 1M NaOH for half an hour under constant stirring. The excess polymer was removed by filtering on a Buchner Funnel fitted with a polycarbonate membrane (Sigmar-Aldrich, pore size: 10μm). All of the handsheets were prepared via wet pressing under 50 psi for 5mins. The wet handsheets were dried at room temperature or on a speed dryer (Labtech Instruments Inc.) for 10 min at 120°C. After preparation, all of the handsheets were conditioned at 23 °C and 50% relative humidity (TAPPI standard T402 sp-98) overnight before measurements. For each test, at least five handsheets were prepared.

5.2.6 Binding isotherm of polymer to oxidized pulp fibers

The unabsorbed PVAm was determined by titrating the filtration solution through conductometric titration while the unabsorbed PVAm-abs-MG was measured by titrating the filtration solution by polyelectrolyte titration. The amount of polymer adsorbed onto the pulp fiber was calculated by deduction of the polymer left in solution from the total amount of polymer added into the pulp.

5.2.7 Wet tensile tests

Tensile strength was measured by the Instron 4411 universal testing system fitted with a 50N load cell (Instron Corporation, Canton, MA) according to TAPPI method T494 om-96. The paper specimen was soaked into deionized water for 5 min and the excess water was removed by pressing between blotting paper. Two strips were cut from each handsheet and at least ten measurements were required for each experimental condition.

5.3 Results

The major goal of this study was to investigate the influence of PVAm based wet strength additives on fiber-fiber bonds. Therefore the unbeaten, bleached kraft softwood pulp was used so that the strength of the handsheet was low and sensitive to the degree of inter-fiber bonding. The SKB pulp was treated with 1wt% of PVAm (MW=10kDa, DH=73%) and PVAm-abs-MG based on the weight of dry pulp fibres. The microgel based wet strength agents were prepared by physically adsorbing PVAm onto the surface of charged anionic microgels. The details about preparation of PVAm-abs-MG were described at Chapter 2. All of the handsheets were rewetted in deionized water and the tensile strengths were measured. Figure 1 shows the effect of pulp oxidation on the wet strength of paper. Without oxidation, the wet tensile index of handsheets increased 70% by PVAm 10kDa and 140% by PVAm-abs-MG. After oxidation, the wet tensile index was significantly promoted by polymer additives. The wet tensile index of the handsheets treated with PVAm 10kDa increased from 2.7 $N.m.g^{-1}$to 3.9 $N.m.g^{-1}$ and the wet tensile index of the handsheets treated with PVAm-abs-MG increased from 3.4 $N.m.g^{-1}$ to 16.7 $N.m.g^{-1}$. The wet tensile index of blank handsheets also increased after pulp oxidation. However, considering the error bars representing the standard deviation of the measurements, the wet strength of blank handsheets was not sensitive to oxidation.

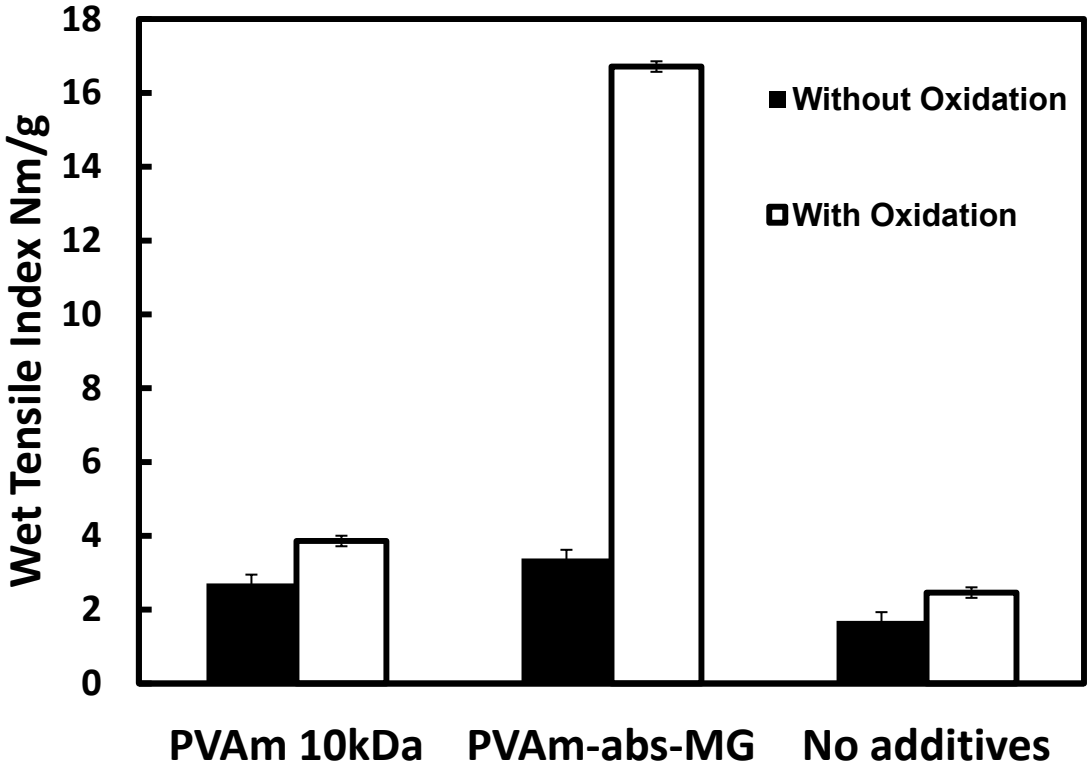

Figure 1. The wet tensile index of handsheets prepared from oxidized cellulose fibers with 1 wt% polymer

After handsheets were formed, they were dried either in a conditioned room at 23°C or in a speed dryer at 100°C. The effect of drying temperature was shown in Figure 2. The drying temperature had no impact on handsheets prepared without additives. For the handsheets treated with PVAm and PVAm-abs-MG, the wet tensile index of handsheets dried at higher temperatures was raised by one third compared with that dried at room temperature.

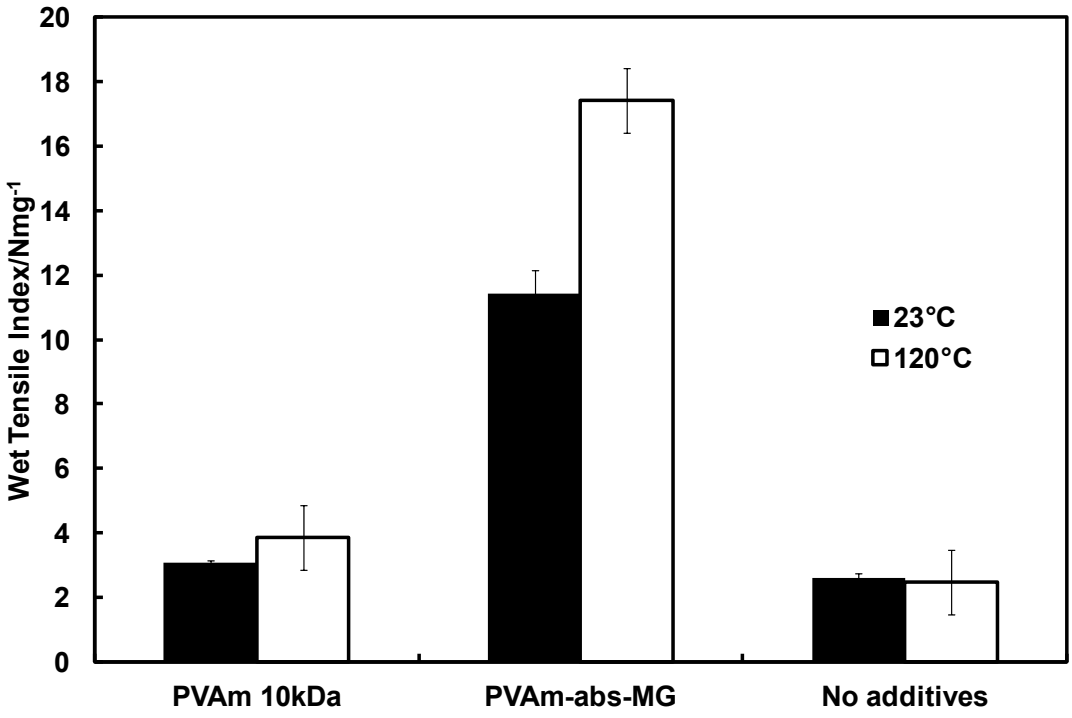

Figure 2. The effect of drying temperature on handsheets prepared by oxidized cellulose with 1 wt% polymers

Since polymer has to adsorb onto cellulose fiber in order to promote the inter-fiber bonding, polymer added into the paper pulp may not contribute to the paper strength. Therefore, the binding isotherms of PVAm with different molecular weight were measured by titrating the unabsorbed PVAm filtered from pulp solution. As shown in Figure 3, the adsorption plateau increased inversely with the molecular weight of PVAm. The maximum amount of polymer that could be adsorbed onto cellulose fibers was 6.3 mg/g for PVAm 340kDa, 9.4mg/g for PVAm 45kDa, and 9.8mg/g for PVAm 10kDa.

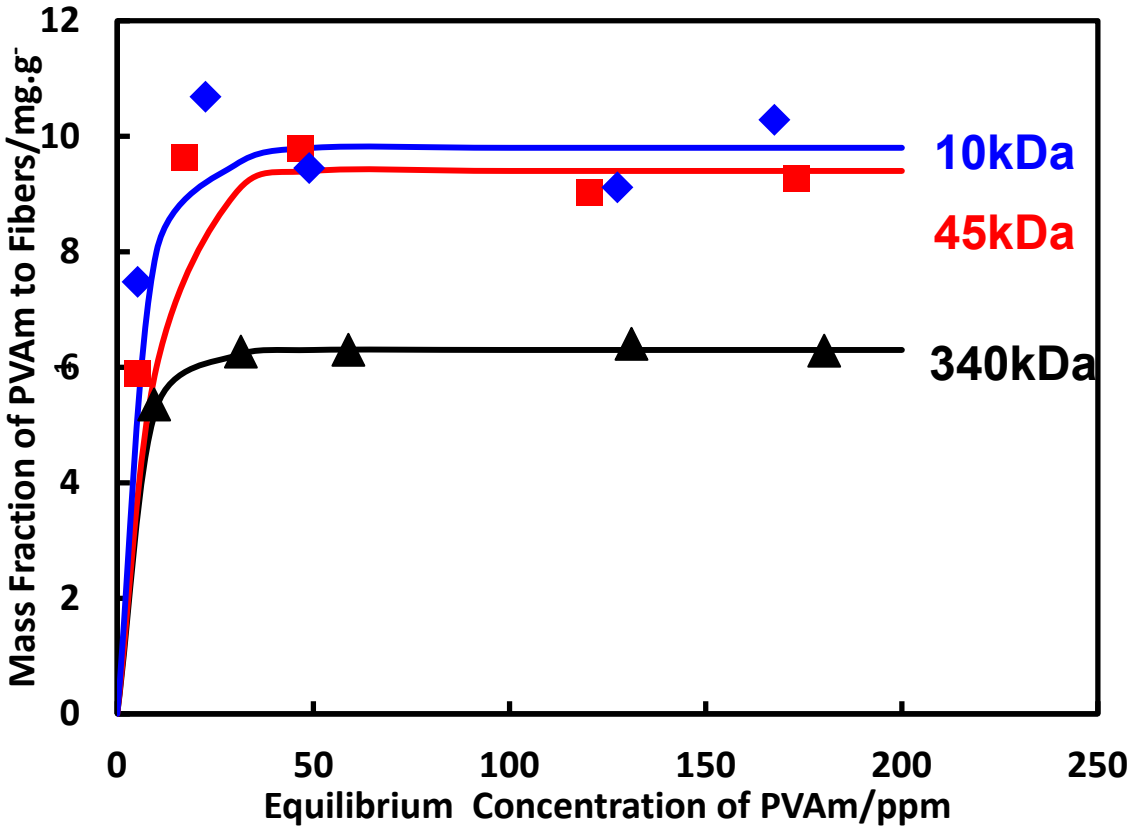

Figure 3. Binding isotherm of PVAm onto oxidized cellulose fibers

Figure 4 shows the response of the wet tensile index to a fluctuation in the amount of PVAm adsorbed onto cellulose fibers. For PVAm 10kDa and PVAm 340kDa, the wet tensile index increased along with the amount of polymer adsorbed. It was found that once the polymer reached the maximum adsorption onto cellulose fibers the molecular weight of PVAm did not make any difference in terms of wet strength enhancement. However, the maximum amount of PVAm 10kDa adsorbed onto cellulose fibers was 50% higher than that of PVAm 340kDa.

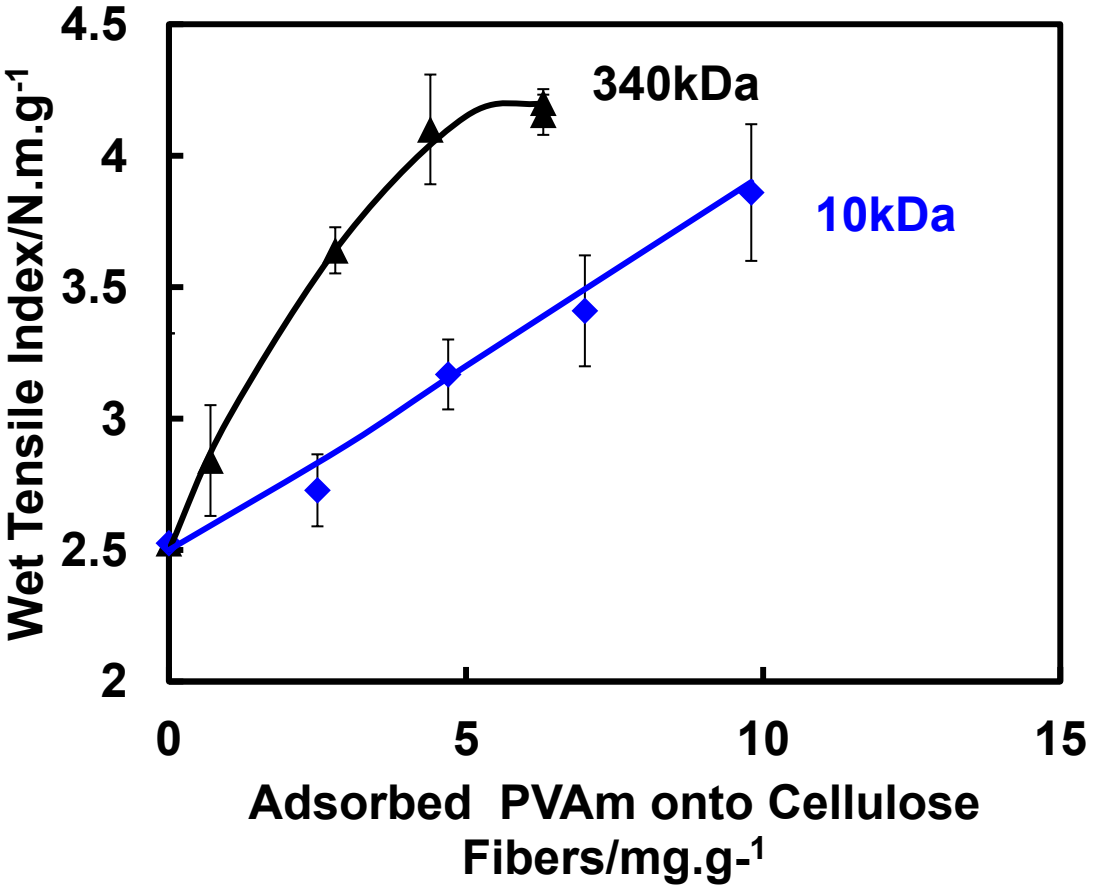

Figure 4. The molecular weight effect of PVAm on wet paper strength

To study the molecular weight effect on microgel based adhesives, PVAm-abs-MGs were prepared by adsorbing PVAm with different molecular weights onto VAA-NIPAM MGs. Specifically, 1wt% of PVAm-abs-MGs were added into pulp and the unabsorbed PVAm-abs-MGs were removed by filtration through a Buchner Funnel fitted with a polycarbonate membrane. The pulp was then redispersed in 1mM NaCl and the amount of PVAm-abs-MG was determined by polyelectrolyte titration. The tensile tests were employed to measure the wet tensile index. The results are summarized in Table 2. The amount of microgels adsorbed onto cellulose fibers was not sensitive to the molecular weight of PVAm. Considering the standard deviation of the wet tensile index displayed in Table 2, the microgels adsorbing PVAm with different molecular weights had equal performance with respect to the wet strength of paper.

Table 2. The influence of PVAm molecular weight adsorbed on MG to wet paper strength (the dosage of MG in pulp is 1wt%)

Molecular Weight kDa	Particle Size at pH 7 nm	Γ(Wmg/Wfiber) $mg.g^{-1}$	Γ(Wpvam/Wmg) $g.g^{-1}$	Wet Tensile Index $N.m.g^{-1}$
10	268±5.4	9.2	0.11	16.7±3.6
45	305±4.4	9.1	0.12	15.8±2.8
340	563±11.3	9.2	0.14	17.24±4.2

Figure 5 shows the wet tensile index as a function of amine content in microgels. The amine content was expressed as the mass fraction of PVAm in microgels. A series of PVAm-abs-MGs were prepared by adsorbing different amounts of PVAm 10kDa to VAA-NIPAM MG. The excess PVAm was removed via centrifugation. The amine content of PVAm-abs-MGs was determined by conductometric titration of centrifuge supernatant. The polymers prepared, 0.3wt% of PVAm-abs-MGs, were added into SKB pulp to make modified handsheets. As shown in Figure 5, the wet tensile index increased with the amine content of PVAm-abs-MG. In fact, 3wt% of PVAm in microgels provided double the wet tensile strength to handsheets compared with unmodified handsheets. The highest wet tensile index was provided by microgels containing 10wt% PVAm.

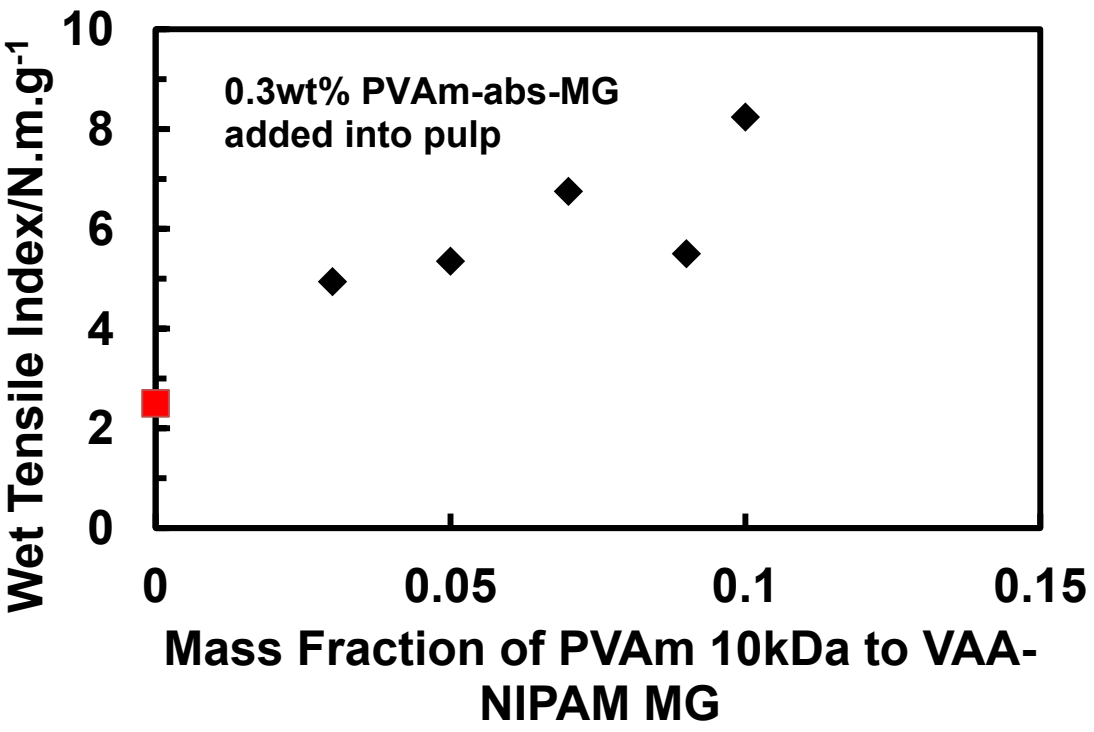

Figure 5. The influence of amine content in microgels to wet paper strength(Drying temperature of handsheet 120°C)

To study the effect of polymer stiffness on the wet paper strength the wet tensile strength of paper was measured as a function of the dosage of different PVAm based adhesives. PVAm-abs-MG and PVAm-abs-PS are colloidal particles with a PVAm coating on the surface, whereas PVAm 340kDa is high molecular weight linear polymer. Polystyrene latexes with a similar size as PNIPAM microgels were introduced to study the influence of deformation on the performance of wet strength resins. Polystyrene latexes are solid particles that maintain a permanent structure while microgels are a network of polymers that will experience a change in shape during the formation of handsheets. The preparation method of PVAm-abs-PS was the same as PVAm-abs-MG by mixing PVAm solution with colloidal particle dispersion and the diameter of PS latex was 200nm which was similar with the diameter of microgels. The mass fraction of PVAm 10kDa in MGs was 10wt% while the mass fraction of PVAm 10kDa absorbed on carboxyl latex was 6wt%. As shown in Figure 6, the wet tensile index increased along with polymer dosage. The wet strength of handsheets treated with PVAm-abs-PS and PVAm 340kDa reached the plateau indicating that the pulp fiber surfaces were fully covered by polymeric adhesives. Therefore, the addition of PVAm-abs-PS and PVAm 340kDa didn't contribute to the wet strength enhancement. Compared with PVAm-abs-PS and PVAm 340kDa, PVAm-abs-MG gave the highest wet tensile index at the same dosage of polymer in pulp.

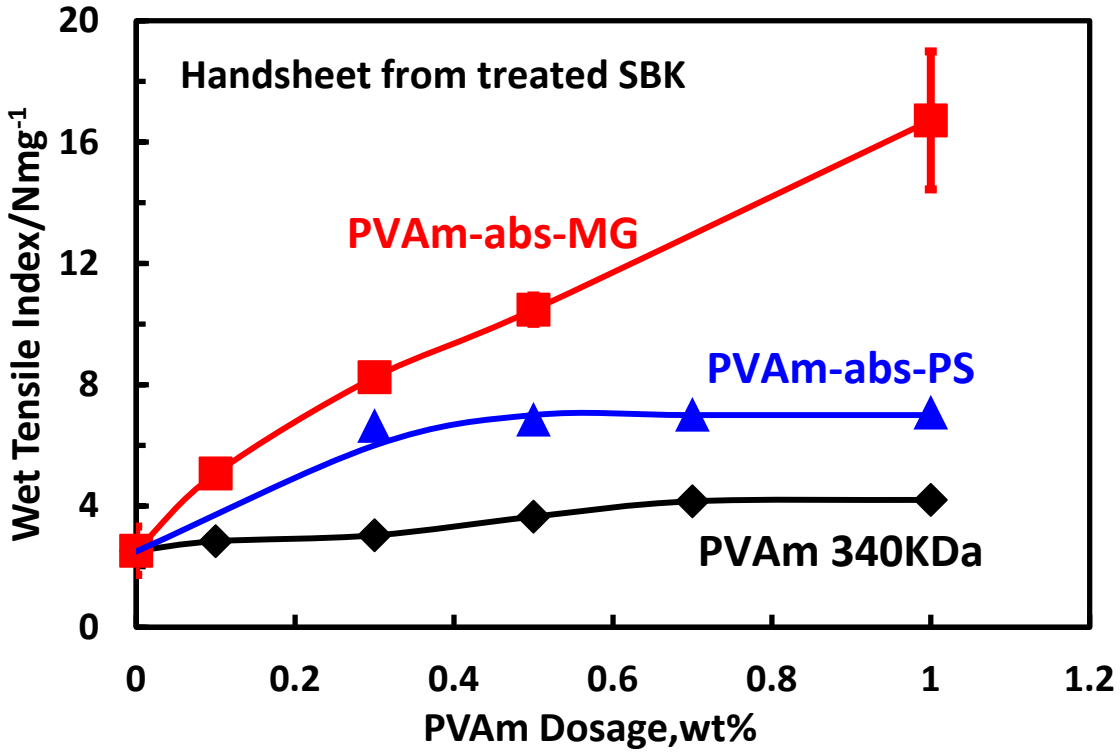

Figure 6. The effect of polymer morphology on the wet strength of paper

5.4 Discussion

The adsorption of cationic polymer to cellulose fibers is driven by the electrostatic interaction between carboxyl groups on cellulose fibers and cationic charges of polymers. Usually polymers can only form a monolayer on surfaces at the coverage of 0.1-1 mg/m^2. In addition, high molecular weight polymers are able to absorb more due to their larger gyration radius [20]. As shown in Figure 3, the adsorption of PVAm onto cellulose fibers followed the typical behaviors of polymer adsorption onto surfaces. However, the maximum amount of polymer absorbed was reduced with increasing molecular weight. The explanation for this response is the porous surface of cellulose fibers. According to the study conducted by Andreasson et al., the pore radius is in the scale of 10nm[21]. It was shown that polymers smaller than 9nm in diameter could penetrate into the cellulose fibres[22]. Therefore, it is possible for polymers with small molecular weights to enter the pores on cellulose fiber walls. The florescent study on adsorption of labeled polyallylamine hydrochloride (PAH) onto cellulose fibers showed that PAH 15kDa could access into fiber walls[23]. Theoretically, the gyration radius of PVAm 10kDa is 4.2 nm and PVAm 340kDa is 34.1nm at pH2.[24] Since the dissociation degree of amine groups is reduced with increasing pH, the gyration radius of PVAm10kDa is less than 4.2nm at pH7. Thus, PVAm 10kDa could easily enter the fiber wall during adsorption while PVAm 340kDa could only adsorb on the surface of cellulose fibers.

To contribute to inter-fiber bindings, the polymer has to be adsorbed onto the exterior of the cellulose fiber walls. Therefore, PVAm 10kDa which can enter the pores on the fiber walls does not effectively enhance the fiber-fiber bonds. As shown in Figure 4, for the same amount of PVAm adsorbed, PVAm 340kDa gave a higher wet tensile index. However, once the amount of polymer reaches the plateau of the binding isotherm the wet strength of the handsheets are not sensitive to the molecular weight of PVAm. It is believed that the wet tensile index depends on the surface coverage of PVAm. The layer thickness contributed by the molecular weight of PVAm is not necessary for wet strength enhancement.

As can be observed from Figure 4 and Table 2, the amount of polymer adsorbed onto cellulose fibres is the same degree. However, the wet tensile index of handsheets treated with PVAm-abs-MG is quadruple of that treated with linear PVAm. Similar research has been done with polyelectrolyte complexes of cationic poly(amideamine) epichlorohydrin condensate (PAE) and anionic carboxymethylcellulose (CMC) to enhance the wet paper strength[25]. However, the influence of polymer size on wet paper strength was not clear due to the broad size distribution. In contrast, this research introduced the mono-dispersed microgels. The possible reason for the effect of wet strength enhancement is the size difference between linear PVAm and PVAm-abs-MG.

Since the mechanism of wet strength enhancement contributed by PVAm is the covalent bonds between primary amine groups of PVAm and aldehyde groups of cellulose [14], the increment of wet strength depends on the number of covalent linkages between PVAm and pulp fibres. As shown in Figure 6, both PVAm-abs-PS and PVAm-abs-MG gave stronger wet strength. In fact, for the same dosage of polymer in handsheet, the primary amine content of PVAm-abs-MG and PVAm-abs-PS are lower than that of PVAm by at least an order of magnitude. Thus the number of covalent bonds formed between colloidal particles and the cellulose fibers is most likely less than linear PVAm. However, the paper treated with PVAm-abs-MG and PVAm-abs-PS achieved a higher wet strength since the colloidal particles created a larger contact area for fiber-fiber interactions. According to Page's theory, tensile strength of paper is defined as: [3]

$$\frac{1}{T} = \frac{9}{8Z} + \frac{12A\rho g}{bPL(RBA)} \qquad \text{Equation 1}$$

Where T is the tensile strength expressed in breaking length; Z is the zero-span tensile strength (measure of fiber strength) of the sample expressed as a breaking length; A is the mean fiber cross sectional area; ρ is the density of the fibrous material; g is acceleration due to gravity; b is the shear strength per unit area of the fiber-fiber bonds and is a function of the sheet structure (related to RBA); P is the average perimeter of fiber cross section; L is the mean length of fiber; RBA is short for relative bonded area which is the fraction of fiber surface that is bonded in the sheet.

Since the type of pulp and papermaking conditions was kept the same for different types of wet strength adhesives, the following variables: A, ρ, g, P and L are fixed as well. Thus, Equation 1 could be derived as[26]

$$\frac{1}{T} = \frac{9}{8Z} + \frac{C}{b_f (RBA)^2} \qquad \text{Equation 2}$$

Where C is the constant for fiber characteristics of a given pulp and b_f is the shear strength per unit of fiber-fiber bonds. The first term of the right-hand side is determined by the intrinsic fiber strength, whereas the second term is determined by the fiber-fiber bonds.

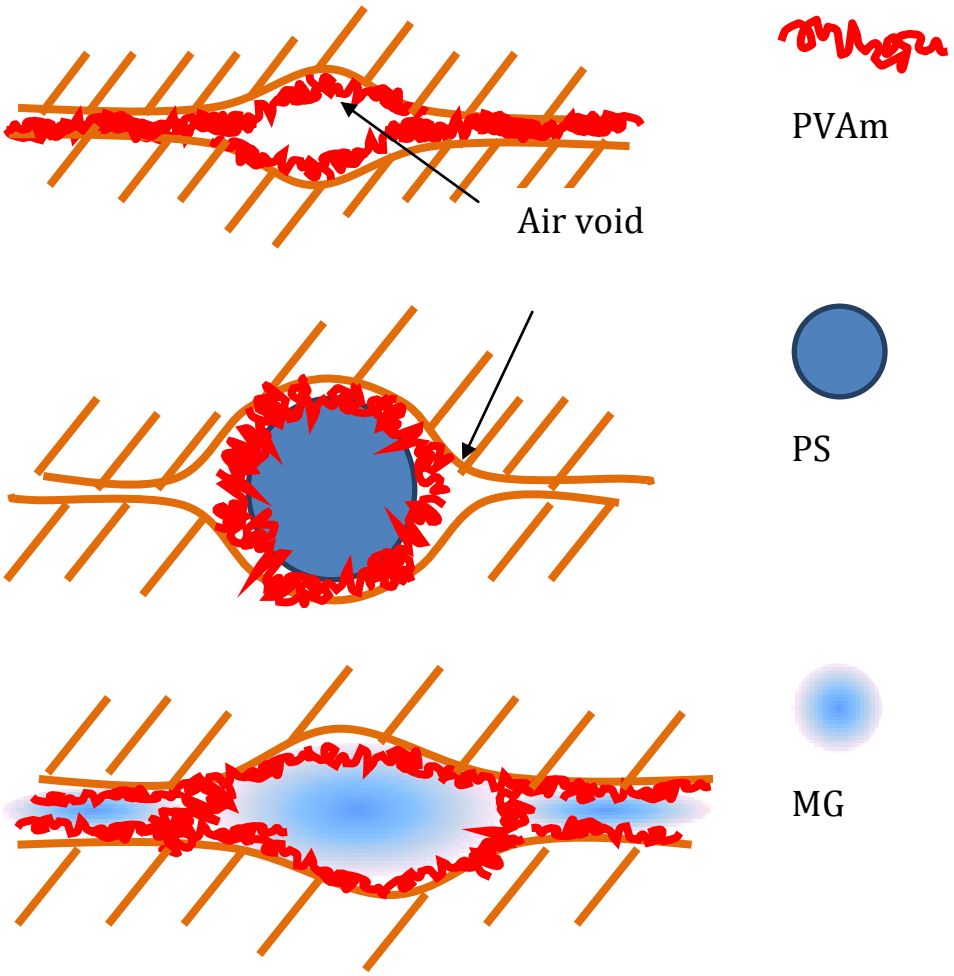

Figure 7. Scheme of relative bonded area between two fibers

This study focused on the wet tensile strength of paper which is mainly provided by the covalent linkage between amine groups from adhesives and the aldehyde groups from pulp fibers. Thus, the b_f is the same for different types of wet strength adhesives involved in this research. Referring to Equation 2, the only cause of different performances of wet strength adhesives is due to the total bonded area reinforced by wet strength additives in the handsheets. In the papermaking system, linear PVAm could only hold the fibers together by covalent bonds at a molecular contact area due to the limitation of polymer size. Compared with the gyration radius of linear PVAm, the sizes of PVAm-abs-PS and PVAm-abs-MG are larger by at least an order of magnitude. As shown in Figure 7, the fiber surfaces are quite rough and forms voids between fiber-fiber bonds.[17] PVAm-abs-MG and PVAm-abs-PS could fill in the voids between fibers and create more contact area for fiber-fiber bonds.

PS Latex could be used as filler particles. The interaction between filler particles and cellulose fibers are usually weaker than inter-fiber bonds[27]. However, according to the study completed by Alince et al., by providing bridging agents between filler particles and pulp fibers, the wet strength of paper is enhanced[28]. Therefore, PVAm acts as a bridging agent that can attach to cellulose fibers and latex particles. However, latex particles are solid and retained their morphology during handsheet formation, which can lead to voids between fibers and destruct the fiber-fiber interactions[4]. Therefore, the tensile strength of paper is reduced by the introduction of a filler particle. Additionally, the water content of PVAm-abs-MG at pH 7 is 82.4%. When the same amount of polymer is added into pulp suspension, PVAm-abs-MG could cover more surface area of cellulose fibers than PVAm-abs-PS. In this case, paper treated with PVAm-abs-PS did not achieve the same degree of wet strength as PVAm-abs-MG.

5.5 Conclusion

The oxidation of pulp promotes the wet adhesion between cellulose fibers and PVAm.

For the same amount of PVAm adsorbed onto cellulose fibers higher molecular weight PVAm treated paper gave a higher wet strength. However, once the fiber surface was fully covered by PVAm the wet strength of paper was not sensitive to the molecular weight of PVAm.

VAA-NIPAM Microgels with a 10wt% PVAm coating gave comparable wet paper strength as PVAm microgels.

The molecular weight of PVAm adsorbed onto the surface of microgels does not influence the wet strength of handsheets.

PVAm coated polystyrene latex has a higher performance as a wet strength resin than PVAm itself. However, the hard latex leads to a reduction of wet paper strength compared with microgels.

5.6 References

1. Smook, G. A., *Handbook for pulp & paper technologists* 2nd ed. ed.; Angus Wilde Publications: Vancouver, 1992.

2. Espy, H. H., The mechanism of wet-strength development in paper: a review. *Tappi* **1995,** *78* (4), 90.

3. Page, D. H., A theory for the tensile strength of paper. *Tappi* **1969,** *52* (4), 674-680.

4. Roberts, J. C., *Paper chemistry*. Blackie ;Chapman and Hall: Glasgow,New York, 1991; p xiii, 234 p.

5. Chan, L. L.; Technical Association of the Paper and Pulp Industry. Papermaking Additives Committee., *Wet-strength resins and their application*. TAPPI Press: Atlanta, Ga., 1994; p xii, 120 p.

6. Obokata, T.; Yanagisawa, M.; Isogai, A., Characterization of polyamideamine-epichlorohydrin (PAE) resin: Roles of azetidinium groups and molecular mass of PAE in wet strength development of paper prepared with PAE. *J Appl Polym Sci* **2005,** *97* (6), 2249-2255.

7. Kurosu, K.; Pelton, R., Simple lysine-containing polypeptide and polyvinylamine adhesives for wet cellulose. *J Pulp Pap Sci* **2004,** *30* (8), 228-232.

8. Pelton, R.; Hong, J., Some properties of newsprint impregnated with polyvinylamine. *Tappi J.* **2002,** *1* (10), 21.

9. Saito, T.; Isogai, A., Wet Strength Improvement of TEMPO-Oxidized Cellulose Sheets Prepared with Cationic Polymers. *Ind. Eng. Chem. Res.* **2006,** *46* (3), 773-780.

10. Yang, C. Q.; Xu, Y.; Wang, D., FT-IR Spectroscopy Study of the Polycarboxylic Acids Used for Paper Wet Strength Improvement. *Ind. Eng. Chem. Res.* **1996,** *35* (11), 4037-4042.

11. Xu, G. G.; Yang, C. Q.-X., Comparison of the kraft paper crosslinked by polymeric carboxylic acids of large and small molecular sizes: Dry and wet performance. *J Appl Polym Sci* **1999,** *74* (4), 907-912.

12. Chen, N.; Hu, S.; Pelton, R., Mechanisms of Aldehyde-Containing Paper Wet-Strength Resins. *Ind. Eng. Chem. Res.* **2002,** *41* (22), 5366-5371.

13. Xu, G. G.; Yang, C. Q.; Deng, Y., Combination of bifunctional aldehydes and poly(vinyl alcohol) as the crosslinking systems to improve paper wet strength. *J Appl Polym Sci* **2004,** *93* (4), 1673-1680.

14. John-Louis, D.; Robert, B.; Robert, P.; Marc, L., The mechanism of polyvinylamine wet-strengthening. **2005**.

15. Geffroy, C.; Labeau, M. P.; Wong, K.; Cabane, B.; Cohen Stuart, M. A., Kinetics of adsorption of polyvinylamine onto cellulose. *Colloids and Surfaces A: Physicochemical and Engineering Aspects* **2000,** *172* (1-3), 47.

16. Feng, X.; Pouw, K.; Leung, V.; Pelton, R., Adhesion of Colloidal Polyelectrolyte Complexes to Wet Cellulose. *Biomacromolecules* **2007,** *8* (7), 2161.

17. Miao, C.; Pelton, R.; Chen, X.; Leduc, M., Microgels versus Linear Polymers for Paper Wet Strength - Size Does Matter. *Appita Journal: Journal of the Technical Association of the Australian and New Zealand Pulp and Paper Industry* **2007,** *60* (6), 465.

18. Hoare, T.; Pelton, R., Highly pH and Temperature Responsive Microgels Functionalized with Vinylacetic Acid. *Macromolecules* **2004,** *37* (7), 2544.

19. Kitaoka, T.; Isogai, A.; Onabe, F., Chemical modification of pulp fibers by TEMPO-mediated oxidation *Nordic Pulp & Paper Reserach Journal* **1999,** *14* (4), 279-284.

20. Fleer, G. J. C. S., M. A.; Scheutjens, J. M. H. M.; Cosgrove,; T.; Vincent, B., *Polymers at interfaces*. 1st ed. ed.; London ;: Chapman & Hall, 1993.

21. Andreasson, B.; Forsström, J.; Wågberg, L., Determination of Fibre Pore Structure: Influence of Salt, pH and Conventional Wet Strength Resins. *Cellulose* **2005,** *12* (3), 253-265.

22. Wågberg, L.; Hägglund, R., Kinetics of Polyelectrolyte Adsorption on Cellulosic Fibers. *Langmuir* **2001,** *17* (4), 1096-1103.

23. Gimåker, M.; Wågberg, L., Adsorption of polyallylamine to lignocellulosic fibres: effect of adsorption conditions on localisation of adsorbed polyelectrolyte and mechanical properties of resulting paper sheets. *Cellulose* **2009,** *16* (1), 87-101.

24. Wen, Q. V., A. M.; Pelton, R., Cationic Polyvinylamine Binding to Anionic Microgels Yields Kinetically Controlled Structures. *Journal of Colloid and Interface Science* **2012**, accepted.

25. Gärdlund, L.; Wågberg, L.; Gernandt, R., Polyelectrolyte complexes for surface modification of wood fibres: II. Influence of complexes on wet and dry strength of paper. *Colloids and Surfaces A: Physicochemical and Engineering Aspects* **2003,** *218* (1-3), 137-149.

26. Yoon, S.-Y.; Deng, Y., Experimental and Modeling Study of the Strength Properties of Clay−Starch Composite Filled Papers. *Ind. Eng. Chem. Res.* **2007,** *46* (14), 4883-4890.

27. Li, L. C., A.; Pelton, R., A new analysis of filler effects on paper strength. *J Pulp Pap Sci* **2002,** *28* (8).

28. Alince, B.; Bednar, F.; van de Ven, T. G. M., Deposition of calcium carbonate particles on fiber surfaces induced by cationic polyelectrolyte and bentonite. *Colloids and Surfaces A: Physicochemical and Engineering Aspects* **2001,** *190* (1-2), 71-80.

Chapter 6 Concluding Remarks

Recent studies have applied polyelectrolyte complexes to papermaking systems as wet strength additives. However, the mechanism whereby complexes reinforce the wet strength of paper is not well defined. Our work studies the interactions between modified microgels and wet cellulose by wet adhesion measurements of cellulose laminates and tensile tests of handsheets. The major contributions of this work are as follows:

1. The colloidal properties of PVAm-abs-MG were determined by their composition, and the charge locations in the microgels. The swelling behaviours and electrophoretic mobilities of microgels were studied under varying pH, resulting from the dissociation of amine groups from PVAm and carboxyl groups from microgels.

2. The binding of PVAm to carboxylated microgels was studied in terms of salt concentration, pH, PVAm molecular weight and mixing orders. The PVAm content of PVAm-abs-MG could be kinetically controlled according to the mixing orders. The final configuration of PVAm in microgels was determined by the balance between the rate of initial attachment of PVAm, and the rate of chain spreading of PVAm.

3. The adhesive properties of PVAm modified microgels were correlated to PVAm content in microgels, molecular weight of PVAm, elasticity of microgels, and the coverage of adhesives on the cellulose. The results showed that microgels with low elasticity and high PVAm content gave stronger wet adhesion with cellulose. The molecular weight of PVAm did not impact the wet adhesion with cellulose.

4. A simple peeling model was developed to predict the influence of microgel diameter, microgel elasticity and coverage on wet delamination force. Microgels are treated as ideal springs and PVAm coatings are stickers. The failure of adhesion during peeling is recognized as detachment of PVAm from microgels.

5. Cellulose model films were prepared by casting from ionic liquid. The surface roughness was controlled by the roughness of the substrate and the deposition rate of cellulose from the ionic liquid. The influence of microgel size on wet adhesion with cellulose was studied, based on cellulose model films. Large microgels could fill in the voids between rough cellulose surfaces to benefit wet adhesion.

6. The effect of PVAm modified microgels as wet strength adhesives was studied by handsheet preparation. The wet paper strength increased with PVAm content in microgels, and 10wt% of PVAm in microgels gave wet paper strength comparable to PVAm microgels. In the case of PVAm worked as wet strength adhesive, PVAm with

high molecular weight gave higher wet paper strength. By contrast, the molecular weight of PVAm coated on microgels did not influence the wet paper strength.